DESIGN OF A SKID-STEER LOADER

A THESIS SUBMITTED TO
THE GRADUATE SCHOOL OF NATURAL AND APPLIED SCIENCES
OF
MIDDLE EAST TECHNICAL UNIVERSITY

BY

TUĞÇE YALÇIN

IN PARTIAL FULFILLMENT OF THE REQUIREMENTS
FOR
THE DEGREE OF MASTER OF SCIENCE
IN
MECHANICAL ENGINEERING

SEPTEMBER 2012

Approval of the thesis:

DESIGN OF A SKID-STEER LOADER

submitted by **TUĞÇE YALÇIN** in partial fulfillment of the requirements for the degree of **Master of Science in Mechanical Engineering Department, Middle East Technical University** by,

Prof. Dr. Canan Özgen _____
Dean, Graduate School of **Natural and Applied Sciences**

Prof. Dr. Suha Oral _____
Head of Department, **Mechanical Engineering**

Prof. Dr. Eres Söylemez _____
Supervisor, **Mechanical Engineering Dept., METU**

Examining Committee Members:

Prof. Dr. Kemal Özgören _____
Mechanical Engineering Dept., METU

Prof. Dr. Eres Söylemez _____
Mechanical Engineering Dept., METU

Prof. Dr. Reşit Soylu _____
Mechanical Engineering Dept., METU

Asst. Prof. Ender Ciğeroğlu _____
Mechanical Engineering Dept., METU

Ferhan Fıçıcı, M.Sc. _____
Team Leader of R&D, Hidromek Inc.

Date: 13.09.2012

I hereby declare that all information in this document has been obtained and presented in accordance with academic rules and ethical conduct. I also declare that, as required by these rules and conduct, I have fully cited and referenced all material and results that are not original to this work.

Name, Last name: Tuğçe YALÇIN

Signature :

ABSTRACT

DESIGN OF A SKID-STEER LOADER

Yalçın, Tuğçe
M.S., Department of Mechanical Engineering
Supervisor : Prof. Dr. Eres Söylemez

September 2012, 133 pages

Skid-steer loaders are also called mini loaders. Skid-steer loaders are capable of zero turning radiuses, which make them extremely maneuverable and suitable for confined spaces. The aim of this thesis study is to design the loader mechanism for skid-steer loaders. Primarily, the loader mechanism synthesis will be performed to determine the basic link dimensions for the mechanism of the loader. Genetic algorithm will be used in the design process. Besides, the hydraulic cylinders dimensions and working pressure of the loader mechanism will be chosen according to the forces that will be applied. After the link dimensions of the loader are determined, 3D modeling of the loader mechanism will be performed. Afterwards, the finite element analysis of the system will be carried out. Finally, improvements will be made on the model according to the results of the analysis.

Keywords: Skid-steer loader, Mechanism synthesis, Burmester theory, Genetic algorithm

ÖZ

MİNİ YÜKLEYİCİ TASARIMI

Yalçın, Tuğçe
Yüksek Lisans, Makina Mühendisliği Bölümü
Tez Yöneticisi : Prof. Dr. Eres Söylemez

Eylül 2012, 133 sayfa

Mini yükleyici, nokta dönüşü yapabilmesi sebebiyle manevra kabiliyeti yüksek olan ve bu sebeple dar alanlarda oldukça fazla tercih edilen bir iş makinesidir. Bu tez çalışmasının amacı, mini yükleyicideki yükleyici kolun tasarımının yapılmasıdır. Öncelikle, yükleyici kol tasarım parametrelerinin belirlenebilmesi için mekanizma sentezi yapılacaktır. Tasarım sürecinde genetik algoritmadan faydalanılacaktır. Bu sırada, uygulanacak yükler göz önünde bulundurularak hidrolik silindir seçimi ve sistemde kullanılacak olan çalışma basıncı seçimi yapılacaktır. Kol üzerindeki bütün mafsal noktalarının konumlandırılmasının ardından, yükleyici kol 3 boyutlu olarak modellenecektir. Daha sonra, tasarlanmış olan yükleyici kolun sonlu elemanlar analizi yapılacaktır. En son olarak da analizde çıkan sonuçlara göre mevcut modelde iyileştirmeler yapılacaktır.

Anahtar kelimeler: Mini yükleyici, Mekanizma sentezi, Burmester teorisi, Genetik algoritma

go confidently in the direction of your dreams!
live the life you've imagined…
Thoreau

ACKNOWLEDGMENTS

First of all, I would like to express my deepest gratitude to Prof. Dr. Eres Söylemez for being such a great educator, his willingness to answer my endless questions, beguiling me by suggesting me to be a thesis student of him and his guidance and criticism throughout the study.

I would like to share my sincere appreciation to Hasan Basri Bozkurt, general manager of Hidromek Inc., for his efforts to motivate me by providing lots of skid-steer loader models, his everlasting willingness to enlighten me and the twinkle in his eyes showing his faith in me.

I would like to thank my colleagues Ferhan Fıçıcı for inspiring me to be a better engineer with his engineering knowledge; Erkal Özbayramoğlu for staying in the office after working hours without a second of hesitation to teach me genetic algorithm, being the one to consult when I have difficulties about engineering and solving all the mentioned problems even if the way he does is not always the way that I wanted; and Serdar Tekin for helping me with the finite element analysis and teaching me various Visual Basic commands like "Application.ScreenUpdating = False" which saves quite a bit of time.

I would like to appreciate Rasim Aşkın Dilan checking my thesis in detail and correcting the mistakes, as carefully as me, over and over again and knowing that he is there for me if I needed him.

Finally, I owe thanks to Sema Yalçın for being the best mum in the world; Serdar Yalçın for his love and support during my life; and Rose for giving joy to my life, sensing my mood perfectly and acting accordingly and giving me the feeling that she is always there for me.

TABLE OF CONTENTS

LIST OF TABLES

TABLES

LIST OF FIGURES

FIGURES

CHAPTER 1

INTRODUCTION

The aim of this thesis is to design the loader mechanism of a skid-steer loader including its structural shape of the loader mechanism.

A brief history of kinematics, the types of synthesis both for type synthesis and dimensional synthesis related to the kinematic design of the loader mechanism can be found in Appendix.

Earth-moving machinery are machines designed to perform excavation, loading, transportation, drilling, spreading, compacting or trenching of earth, rock and other materials by their equipment or working tools [1].

A skid-steer loader is earth-moving machinery and can be depicted as a mini loader. Skid-steer loaders' weight changes from 1 ton to 5 tones and their net power changes from 10kW to 70kW; both of the values are much less than those of the standard loaders. A skid-steer loader is defined as "loader which normally has an operator station between attachment-supporting structures and which is steered by using variation of speed, and/or direction of rotation between traction drives on the opposite sides of a machine having fixed axles on wheels or tracks" [2]. A great amount of attachments can be attached to the lift arm of the skid-steer loader. These attachments can be listed as backhoe, hydraulic breaker, pallet forks, angle broom, sweeper, auger, mower, snow blower, stump grinder, tree spade, trencher, dumping hopper, ripper, tillers, grapple, tilt, roller, snow blade, wheel saw, cement mixer, and wood chipper machine. Hence, skid-steer loader is capable of accomplishing all these jobs other than its usual jobs like excavation and loading.

According to their lift arm skid-steer loaders can be classified in two types. One type uses a simple inverted-slider crank mechanism as its structure. A piston-cylinder

rotates the lift arm. The type is named as Type I mechanism. In this mechanism, the hinge pin joining the bucket and the lift arm draws an arc of a circle. The other type uses a four-bar mechanism; again a piston-cylinder drives the four-bar chain. That type is named as Type II mechanism. In this mechanism, the hinge pin can trace any path wanted by making a three or four position synthesis. These two possibilities for loader mechanism can be seen in Figure 1-1.

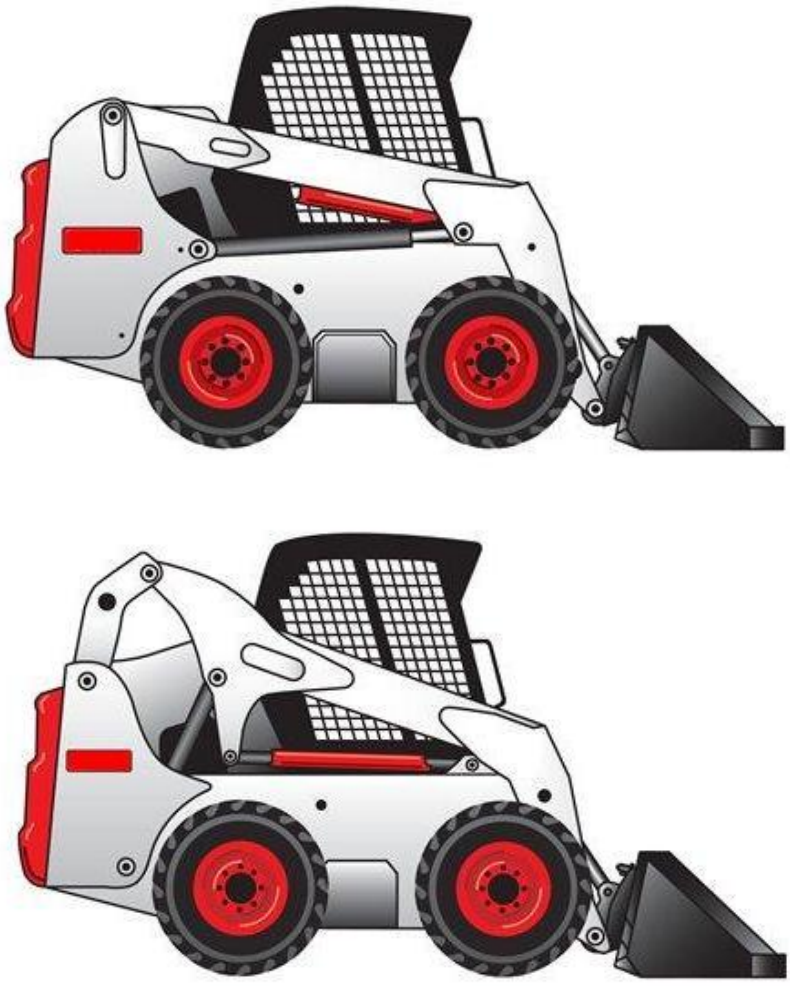

Figure 1-1 – Types of skid-steer loaders according to loader mechanism (above: Type I mechanism, below: Type II mechanism) [3]

Basically, the motion of a skid-steer loader consists of filling the bucket with diggings, bringing the bucket to a position that the diggings will not spill during the cycle, lifting the load and dumping it to a truck. As usual, the simplest solution is the best solution. The simplest mechanism satisfying the motion described above is a Type I mechanism as shown in Figure 1-1. If the motion of the hinge pin is required to be controlled, the simplest mechanism becomes a Type II mechanism. Six-link mechanism, plus a piston-cylinder driving the mechanism, or any other mechanism satisfying the motion can also be a solution but it will be pointless because it would make the system more complex than necessary. The schematic views of these two possible mechanisms can be seen in Figure 1-2. The links in red shows the lift arm; the blue and green links show the connecting rods and the orange ones show the hydraulic piston-cylinder pairs schematically.

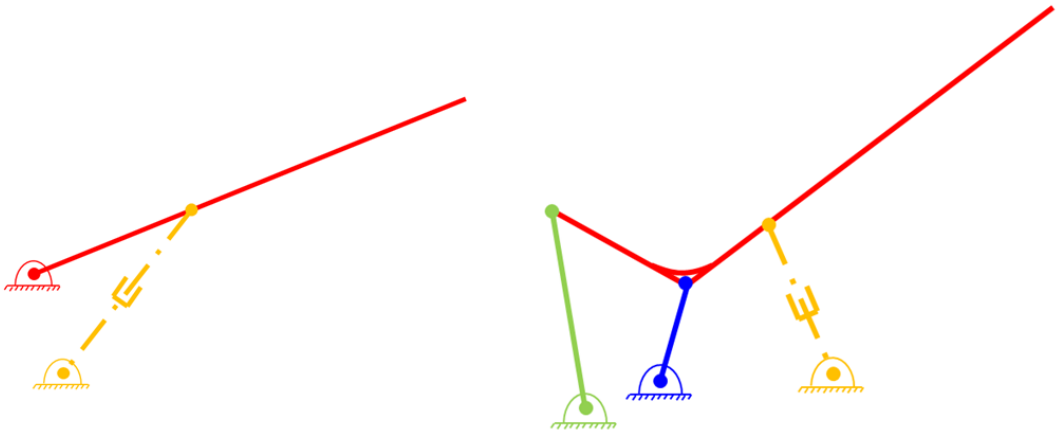

Figure 1-2 – Schematic views of two possible loader mechanisms (left: Type I mechanism, right: Type II mechanism)

A skid-steer loader consists of lower frame, upper frame, lift arm, cab, bucket and piston-cylinder pairs. If a Type II mechanism exists instead of a Type I mechanism, connecting rods are also added to the construction. All these parts can be seen in

Figure 1-3. The lift arm - bucket mechanism is a two-degree of freedom system controlled by piston-cylinder pairs namely lift and tilt cylinders. Two lift cylinders, mounted on the left and on the right of the upper frame, are parallel actuators and give motion to the lift arm, for lift arm to go up or down. Besides two tilt cylinders, which are mounted on the lift arm, rotate the bucket with respect to the lift arm to load or dump the diggings.

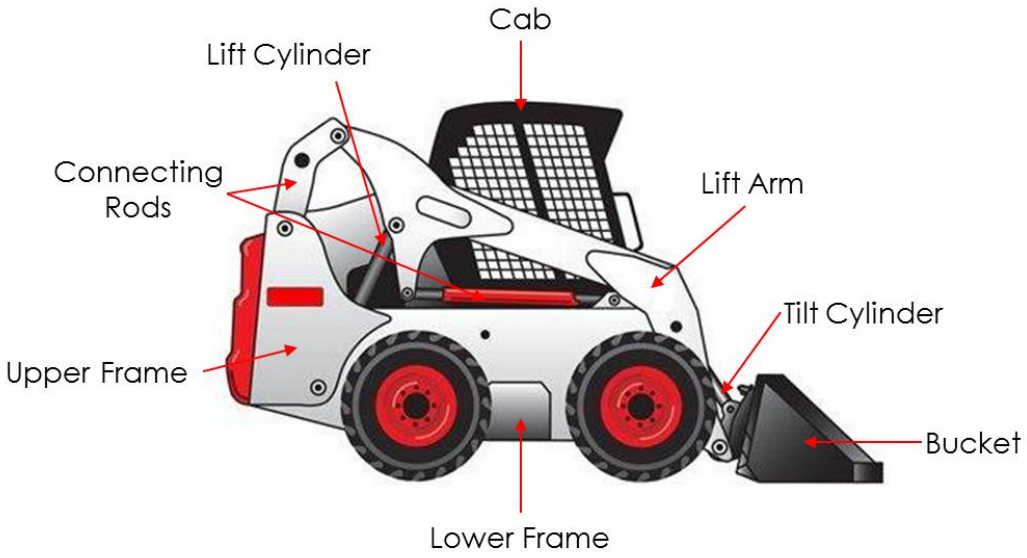

Figure 1-3 – Parts of a typical skid-steer loader with Type II mechanism [3]

Skid-steer loaders, as shown in Figure 1-4, can be equipped either with tracks or wheels. If it is equipped with wheels, typically it will be a four-wheel drive vehicle. Like a skid-steer loader with tracks, the left side drive wheels will be independent of the right side drive wheels. By having the left and right sides independent of each other, skid-steer loaders are capable of zero-turning radius which makes them extremely maneuverable and suitable for confined places.

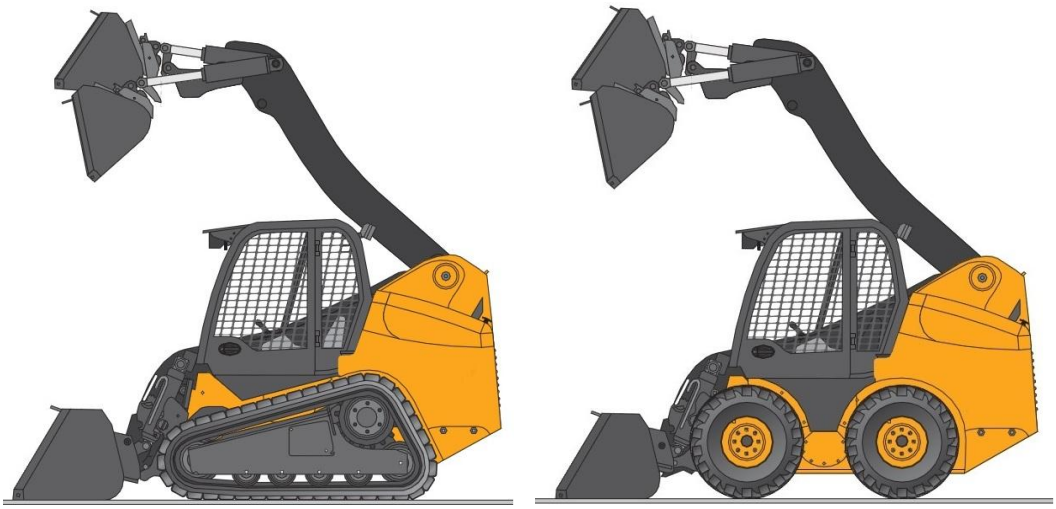

Figure 1-4 – Types of skid-steer loaders according to travel train (left: tracks, right: wheels) [4]

The objective of this study is to design a skid-steer loader mechanism with an inverted-slider (Type I) mechanism and a four-bar (Type II) mechanism. Four multiply separated position synthesis is used for the design of the Type II mechanism. The first reason for selecting four multiply separated positions is to have an infinite number of solutions unlike five multiply separated one. The second reason is to be more accurate than the three multiply separated one. In four-bar linkage system, motion generation is used for prescribed position synthesis, because the hinge pin is wanted to pass from those four prescribed points exactly. The usable ranges of the center-points should be determined. Among the ∞ solutions, the designer has to use his/her intuition and experience while selecting the most suitable mechanism dimensions out of the possible combinations. That is why the designer plays a major role in kinematics synthesis of mechanisms.

After the kinematic synthesis is accomplished then kinematic, force and stress analysis will be carried out all together to achieve an acceptable solution. When all analysis procedures are completed, a design optimization should be performed to derive maximum benefit from the available resources. Genetic algorithm is one of

the most popular optimization algorithms, which is known for its robustness and ability to search complex and noisy search spaces [5]. There are lots of restrictions while designing the loader part of a skid-steer loader and its general view can be seen in Figure 1-5. A few of them can be sorted as the skid-steer loader portion should satisfy the target height, the skid-steer should not spill over any diggings when the bucket is loaded both at its lowest and highest position and the skid-steer should be able to dump all the diggings when the bucket is at its highest position with the bucket cylinder is fully opened. It is difficult to design a skid-steer satisfying all those criteria listed above and like. Moreover, the mechanism satisfying all geometrical criteria should also have a good transmission angle and force distribution. It is more austere to design a mechanism having a good transmission angle and force distribution, so genetic algorithm is used as an optimization algorithm to find the best possible solutions.

Figure 1-5 – General view of a skid-steer loader [6]

CHAPTER 2

LITERATURE SURVEY AND STATE OF ART

2.1 LITERATURE SURVEY

Modern kinematics had its beginning with Reuleaux. Reuleaux believed that a mechanism could be seen as a kinematic chain of connected links, one of which is fixed. Moreover, he introduced symbolic notation to describe kinematic chains in 1876. Burmester was in agreement with the fundamental concepts, nomenclature and definitions that Reuleaux was using. By applying mathematical principles and taking displacement, velocity and acceleration into account, Burmester showed the way to synthesis [7]. Three different methods for generating Burmester center-point and circle-point curves representing the total locus of solutions to synthesize a mechanism guiding a body through four finite positions have gained significant popularity. The first one is the graphical procedure, the second one is the algebraic formulation and the third one is solving a set of loop displacement equations [8].

In the beginning of the 20th century, the graphical methods of synthesizing planar mechanisms have been studied. By using the overlay method, the graphical synthesis techniques for two, three and four positions for motion, path and function generators are given by Harrisberger [9].

Freudenstein, Father of Modern Kinematics, used a simple algebraic method to designate the displacement equations for three precision point function generation. This method determines the position of the output link in a linkage mechanism. Freudenstein's technique can be extended to four and five precision points [10]. Freudenstein and Sandor [11, 12], the first Ph. D. student of Freudenstein, adapted the graphical-based techniques presented by Burmester [13] to the computer for linkage synthesis and rearranged these techniques for the computer solution.

Starting from the first one, Freudenstein's publications can be indicated as a reference.
Sandor introduced the general closed form method of planar kinematic synthesis. Complex numbers are used to illustrate link vectors. Sandor and Erdman [14] applied the closed form solution to the synthesis of a geared five-bar linkage for function generation. A method is demonstrated for three first-order and three second-order totally six precision conditions. Furthermore, Erdman, with Sandor introduced dyadic approach with which the motion generation, path generation with prescribed timing, and function generation can be performed [10]. Moreover, Sandor and Erdman [15] introduced the concept of the "compatibility linkage", which is the equation of closure of a four-bar linkage involving one fixed, three movable links and three angles measured from the starting position of the compatibility linkage. It is shown that the center-point curve can be parameterized based on the crank angle of the compatibility linkage.

Chase et al. [8] observed that the motion type of the compatibility linkage affects the shape of the center-point curve. They showed that a Grashof compatibility linkage generates a dis-joined center-point curve, while a non-Grashof compatibility linkage generates a continuous center-point curve.

McCarthy [16] showed that the opposite pole quadrilateral serves as a compatibility linkage. Moreover, to parameterize the center-point curve, it uses the crank angle. Two-dimensional set of quadrilaterals being able to generate a given center-point curve is stated by Murray and McCarthy [17].

Murray and Myszka [18] introduced a procedure to identify four finitely separated positions forming different shapes of the opposite pole quadrilateral. The poles in specific shapes, like open and closed forms of a rhombus, kite, parallelogram, can be arranged by this study.

The angular unknowns are considered as candidate for parameters on which the locations of the fixed and moving pivots of the solution dyads will depend. Loerch [19] discovered that, for three precision conditions, if an arbitrary value is selected for one nonprescribed angular parameter while the other angular parameter is allowed

to assume all possible values, the fixed pivots m and the moving pivots k_1 of all possible dyads must lie on respective circular loci. Graphical methods based on this theory give rise to a new, kinematic derivation of the geometric construction of Burmester's center-point and circle-point curves for four prescribed positions.

Kramer and Rigelman [20] worked on the optimization method for synthesizing planar four-bar mechanisms satisfying specified kinematic and dynamic conditions. This method can be used for path, motion and function generation or a combination of these. To express the kinematic conditions in terms of a specification plus an allowable deviation from the specification, Selective Precision Synthesis (SPS), is used. By using Generalized Reduced Gradient (GRG) method, the nonlinear optimization problem is solved. The order and branch problems are the common problems when analytical methods are used for synthesizing mechanisms. It means that the four-bar mechanisms are either not able to move continuously between the prescribed positions although mountable in those prescribed positions or the movement is continuous but the sequence is wrong. These problems were studied by Filemon [21] and he constituted the basis of the theory.

Chen and Fu [22] present a computational method to locate the regions of the Burmester center-point curve which gives the driving cranks of crank-rocker or drag-link linkages when combined with a given driven link. The order and branch problems are avoided with this simple and rapid numerical method.

Lee et al. [23] investigated the relationship between the sensitivity to variations of link lengths and the location of the moving pivots of four-link mechanisms for three and four position synthesis.

Kinematic synthesis software for design of planar mechanisms has developed at a slower rate than analysis software, which was committed on 1951 [24]. However, the first mechanism synthesis package to use interactive graphics, KINSYN, was developed by Kaufman in the late 1960's [25]. KINSYN I should be recognized as a milestone in kinematic design. By the mid 1970's, several software packages for synthesis and analysis became available like RECSYN, LINCAGES, etc. The first version of today's one of the most important mechanism synthesis packages, LINCAGES

introduced by Erdman [26] in 1977. LINCAGES 4 is used for four-bar and LINCAGES 6 is used for six-bar mechanisms. Three and four finitely separated positions for path, motion and function generation can be synthesized. Sufficient information for LINCAGES can be obtained from [27].

In Alankuş's thesis [28], a method has been developed to design planar mechanisms to guide a rigid body through the given finitely and/or infinitesimally separated positions, and POSSYN, Position Synthesis Program, has been prepared for the automation of the method. A synthesis program, MECSYN (MEChanism SYNthesis) is developed by Polat [29] for synthesizing four-link mechanisms to move a moving plane through three or four finitely and/or infinitesimally separated positions. A visual, interactive computer program named Quad-link is developed by Sezen [30] to carry out the synthesis and analysis of planar four-bar mechanisms. In synthesis, the dyadic approach and in analysis Freudenstein's equation is used as the main solver. So, the instant motion characteristics and kinematic entities can be found. There are 9 test cases in the thesis. In one of them, a skid-steer loader, which goes up on a vertical line, is designed. Demir [31] developed a program named CADSYN (Computer Aided Design SYNthesis) making synthesis and analysis of planar four-bar mechanisms very similar to Sezen [30]. One of the test cases of the synthesis in Sezen's thesis can be seen in Figure 2-1.

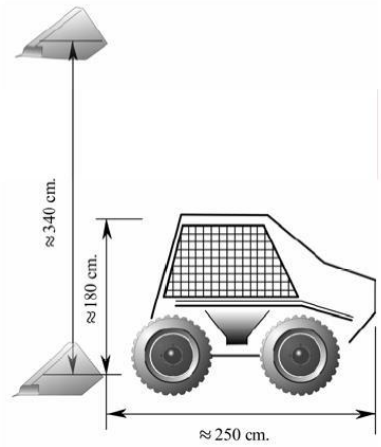

Figure 2-1 – Desired maximum height to reach for a schematic skid-steer loader [30]

Holte [32] states that a little change in positions may change the solution curve entirely. Mlinar [33] was curious about the rate of change of solution curves with a change of the input positions. Mlinar and Holte worked on a sensitivity analysis and found that the solution curves may change drastically by making a minor change in the inputs.

In the thesis prepared by Duran [34] a new mechanism design for opening hatchback-car baggage door is introduced. In this design the door is opened vertically and thus occupies less space behind the car during the opening. With the help of Burmester theory, motion generation is applied. Four positions of the new designed hatchback-car baggage door can be seen in Figure 2-2.

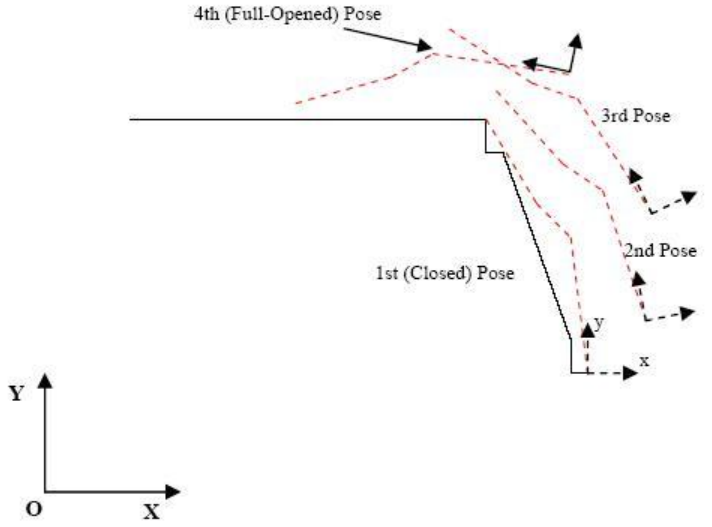

Figure 2-2 – 4 prescribed positions of the new designed hatchback-car baggage door [34]

Drawing Burmester curves, namely center-point and circle-point curves can be achieved by a simple set of equations in Microsoft Excel. The difficult part is to select the points that the crank and rocker are fixed, the lengths of the links, to determine the forces on links when the bucket is loaded and to designate the change in the coupler angle from its lowest position to its highest position. The optimization of the properties listed above can be achieved by various approaches.

The book that initiated the genetic algorithm was written in 1975 by Holland [35]. The practical benefit of genetic algorithm cannot be understood up to another book written in 1989 by Goldberg [36], a Ph. D. student of Holland. With this book, Goldberg showed with 83 applications that the range of usage of genetic algorithm is very large. Suganthan [37] presented a genetic algorithm based optimization procedure to solve a structural pattern recognition problem in 1999. The population was selected randomly and integer strings represented the candidate solutions. Silhoutte images and line patterns are used for sub graph isomorphism to pattern recognition. Jakiela et al. [38] derived an important advantage of genetic algorithm, that is, genetic algorithms being applied to problems for which little is known about the nature of the design domain, because genetic algorithms only require zeroth order functions.

Hasançebi and Erbatur [39] presented two new crossover techniques, with which a better efficiency of genetic algorithms can be obtained. In genetic algorithms, constraints are mostly handled by using the concept of penalty functions, which penalize infeasible solutions by reducing their fitness values. Generally, constant coefficients, specified at the beginning of the problem, are employed by penalty schemes throughout the entire calculation. To prevent having a too weak or too strong penalty during different phases of the evaluation, a new penalty scheme being able to adjust itself during the evaluation is developed by Nanakorn and Meesomklin [40].

When disadvantages and advantages are considered, İpek [41] claimed that heuristic methods are more preferable when there are too many parameters and constraints exist, because they are easy to implement. Among the heuristic methods, genetic algorithm, a search method influenced by natural genetics, is selected.

Genetic algorithm develops a population of solutions to a problem by its genetic operators and then assigns a fitness value to each individual. Better solutions in the population are combined with each other to have individuals having higher fitness values. İpek [41] studied to develop a computer program to optimize the loader mechanism in backhoe-loaders. Finally, among the four runs the best one achieved 13.7% increase in arm breakout force, 6.8% increase in bucket breakout force and 2.7% increase in lifting capacity at the same time still achieving the required dumping height and digging depth constraints. The loader mechanism before the optimization and after the optimization can be seen in Figure 2-3.

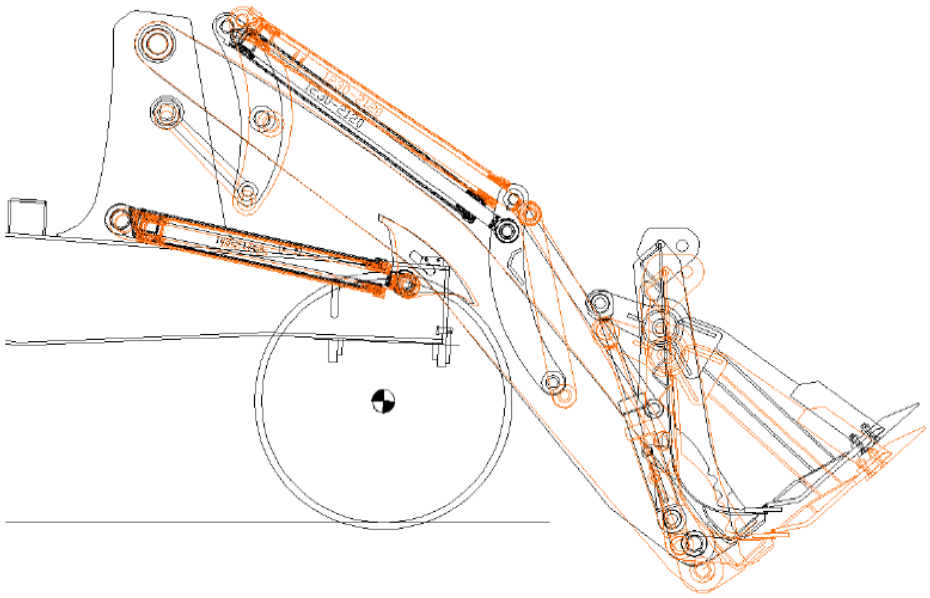

Figure 2-3 – The best optimized loader mechanism [41]

Structural optimization became usable among the engineers because the efficiency and reliability of manufactured goods generally related with the geometry. To seek for a better excavator boom and to select the optimum, Uzer [42] chose genetic algorithm from heuristic search strategies. Uzer mentioned two reasons for selecting

the genetic algorithm. The first reason is that genetic algorithm can be easily applied to many applications because it does not require specific information about the subject. The second reason is that genetic algorithm searches a wide multi-dimensional solution space so it has the capability of finding a solution of local or global maxima's (or minima's). There are some design criteria that should be satisfied some of which are the boom to have a Von Mises stress that will not exceed allowable design stress value and to minimize the weight of the boom to have less fuel consumption and digging cycle time. Finally, boom geometry 4.6% lighter than the initial design was achieved while the design stress criteria are satisfied. The excavator boom before the optimization and after the optimization can be seen in Figure 2-4.

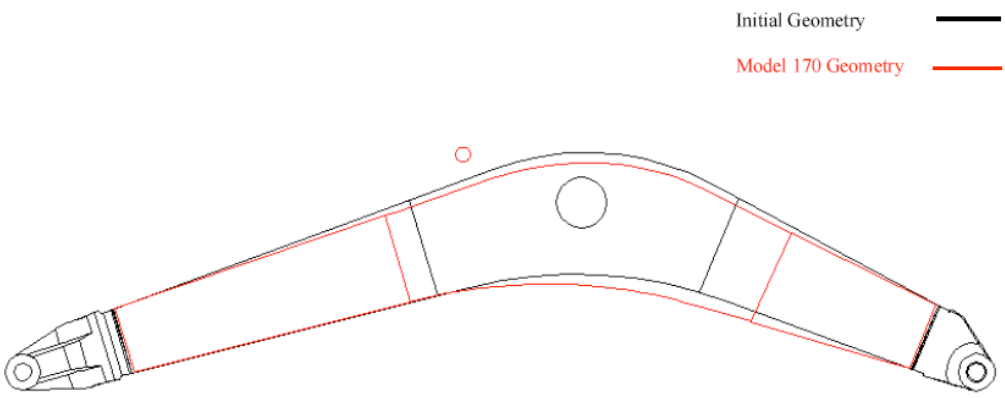

Figure 2-4 – The best optimized excavator boom [42]

In engineering design, optimization became so popular because design engineers mostly concentrate on improving the existing system. The objective for the thesis studied by Özbayramoğlu [43] is to minimize the mass of the lower chassis while the structure still satisfies the required fatigue resistance. When the study was finalized, variables are adjusted to have 4 optimum solutions. Özbayramoğlu designated 4

critical welded regions and compared the advantages and disadvantages of these 4 critical welded regions, which can be seen in Figure 2-5, of all 4 optimum solutions.

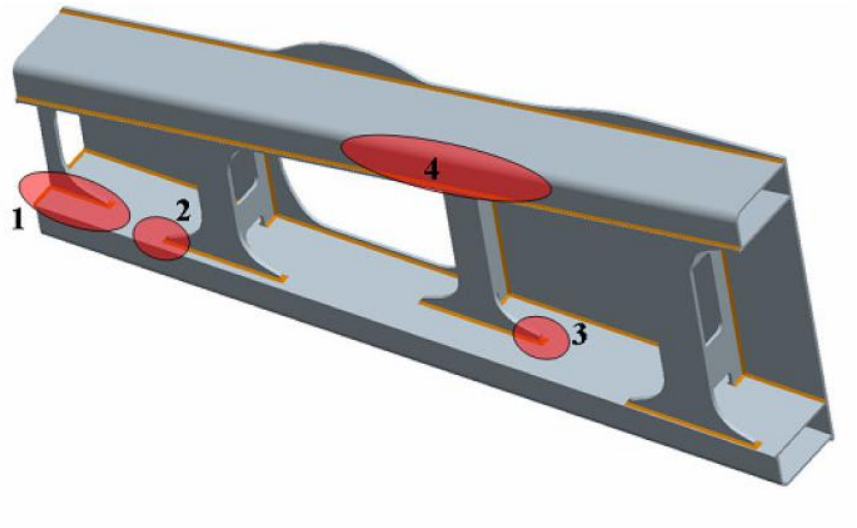

Figure 2-5 – 4 critical welded regions of a lower chassis [43]

Chen [44] developed an optimization code based on genetic algorithm working with the finite element modeling for the shape optimization of plane stress problems. Four 2D example problems were solved and compared with the results presented previously on literature. From the results it can be concluded that the mutation probability was increased to get global optimum instead of local ones. Furthermore, the randomness in the optimization causes uniqueness and also gives a stable result. Moreover, it was concluded that a low crossover probability might not converge as fast as expected and a high crossover probability does not necessarily give the best fitness result. Unfortunately, an absolute solution about crossover probability cannot be achieved. Also, increasing the size of the population creates high probability of convergence because the individuals in the population guide the process.

Çakır [5] developed a design procedure with Visual Fortran including a genetic algorithm for the optimization of the wing structure of a special aircraft. The weight and the stress values of the structure are the most important characteristics of an aircraft for the performance. Çakır selected genetic algorithm as the optimization method due to its robustness and ability to search complex and noisy search spaces. Moreover, Çakır thought finding better solutions instead of trying to search for the exact optimum solution is another advantage for the genetic algorithm. When optimization process was finalized, the weight is reduced to 91% of its initial value and the Von Mises stress in the FE model is reduced to 85% of its preliminary value. Furthermore, stress is more uniformly distributed around the members after the optimization process. The wing structure before and after the optimization can be seen in Figure 2-6.

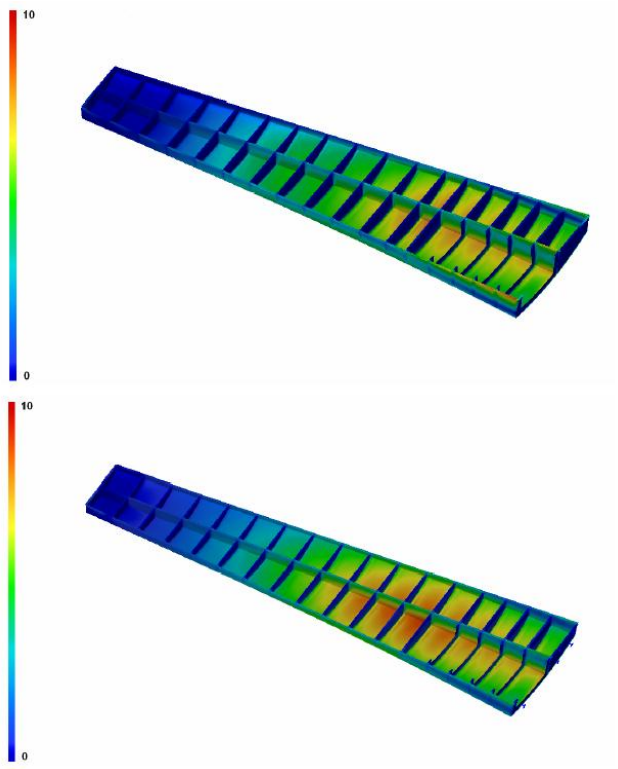

Figure 2-6 – Von Mises stress distribution at a section cutting wing structure in optimized (upper) and in initial (lower) models [5]

2.2 STATE OF ART

Skid-steer loaders are commonly used in daily life. There are two types of loader mechanisms that skid-steer loaders are using. One of them uses a simple inverted-slider crank mechanism and a piston-cylinder rotates the lift arm. The hinge pin, joining the bucket and the lift arm, on a Type I mechanism draws an arc of a circle. The other type uses a four-bar mechanism; again a piston-cylinder drives the four-bar chain. By making a three or four position synthesis the hinge pin can trace any path wanted or can be at those prescribed positions that selected.

In the patent numbered as US 3215292 and named Material Handling Apparatus - Front Lift Type [45], a material load handling apparatus for using on tractor type vehicles is invented in 1965. This invention involves a loader arrangement that enables the end of the arms to rise along a nearly vertical path instead of an arcuate path of the conventional loader. The reasons to design such an apparatus is to reduce the shifting of gravity of the unit forward as the load is raised and to provide a higher lifting height than a conventional pivoting arm loader. The various positions of the bucket during the operation from lowered position to raised and dump positions can be seen in Figure 2-7.

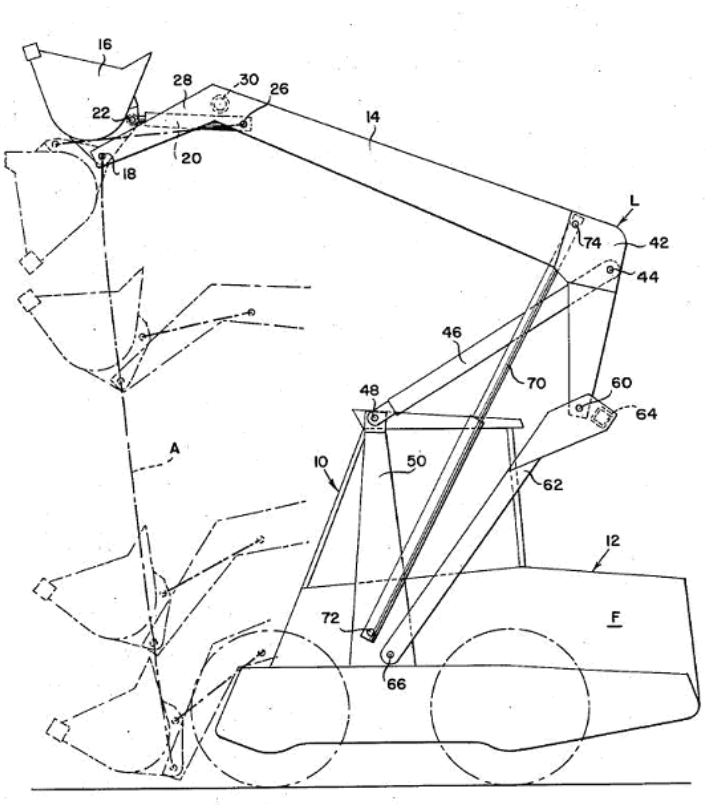

Figure 2-7 – 4 positions of a front-lift tractor [45]

Another example of a Type II mechanism for a skid-steer loader can be seen in United States Patent numbered as US 5542814 and named Method of Lifting a Skid-Steer Loader Bucket [46]. Same company, which made the material load handling apparatus, patented this Type II loader mechanism in 1996. Both of the patents are similar in mechanism-wise but the latter is more particularly for skid-steer loaders. The hinge pivot has a lift path, including a substantially vertical direction from the lowered position to an intermediate position in the lift path, a slightly forwardly inclined direction up to a second intermediate position in the lift path and a substantially vertical direction up to the raised position. The difference of lift paths between a Type I mechanism and a Type II mechanism can be seen in Figure 2-8. On one hand the long dash dot line type shows the lift path of Type I mechanism; on the other hand the continuous line type shows the lift path of Type II mechanism.

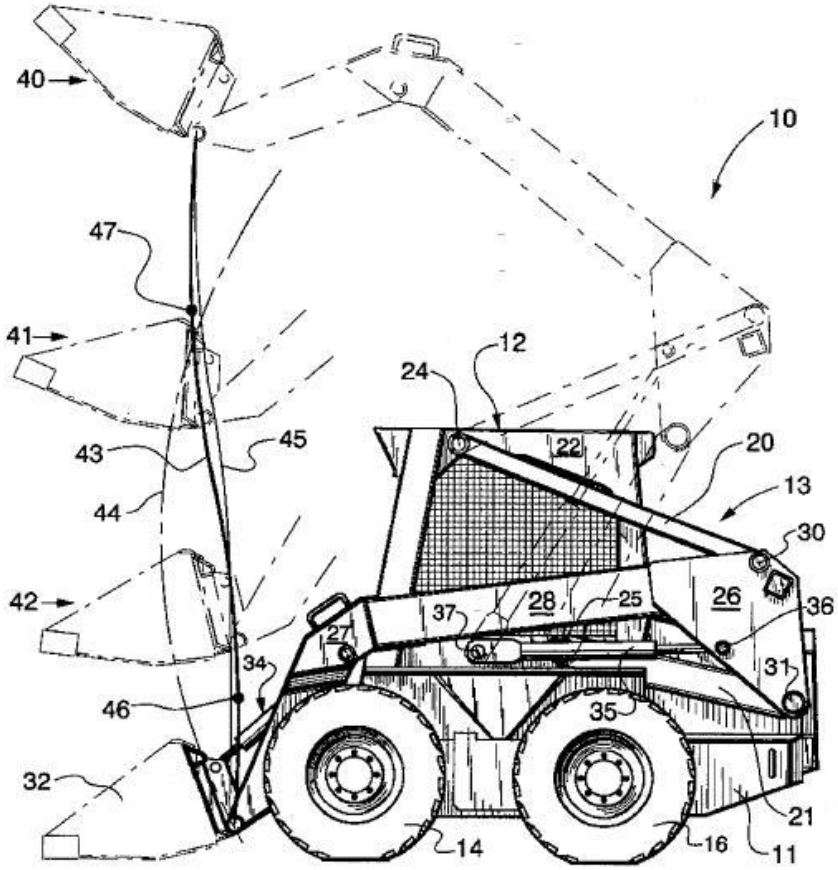

Figure 2-8 – 4 positions of a skid-steer loader [46]

Another example of a Type II loader mechanism for a skid-steer loader can be seen in WO 2004 / 104304 A2 named Folding Lift Arm Assembly for Skid-Steer Loader [47]. The main difference between this patent and the others is the extendable and retractable actuator is pivotally between the first and the second arm link as can be seen in Figure 2-9. The control link guides the end of the second lift arm link in a substantially vertical path as the actuator is retracted and extended which can be seen in Figure 2-10.

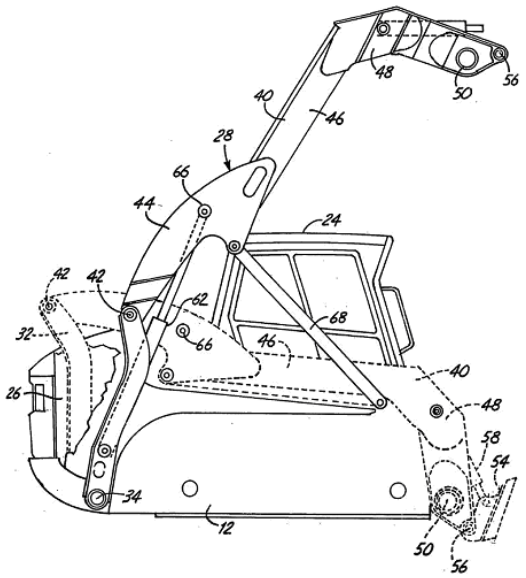

Figure 2-9 – Folding lift arm assembly for skid-steer loader [47]

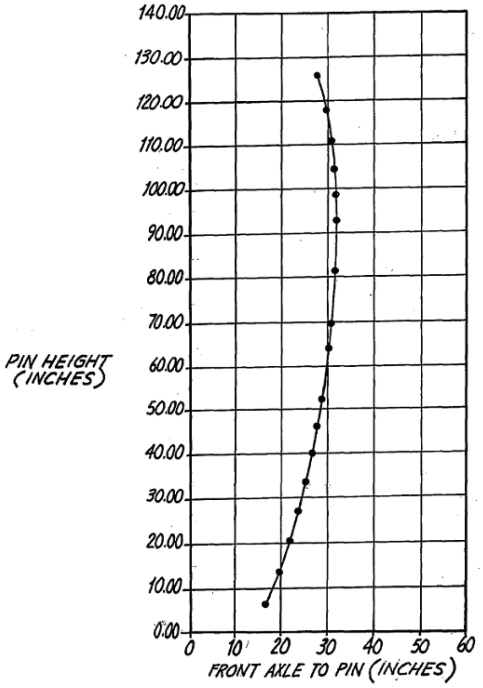

Figure 2-10 – The path of the end of the second lift arm link [47]

In a Canadian Patent numbered as 1166198 and named Lift Arm and Control Linkage Structure for Loader Buckets [48], a skid-steer loader using a Type II mechanism for lifting is introduced. The bucket makes a fairly vertical movement between the lowered and raised positions as can be seen in Figure 2-11. The bucket is never rearward of the line that passes vertically from the tip of the bucket at the lowered position. Moreover, the bucket maintains its position relative to ground by the help of a self-leveling linkage between the lowered position and raised position.

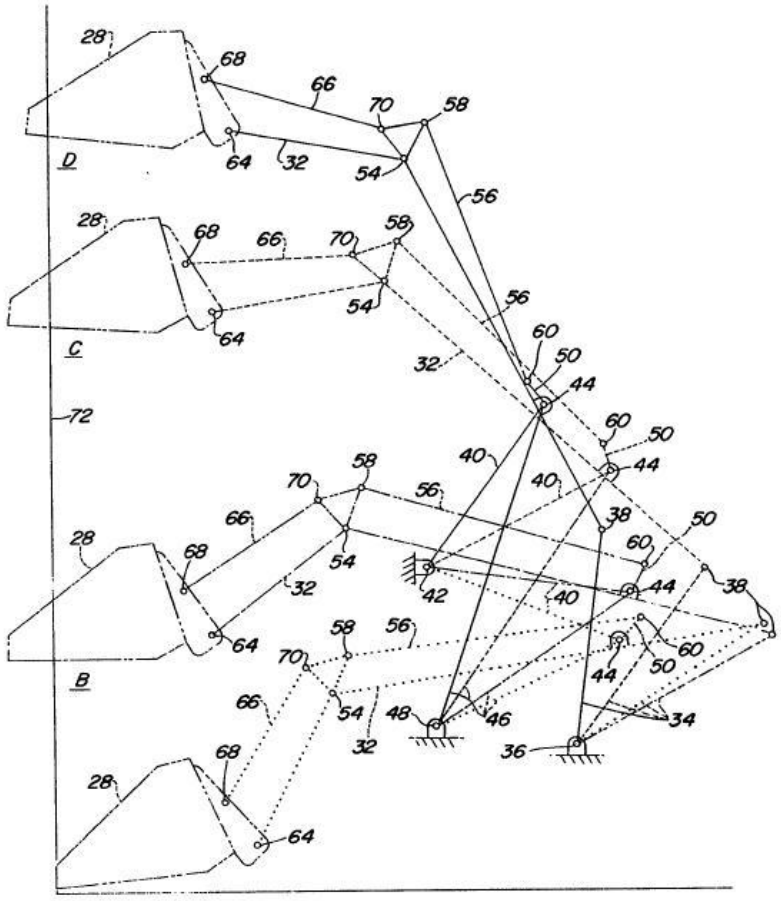

Figure 2-11 – 4 positions of a skid-steer loader mechanism [48]

CHAPTER 3

DESIGN CRITERIA

There are lots of restrictions while designing the loader part of a skid-steer loader as mentioned in the Introduction part. Some restrictions are valid for both four-bar (Type II) and inverted-slider (Type I) mechanism; some restrictions are just for Type II mechanism.

3.1 TARGET HEIGHT

This criterion is valid for both mechanism types. The skid-steer loader portion should satisfy the target height reached when the lift cylinders are fully opened. A benchmark study is conducted before the beginning of the design. 125 models of 18 companies are compared. When the benchmark study is conducted, it is seen that the maximum height the hinge pin reaches changes from 2400 mm to 3600 mm. In this study, maximum height the hinge pin reaches, the illustration of which can be seen in Figure 3-1, is selected between 2900 mm and 3300 mm. The dimensions of the links are generated according to the selected range. Selecting a range is not a loss for the study because scaling all the link dimensions makes the whole system applicable to any target height.

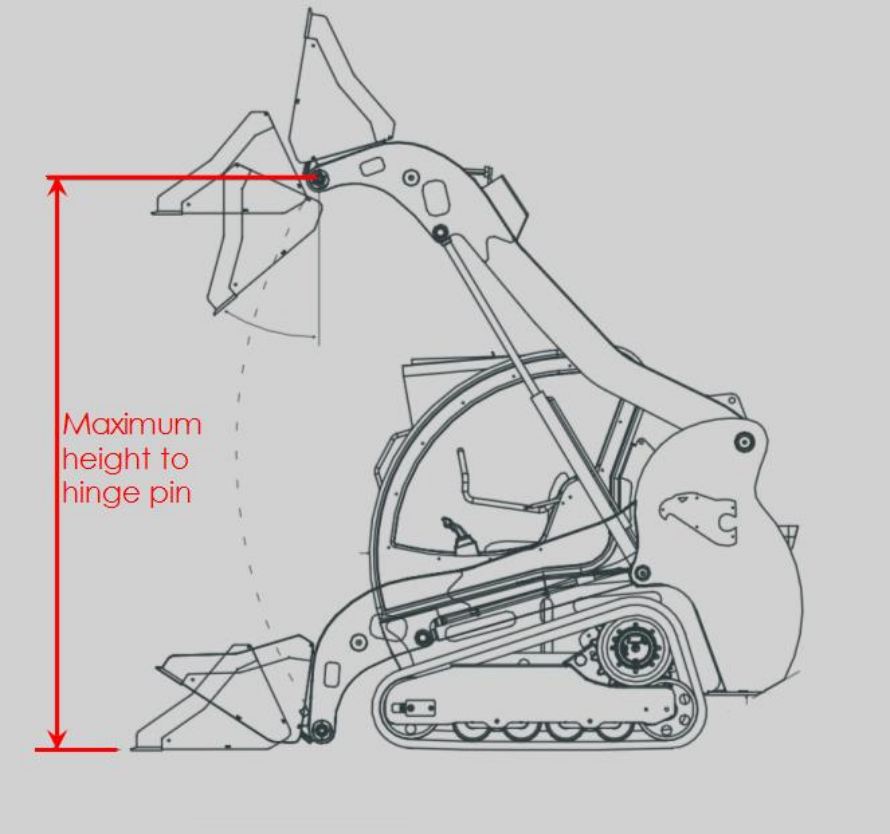

Figure 3-1 – A design criterion - the maximum height to hinge pin [49]

3.2 PATH OF THE HINGE PIN

The path of the hinge pin also plays an important role as a design criterion. This criterion is valid just for a four-bar (Type II) mechanism, because the hinge pin of an inverted-slider (Type I) mechanism is only capable of drawing a circular arc. In a skid-steer loader having Type II mechanism, it is either wanted that the hinge pin on the lift arm should move on a vertical line or the hinge pin can be at a forward position at the highest position of the lift arm. Skid-steers are used for the same reasons as loaders. One of these reasons is that to load the bucket with diggings and then dump it to a truck. That is why, it is better to move the bucket on a vertical line or to bring the bucket to a position that is slightly forward than the front side of the machine. In this mechanism study, instead of controlling the whole path of the hinge

pin, only 4 prescribed positions are controlled. The translation and rotation of moving reference frames relative to a fixed reference frame is controlled. For this Type II mechanism study, the moving reference frames are assumed to be at the first, second, third and fourth prescribed positions which are at the hinge pins of the lift arm, and the fixed reference frame is assumed to be at the hinge pin while the lift cylinders are fully closed with having a x-axis parallel to ground and y-axis perpendicular to ground. The moving reference frames can be seen in Figure 3-2.

Figure 3-2 – A design criterion - the path of the hinge pin [50]

3.3 AVOIDANCE OF SPILLING OVER ANY MATERIAL

This criterion is valid both for Type I and Type II mechanisms. The skid-steer loads the bucket from the ground and brings the bucket to a position, by retracting the tilt cylinders, which the bucket will not spill over any material. The tilt cylinders should be able to be retracted up to a length that satisfies this condition. The angle between the bottom plate of the bucket and the ground is called roll back angle. In other words, the roll back angle should satisfy the condition of not spilling any material when the lift and tilt cylinders are fully retracted. From benchmarking, it can be said that the roll back angle is between 25 degrees and 45 degrees. Furthermore, the bucket should not spill over any material when the bucket is loaded at its highest position. The diggings should not be spilled over neither in front of the machine nor the top of the cabin. Not only at the lowest and highest position of the bucket, but also the positions in between should also satisfy the not spilling over any material condition. The highest and lowest positions of the mechanism can be seen in Figure 3-3.

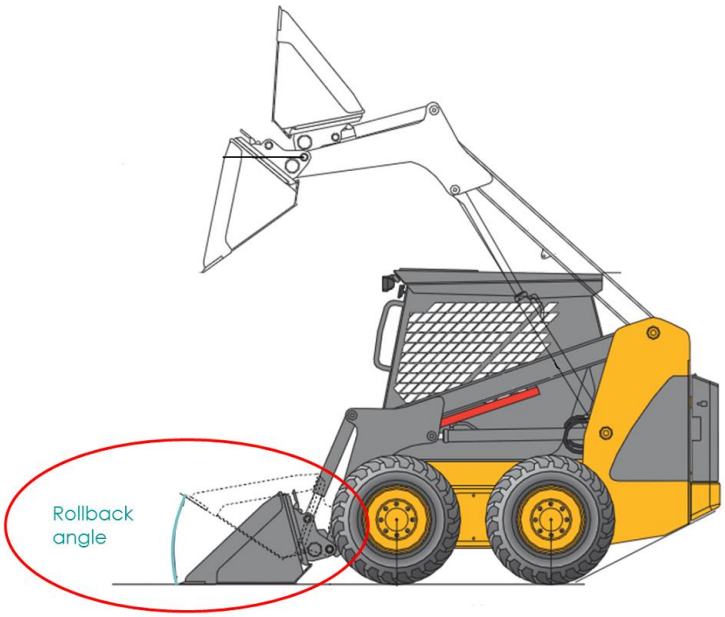

Figure 3-3 – A design criterion - not spilling over any material [51]

3.4 DUMP ANGLE

This criterion is also valid for both mechanisms. At the highest position, when the tilt cylinders are fully extended the bucket should dump all the diggings. The angle between the bottom plate of the bucket and the horizontal line drawn from the hinge pin is called dump angle and can be seen in Figure 3-4. According to the benchmark, the dump angle changes between from 30 degrees to 50 degrees.

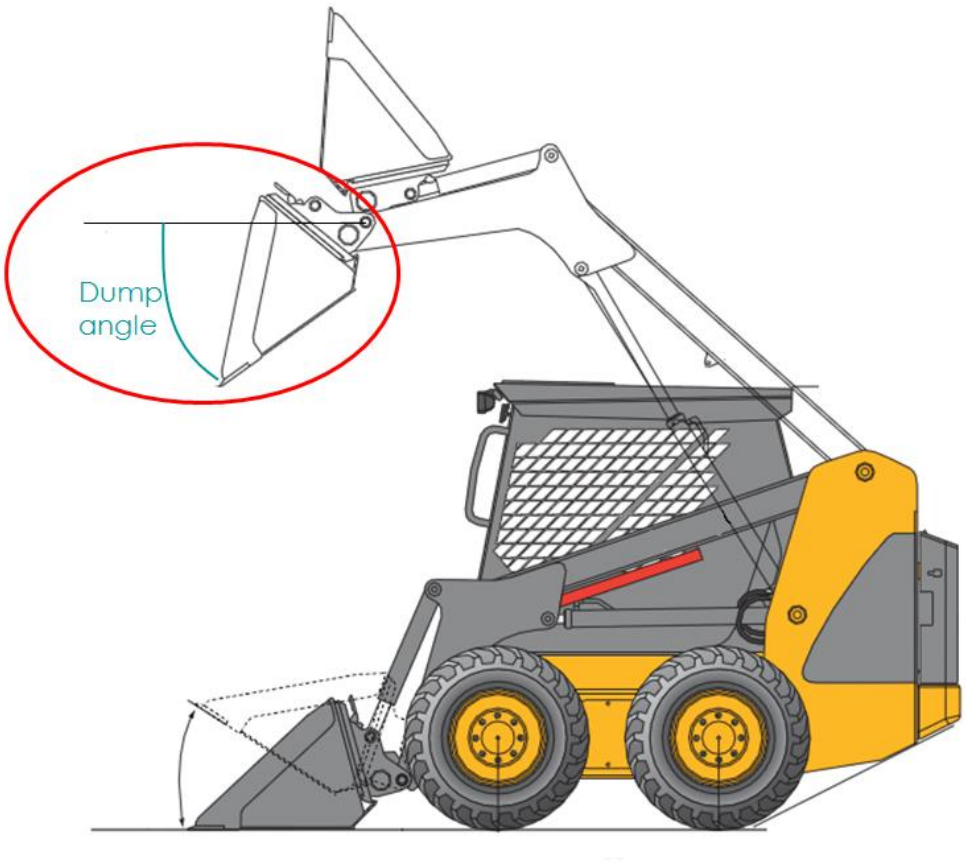

Figure 3-4 – A design criterion - dump angle [51]

3.5 THE POSITION OF CONNECTING RODS

In a Type I loader mechanism, this condition is satisfied naturally; because the lift arm is directly mounted to the back of the upper frame without having any connecting rods. However, in a Type II mechanism the position of the connecting rods is also a design criterion. The connecting rods should not pass beyond the back of the machine as much as possible. Because skid-steers are used especially in confined places so the links being inside the machine is a demand. An acceptable example for the position of the connecting rods can be seen in Figure 3-5.

Figure 3-5 – A design criterion - the position of the connecting rods [52]

3.6 DIGGING DEPTH

This criterion is again for both of the mechanisms. The bottom plate of the bucket should be able to go under the ground at the lowest position and when that plate is parallel to ground. One of the reasons for the buckets' bottom sheet to be able to go under the ground is leveling. Another reason is due to uneven ground shape, especially on an inclined surface, the bucket must be lowered below the ground level defined by the position of the tires to reach the ground. The parallel position of the bucket to the ground can be seen in Figure 3-6.

Figure 3-6 – A design criterion - Digging depth [53]

CHAPTER 4

SYNTHESIS

4.1 TYPE SYNTHESIS

The number of the degrees of freedom required, the appropriateness of the mechanism for the desired motion, the number of links needed and the configuration of these links, etc. are some questions that type synthesis should answer.

According to the design criteria, there should be 2 degrees of freedom for the desired motions. In general, one is for the motion of the lift arm and one is for loading or dumping the bucket. Grübler's equation (4.1) is used to determine the number of degrees of freedom of the mechanism.

$$F = \lambda(l - j - 1) + \sum_{i=1}^{j} f_i \tag{4.1}$$

4.1.1 TYPE II (FOUR-BAR) MECHANISM

In equation (4.1), the general degree of freedom of space (λ) is 3 for planar motion, the number of links (l) is 9; 4 of them from four-bar, 4 from lift and tilt cylinders and 1 for bucket, the number of joints (j) is 11; 9 from revolute pair and 2 from prismatic pair, and degree of freedom of i^{th} joint (f_i) is 11. The number of degrees of freedom is found to be 2 and the lift cylinders and tilt cylinders are inputs. The number of links, the revolute pairs in red and prismatic pairs in green can be seen in Figure 4-1.

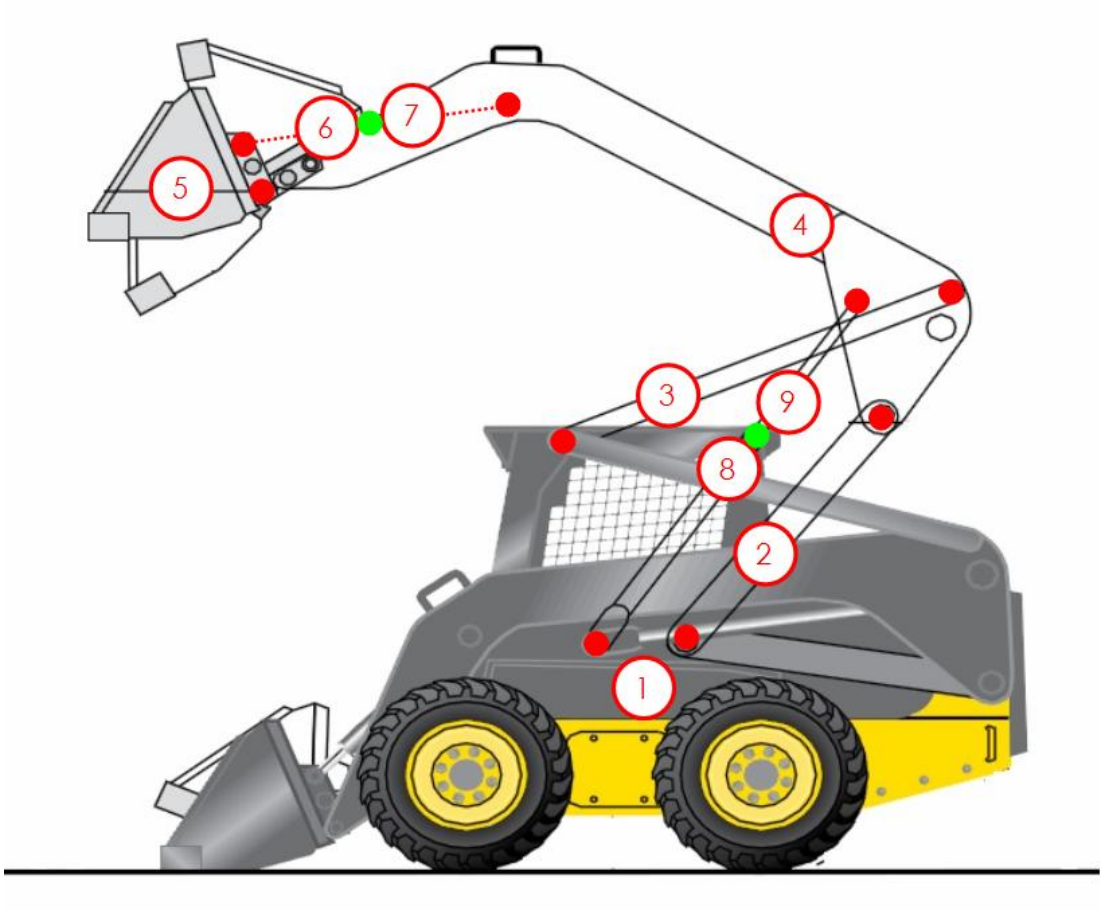

Figure 4-1 – The number of links and joints on a Type II mechanism [6]

4.1.2 TYPE I (INVERTED-SLIDER) MECHANISM

In Type I mechanism case, the number of links (l) is 7; 1 is for the lift arm, 1 is for the frame, 4 from lift and tilt cylinders and 1 for bucket, the number of joints (j) is 8; 6 from revolute pair and 2 from prismatic pair, and degree of freedom of i^{th} joint (f_i) is 8. The number of degrees of freedom is again found to be 2 and the lift cylinders and tilt cylinders are inputs. The number of links, the revolute pairs in red and prismatic pairs in green can be seen in Figure 4-2.

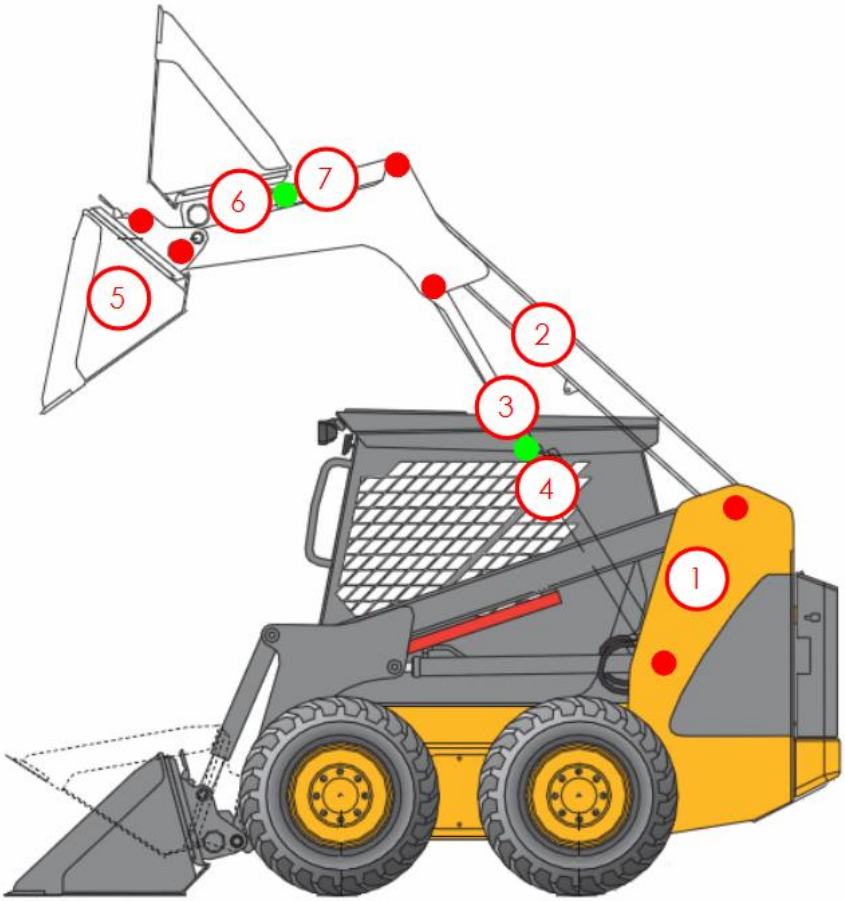

Figure 4-2 – The number of links and joints on a Type I mechanism [51]

4.2 DIMENSIONAL SYNTHESIS

The dimensions and the starting position of the mechanism of predetermined type for a specified task and prearranged performance are the subjects of dimensional synthesis. In this study, the predetermined type of mechanism is either a four-bar (Type II) or an inverted-slider (Type I) mechanism. The pivot-to-pivot distances on binary and ternary links or the constant angles to define ternary links are the dimensions that should be found. Moreover, the starting position can be specified by the angular position of an input link with respect to the fixed reference frame, or in this case by the length of the cylinders.

4.2.1 OPTIMIZATION SYNTHESIS

Optimization synthesis searches for a solution with the least error between the desired output and the realized output. By changing the values of the variables within a determined region, a function is tried to be minimized or maximized. Heuristic algorithms are used widely nowadays, because of the difficulty of setting an exact optimization algorithm for complicated problems including high number of design parameters. Genetic algorithm is selected among the heuristic algorithms because of not requiring special information about the subject and the capacity of searching wide complex multi-dimensional area.

4.2.1.1 TERMINOLOGY OF GENETIC ALGORITHM

Genetic algorithms have a terminology inspired by natural genetics [33].

Population: A population, may also be called as generation, is a collection of individuals that can be on anywhere of the search space.

String: A string is an individual in a population which is a possible solution to the given problem. Parameters of the design are listed in a string.

Gene: Each parameter in a string is called a gene, which can be either real or binary numbers.

Fitness: Fitness is a measure of goodness of a string in the population. Higher fitness value means that string satisfies the required outputs more accurately.

4.2.1.2 BASIC GENETIC ALGORTIHM

As a first step, an initial population is created from many strings. Generally, at the beginning of the optimization, the first population is generated randomly. According to the type of the problem, the population size varies in a wide range. An evaluation

function is used to evaluate each string and to assign a fitness value to each of the possible solutions. Individuals are selected according to their fitness values to reproduce the next generation of individuals. Genetic algorithms rely on the survival of the fittest principle [54]. Therefore, an individual having higher fitness value has a greater chance to be selected for the reproduction. A better position in the search space is reached with this operation. The next population is generated by applying crossover and mutation on selected solutions. The process of generating new populations continues up to achieve the termination condition by evaluating the fitness value of each individual at every new population.

A basic genetic algorithm includes 4 main genetic operators namely, evaluation, selection, crossover and mutation. Moreover, the flowchart of the algorithm can be seen in Figure 4-3.

The parameters used for the evaluation function in a Type II mechanism are more than in a Type I mechanism. However, most of the parameters are either defined as "acceptable" or "not acceptable", so they do not affect the fitness value. If a parameter is not acceptable that string is not a solution anymore, because most of the parameters are a must. To illustrate, the location of the fixed pivot of the four-bar's crank and rocker being inside the possible machine dimensions is a must. In other words, the number of parameters to decide the fitness values is similar in a four-bar (Type II) mechanism and in an inverted-slider (Type I) mechanism.

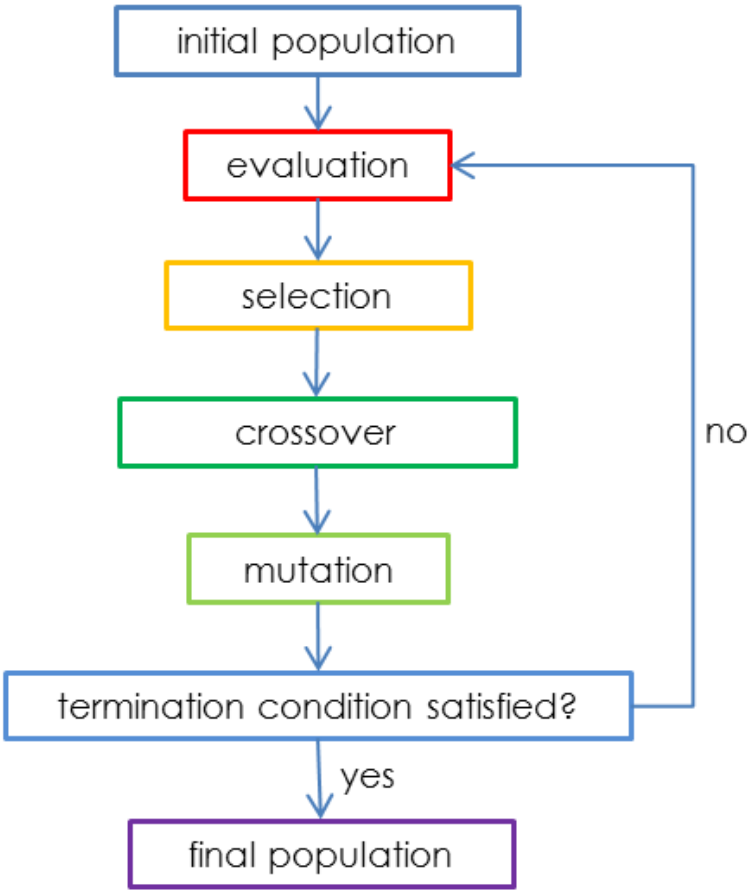

Figure 4-3 – Flow chart of a basic Genetic Algorithm

Evaluation: Each string in the population is evaluated by the fitness function and given a fitness value at this stage. By assigning fitness value to an individual makes the listing possible from weakest to strongest. This stage is the only stage that genetic algorithm uses information about the problem itself.

Selection: Some of the individuals in the population are selected according to their fitness values at this stage. As expected, stronger individuals have more chance to be selected. There are many different methods for selecting individuals in the population. After selection an intermediate population is formed with selected individuals.

Crossover: Next population is generated by coupling the individuals in the intermediate population. At first, the strings in the intermediate population are coupled randomly with each other, called as parents, and then two new strings, called as children, are formed from crossover. Crossover operation differs according to the type of the representation method of strings. It is explained that the format of the strings can be either binary or real. If binary representation is used, crossover is done by exchanging the genes randomly selected or specified sections of the string. On the other hand, a weighted mean function is used to calculate the value of the new gene if real representation is used. In this study, real representation is used.

Mutation: Sometimes, genetic algorithm converges to a local optimum. To avoid the convergence and to keep the variety in the population mutation is applied on some randomly selected strings. There is a parameter which defines the ratio of mutation. Not only the ratio of mutation but also the strategy should be decided rigorously.

4.2.2 PRESCRIBED POSITION SYNTHESIS

In this type of synthesis, the mechanism should pass from those prescribed positions. However, the synthesis does not declare anything about the motion between these prescribed positions. Loop closure equations should be written to find the variables of the mechanism. The number of equations that should be written for the corresponding number of prescribed positions can be seen from the Table 4-1. Up to 4 prescribed position synthesis the solution is infinite. The Burmester theory is very sensitive to small changes, so the designer should be aware of this property while selecting the prescribed positions.

4.2.2.1 THE DYAD FORMULATION

The mechanism that will be synthesized can be thought as combinations of vector pairs called dyads, each of which carries out the motion independently through the prescribed positions [28]. The dyads can be combined to define the entire mechanism. To illustrate, the four-bar mechanism in Figure 4-4 can be perceived as

two dyad pairs, one of them is $\overrightarrow{W}$ and $\vec{Z}$, and the other one is $\overrightarrow{W*}$ and $\overrightarrow{Z*}$. The point P on the coupler moves from P_1 to P_j defined in an arbitrary complex coordinate system by $\vec{R}_1$ and $\vec{R}_j$. Subscript j defines the difference from the first position to the j[th] position. Besides, all vector rotations are measured positive counter clockwise from the starting position. α_j's are the change of the angle of rotation of the coupler, while β_j's are the change of the angle of rotation of the crank. To find the unknown starting position of the vectors of the dyad, a loop closure equation (4.2) should be derived.

$$\overrightarrow{W}e^{i\beta_j} + \vec{Z}e^{i\alpha_j} - \vec{R}_j + \vec{R}_1 - \vec{Z} - \overrightarrow{W} = 0 \quad \text{where j=2,3,...} \tag{4.2}$$

or

$$\overrightarrow{W}(e^{i\beta_j} - 1) + \vec{Z}(e^{i\alpha_j} - 1) = \vec{\delta}_j \quad \text{where j=2,3,...} \tag{4.3}$$

This loop closure equation is easily written by combining the dyads at the 1[st] and j[th] position and the vectors coming from the arbitrary complex coordinate system.

Instead of $\overrightarrow{W}, \vec{R}$ is used since using the center-point (fixed pivot) coordinate vector has a better physical meaning. Moreover, $-\vec{Z}$ is used for the circle-point (moving pivot) coordinate vector. By substituting (4.4) to (4.3) the equation becomes (4.5).

$$\vec{R} = -\vec{Z} - \overrightarrow{W} \tag{4.4}$$

$$\vec{R}(1 - e^{i\beta_j}) + \vec{Z}(e^{i\alpha_j} - e^{i\beta_j}) = \vec{\delta}_j \quad \text{where j=2,3...} \tag{4.5}$$

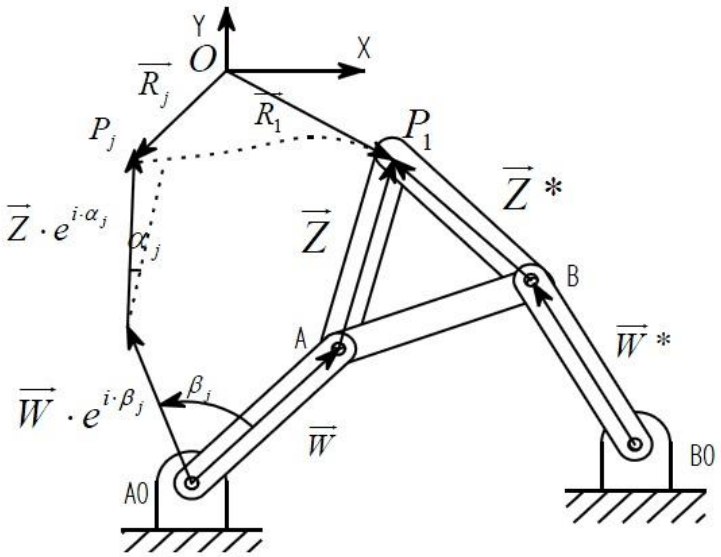

Figure 4-4 – Dyads generating a four-bar [34]

The maximum number of solutions for the unknown dyads $\overrightarrow{W}$ and $\vec{Z}$ when $\vec{\delta}_j$ and α_j are prescribed in the equation (4.3) can be seen in Table 4-1.

Table 4-1 – The relationship between the number of positions and the number of solutions

NUMBER OF POSITIONS j=2,3,..,n	NUMBER OF SCALAR EQUATIONS	NUMBER OF SCALAR UNKNOWNS	NUMBER OF FREE CHOICES	NUMBER OF SOLUTIONS
2	2	5 ($\overrightarrow{W}$, $\vec{Z}$, β_2)	3	∞^3
3	4	6 (above + β_3)	2	∞^2
4	6	7 (above + β_4)	1	∞
5	8	8 (above + β_5)	0	finite

4.2.2.2 SYNTHESIS OF A FOUR-BAR MOTION GENERATOR FOR FOUR PRECISION POINTS

The equations for four prescribed positions of the moving plane can be written by substituting j = 2, 3 and 4 in (4.3). From Table 4-1, it can be seen that 6 equations should be written for four prescribed position synthesis. (4.6), (4.7) and (4.8) are complex equations, one real and one imaginary part exists for any complex equation, therefore the equation number of 6 is satisfied. The parameters in the equation can be seen in Figure 4-5.

$$\vec{W}(e^{i\beta_2} - 1) + \vec{Z}(e^{i\alpha_2} - 1) = \vec{\delta}_2 \tag{4.6}$$

$$\vec{W}(e^{i\beta_3} - 1) + \vec{Z}(e^{i\alpha_3} - 1) = \vec{\delta}_3 \tag{4.7}$$

$$\vec{W}(e^{i\beta_4} - 1) + \vec{Z}(e^{i\alpha_4} - 1) = \vec{\delta}_4 \tag{4.8}$$

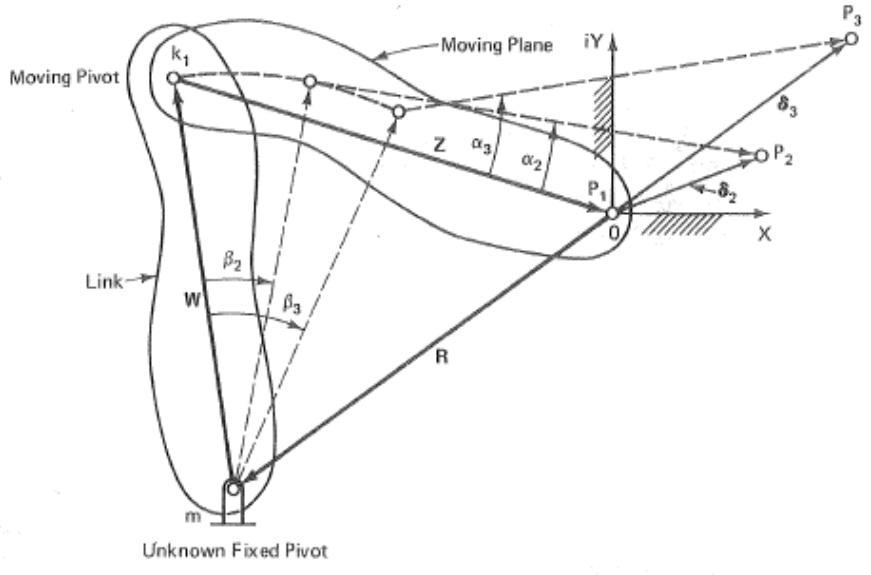

Figure 4-5 – The parameters for the loop closure equations [15]

4.2.2.3 SOLUTION PROCEDURE FOR FOUR PRECISION POINTS

In order for this set of equations to have simultaneous solution for $\vec{Z}$ and $\overrightarrow{W}$, one of the equations from (4.6), (4.7) and (4.8) should be linearly dependent to the other, assuming these set of equations are linear and non-homogeneous. The equation set (4.6), (4.7) and (4.8) can be written in matrix form as (4.9).

$$\begin{vmatrix} e^{i\beta_2}-1 & e^{i\alpha_2}-1 \\ e^{i\beta_3}-1 & e^{i\alpha_3}-1 \\ e^{i\beta_4}-1 & e^{i\alpha_4}-1 \end{vmatrix} \begin{vmatrix} \overrightarrow{W} \\ \vec{Z} \end{vmatrix} = \begin{vmatrix} \vec{\delta}_2 \\ \vec{\delta}_3 \\ \vec{\delta}_4 \end{vmatrix} \tag{4.9}$$

β_2, β_3, β_4, $\vec{Z}$ and $\overrightarrow{W}$ are unknowns ; $\vec{\delta}_2$, $\vec{\delta}_3$, $\vec{\delta}_4$, α_2, α_3 and α_4 are inputs for the matrix. In four precision position synthesis, there exists only one free choice, so one of the β_j's will be a free choice. The system is not in agreement if the rank of the augmented matrix is greater than the rank of the coefficient matrix; on the other hand, it must have at least one solution if the ranks are same. Coefficient matrix is the matrix that is at the left side of the equation (4.9). Augmented matrix, which can be seen in (4.10), is a matrix obtained by combining the columns of two matrices, and in this case combining the coefficient matrix and the result matrix. A matrix has rank r if determinant of [(r+1) x (r+1)] and higher orders are zero; on the other hand [r x r] order is nonzero. So, equation (4.10) should be satisfied to have at least a solution.

$$\left|\begin{array}{cc:c} e^{i\beta_2}-1 & e^{i\alpha_2}-1 & \vec{\delta}_2 \\ e^{i\beta_3}-1 & e^{i\alpha_3}-1 & \vec{\delta}_3 \\ e^{i\beta_4}-1 & e^{i\alpha_4}-1 & \vec{\delta}_4 \end{array}\right| = 0 \tag{4.10}$$

It can be easily seen that the solution of (4.10) is (4.11) by substituting (4.12), (4.13), (4.14) and (4.15) into (4.11).

$$\Delta_2 e^{i\beta_2} + \Delta_3 e^{i\beta_3} + \Delta_4 e^{i\beta_4} + \Delta_1 = 0 \tag{4.11}$$

$$\Delta_1 = -\Delta_2 - \Delta_3 - \Delta_4 \tag{4.12}$$

$$\Delta_2 = \begin{vmatrix} e^{i\alpha_3} - 1 & \vec{\delta}_3 \\ e^{i\alpha_4} - 1 & \vec{\delta}_4 \end{vmatrix} \tag{4.13}$$

$$\Delta_3 = -\begin{vmatrix} e^{i\alpha_2} - 1 & \vec{\delta}_2 \\ e^{i\alpha_4} - 1 & \vec{\delta}_4 \end{vmatrix} \tag{4.14}$$

$$\Delta_4 = \begin{vmatrix} e^{i\alpha_2} - 1 & \vec{\delta}_2 \\ e^{i\alpha_3} - 1 & \vec{\delta}_3 \end{vmatrix} \tag{4.15}$$

The magnitudes and angles of all Δ_j 's are found and if they are expressed as (4.16) and (4.17) the equation will look like a four-bar mechanism loop closure equation. The parameters of a four-bar in (4.23) can be seen in Figure 4-6. Δ_j can be called fixed link if j = 1 and can be called movable links if j = 2, 3 and 4. β_j 's are the link rotations measured from the starting position of the compatibility linkage defined in (4.12).

$\Delta_j = a_j e^{i\gamma_j}$ where i =2 and 3 (4.16)

$\Delta_j = -a_j e^{i\gamma_j}$ where i =1 and 4 (4.17)

$$a_2 e^{i(\beta_2+\gamma_2)} + a_3 e^{i(\beta_3+\gamma_3)} = a_4 e^{i(\beta_4+\gamma_4)} + a_1 e^{i\gamma_1} \tag{4.18}$$

$$a_2 e^{i(\beta_2+\gamma_2-\gamma_1)} + a_3 e^{i(\beta_3+\gamma_3-\gamma_1)} = a_4 e^{i(\beta_4+\gamma_4-\gamma_1)} + a_1 \tag{4.19}$$

$$\theta_{12} = \beta_2 + \gamma_2 - \gamma_1 \tag{4.20}$$

$$\theta_{13} = \beta_3 + \gamma_3 - \gamma_1 \tag{4.21}$$

$$\theta_{14} = \beta_4 + \gamma_4 - \gamma_1 \tag{4.22}$$

$$a_2 e^{i\theta_{12}} + a_3 e^{i\theta_{13}} = a_4 e^{i\theta_{14}} + a_1 \tag{4.23}$$

One of the equations from (4.6), (4.7) and (4.8) is linearly dependent on one other so with two linearly independent one $\vec{Z}$ and $\vec{W}$ can be solved. (4.6) and (4.7) are selected for this purpose and by applying Cramer's Rule, the solutions for $\vec{Z}$ and $\vec{W}$ can be seen in (4.25) and (4.26).

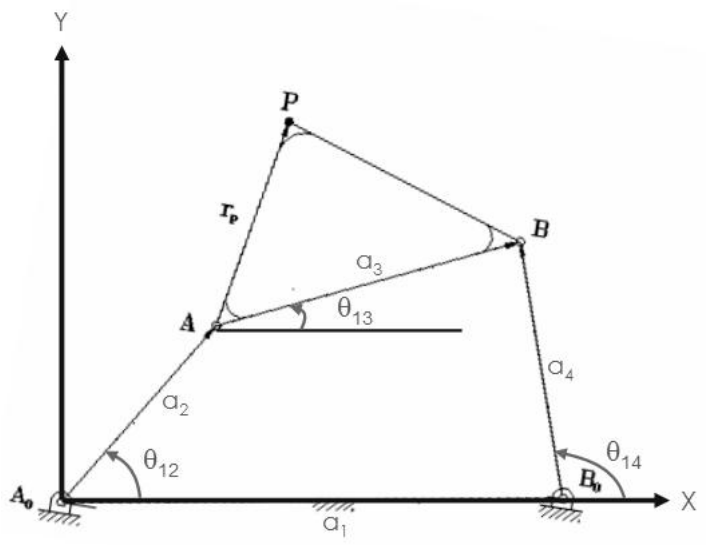

Figure 4-6 – The link dimensions and angles for a four-bar

$$\Delta = \begin{vmatrix} e^{i\beta_2} - 1 & e^{i\alpha_2} - 1 \\ e^{i\beta_3} - 1 & e^{i\alpha_3} - 1 \end{vmatrix} \tag{4.24}$$

$$\vec{W} = \frac{1}{\Delta} \begin{vmatrix} \vec{\delta}_2 & e^{i\alpha_2} - 1 \\ \vec{\delta}_3 & e^{i\alpha_3} - 1 \end{vmatrix} \tag{4.25}$$

$$\vec{Z} = \frac{1}{\Delta}\begin{vmatrix} e^{i\beta_2} - 1 & \vec{\delta}_2 \\ e^{i\beta_3} - 1 & \vec{\delta}_3 \end{vmatrix} \tag{4.26}$$

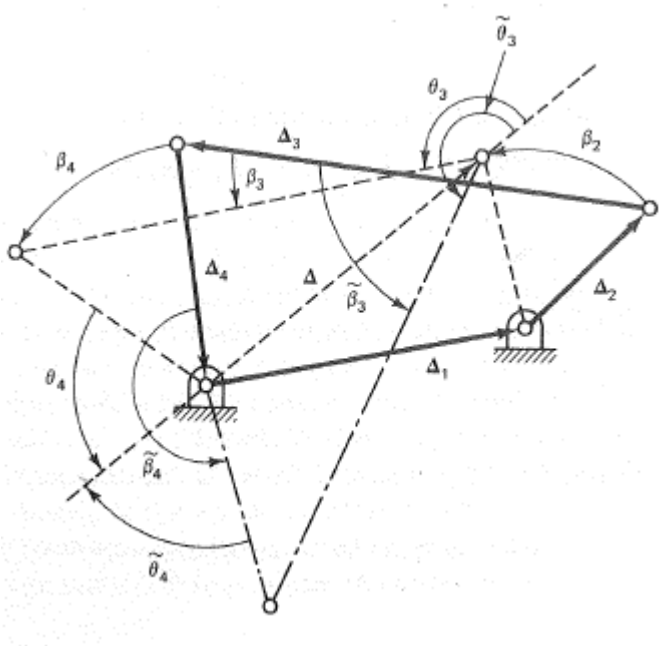

Figure 4-7 – Geometric solution of the compatibility equation [15]

For every position of Δ_2 center-points sweep out two branches: one for β_3 and β_4, one for $\tilde{\beta}_3$ and $\tilde{\beta}_4$. If Δ_2 is able to rotate 360 degrees, these two branches will meet. For each value of β_2, there exist two sets of Burmester point pairs, each consisting of circle-point and a center-point. Every point on a center-point curve is a possibility of a fixed pivot and this fixed pivot can only be connected with its conjugate on circle-point curve. In Figure 4-4, one can see that one half of the four-bar can be constructed having a ground pivot (m), crank $\vec{W}$ pin joint (k_1), coupler link $\vec{Z}$ and terminal point P_1. A four-bar linkage can easily be completed by applying the same procedure explained above two times.

CHAPTER 5

PRACTICALLY USABLE MECHANISMS FOR A FOUR-BAR LINKAGE SYSTEM

The major advantage of using prescribed position synthesis is having infinite number of solutions up to 4 prescribed positions. On the other hand, the main disadvantages can be listed as the convergence of the numerical solution is not guaranteed and the mechanism obtained may not be used practically.

The conditions for a well working skid-steer loader with Type II mechanism will be explained. Satisfying the first three conditions, which will be explained below, is a must. Satisfying the last two conditions is not a necessity but they can be used as elimination items. So after listing all possibilities that satisfies the first three conditions, designer has to select one of the possible solutions by considering the last two conditions.

5.1 BRANCH

The coupler must be moved through all prescribed positions without dismounting or reassembling the linkage system. There are two reasons for branch problem. One of them arises from the configuration of the four-bar mechanism. If at least one prescribed position can be satisfied by a configuration of a four-bar other than the other three prescribed positions' configuration, a branch problem occurs. The other one arises from link dimensions. Burmester claims to satisfy all prescribed positions but he does not mention anything about the motion between these positions. Because of a link's dimension is being short, the mechanism may not be able to pass from one prescribed position to another one even if it satisfies both of the prescribed positions exactly.

5.2 SEQUENCE

The coupler must pass through all prescribed positions in the correct sequence. This condition can be checked by comparing β_j values in Figure 4-5 at every prescribed position. β_j can either increase or decrease continuously while tracing the prescribed positions from 1 to 4.

5.3 CONTINUITY OF CYLINDER STROKE

The cylinder, which moves the coupler through all prescribed positions, must continuously expand through passing the positions in the correct sequence from 1 to 4. The motion of the lift arm will be performed by a piston-cylinder pair, one end of which is connected to the frame and the other end of which is connected to the coupler of the four-bar mechanism. After satisfying first two conditions, while selecting the end positions of the cylinder this criterion is very important and must be checked. If this criterion cannot be satisfied even for a second, for the whole stroke both static and dynamic properties are affected immensely. An example of this effect can be seen from the graph in Figure 5-1.

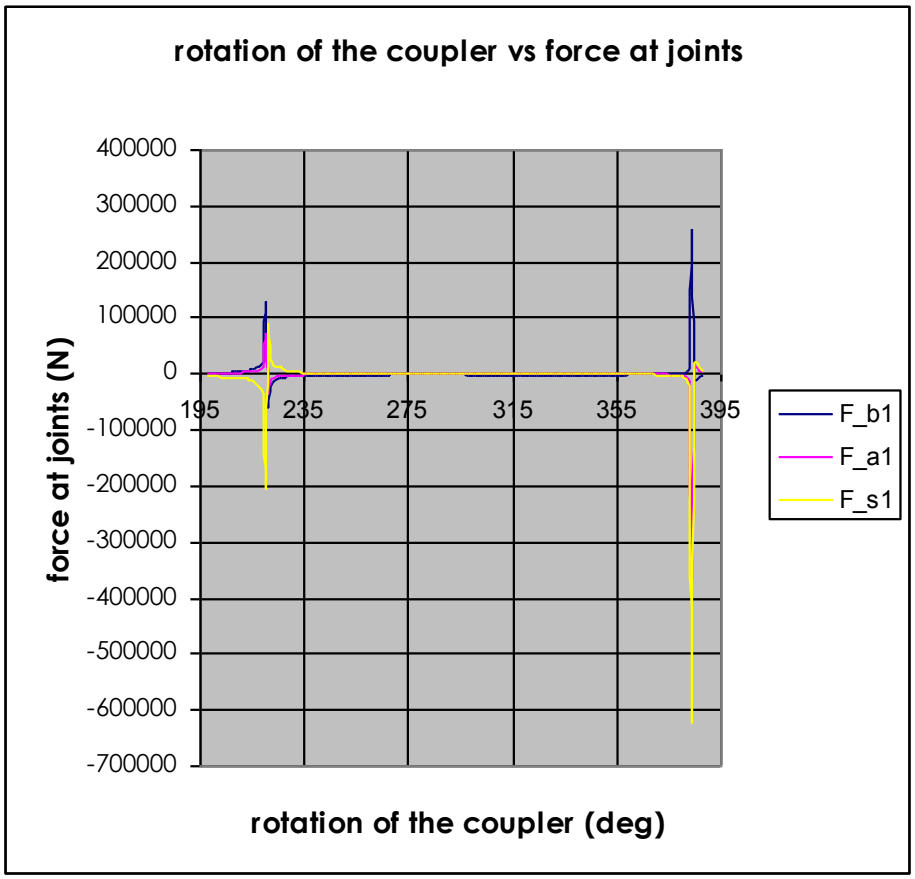

Figure 5-1 – The effect of discontinuity of the cylinder stroke on rotation angle of coupler versus force graph

5.4 LINK LENGTH RATIOS

The link length ratios should be within acceptable limits. The ratio of the longest link to the shortest link is an important criterion for a usable mechanism. The designer desires that ratio to be in a range because if that value is too large, a practical mechanism cannot be constructed.

5.5 STATIC AND DYNAMIC PROPERTIES

Dynamic properties of the mechanism should be within acceptable limits. Both the static and dynamic force distributions on joints throughout the whole stroke of the mechanism are important parameters. If the continuity of the cylinder stroke cannot be satisfied, one can see the effect of this on static forces from Figure 5-1. This is not a dynamic property but it can be an indication to analyze the problem. Besides, the acceleration of the links is another important dynamic parameter.

CHAPTER 6

KINEMATIC ANALYSIS

6.1 TYPE II (FOUR-BAR) MECHANISM

Consider the kinematic chain A_0ABB_0 shown on Figure 6-1. A_0B_0 is the fixed link. The positions of these two fixed pivot points can be found by using Burmester Theorem. $-\vec{R}$ is the coordinate vector showing the center-points, when the configuration of the four-bar is specified.

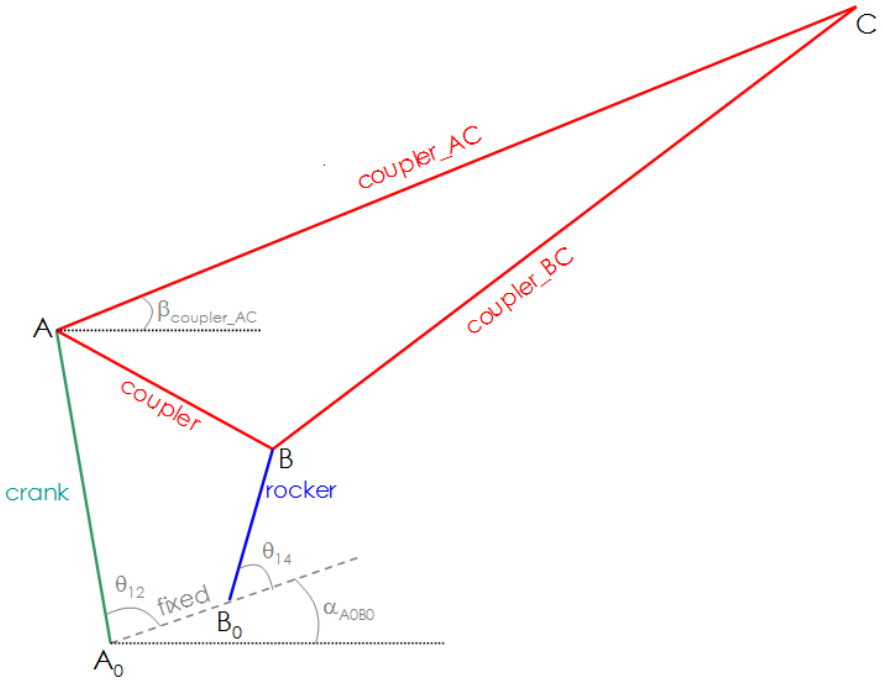

Figure 6-1 – The geometric properties of a lift arm having four-bar mechanism for analysis

The dimensions of the crank, coupler, rocker and fixed links of the four-bar can be found from the dyadic approach. Fixed link dimension can be computed from the difference of the $-\vec{R}$ vectors showing A_0 and B_0. Furthermore, coupler link dimension can be calculated from the difference of the $-\vec{Z}$ vectors, which corresponds to the circle-point of the fixed pivots A_0 and B_0. Moreover, crank and rocker link dimensions can be found from the $\vec{W}$ vectors. All these properties can be computed when the configuration of the four-bar is specified as the position of the fixed pivots.

At the first stages of the design, θ_{12} was the input of the four-bar. A Visual Basic program is used to determine θ_{14} when θ_{12}, the link dimensions and the configuration of the four-bar are specified. Therefore, the positions of the moving pivots A and B can be found when (6.5) is substituted in the equations (6.1), (6.2), (6.3) and (6.4).

$$A_x = A_{0x} + crank \cdot \cos(\theta_{12} + \alpha_{A0B0}) \tag{6.1}$$

$$A_y = A_{0y} + crank \cdot \sin(\theta_{12} + \alpha_{A0B0}) \tag{6.2}$$

$$B_x = B_{0x} + rocker \cdot \cos(\theta_{14} + \alpha_{A0B0}) \tag{6.3}$$

$$B_y = B_{0y} + rocker \cdot \sin(\theta_{14} + \alpha_{A0B0}) \tag{6.4}$$

where

$$\alpha_{A0B0} = a\tan2((B_{0x} - A_{0x});(B_{0y} - A_{0y})) \tag{6.5}$$

The coupler is a ternary link; the second and the third link dimensions of the coupler should be found. The fixed coordinate system of the mechanism is configured at the place of the hinge pin when the lift cylinders are closed. From the positions of the moving pivots A and B, the link dimensions, namely $coupler\_AC$ and

$coupler\_BC$ can be found. Now, also the coordinates of point C can be found when (6.8) is substituted into (6.6) and (6.7).

$$C_x = A_x + coupler\_AC \cdot \cos(\beta_{coupler\_AC}) \tag{6.6}$$

$$C_y = A_y + coupler\_AC \cdot \sin(\beta_{coupler\_AC}) \tag{6.7}$$

where

$$\beta_{coupler\_AC} = a\tan2((C_x - A_x);(C_y - A_y)) \tag{6.8}$$

All of the positions and dimensions up to this point are found from the random selection of del_{2x}, del_{2y}, del_{3x}, del_{3y}, del_{4x}, del_{4y}, α_2, α_3, α_4, configuration of the four-bar, β_3 and β_4. A range is chosen and a triangle is drawn outside the coupler, having each side parallel to the side of the inner triangle and that range away from it. The reason for selecting such a region is because of the cylinder pivot mounted on the coupler. It does not have to be mounted inside the triangle that is constructed by the pivot points on the coupler, because the structure of coupler is definitely greater than the inner triangle in Figure 6-2 and generally the cylinder pivot is near the sides of the structure rather than the middle of it. In order to decide the position of that cylinder pivot, two ratios are selected randomly, namely cyl_ran and cyl_ran2. The definitions of these ratios are in (6.9) and (6.10) and the lengths in the equations can be seen in Figure 6-2. Besides a distance named $dist$ is defined as $|F'F''|$ to determine the position of point F. $dist$ is the minimum distance from F' to the intersection of the perpendicular line passing from F' with either A_3B_3 or B_3C_3. Equations (6.11) and (6.12) show the x and y positions of point F.

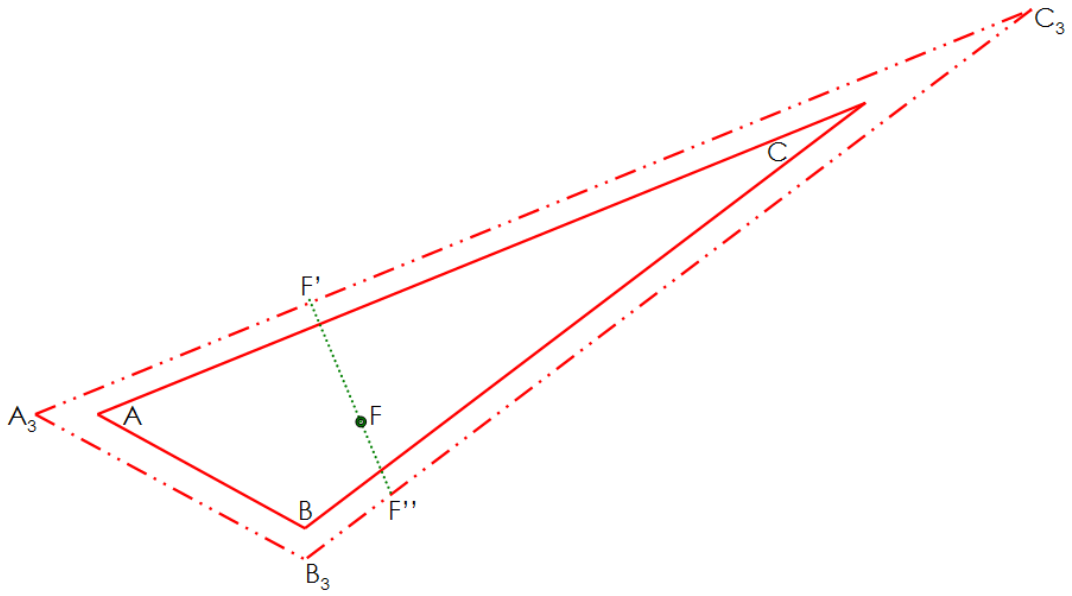

Figure 6-2 – The position of lift cylinder pivot mounted on coupler on a Type II mechanism

$$cyl\_ran = \frac{|F'A_3|}{|A_3C_3|} \tag{6.9}$$

$$cyl\_ran2 = \frac{|FF'|}{|F'F''|} \tag{6.10}$$

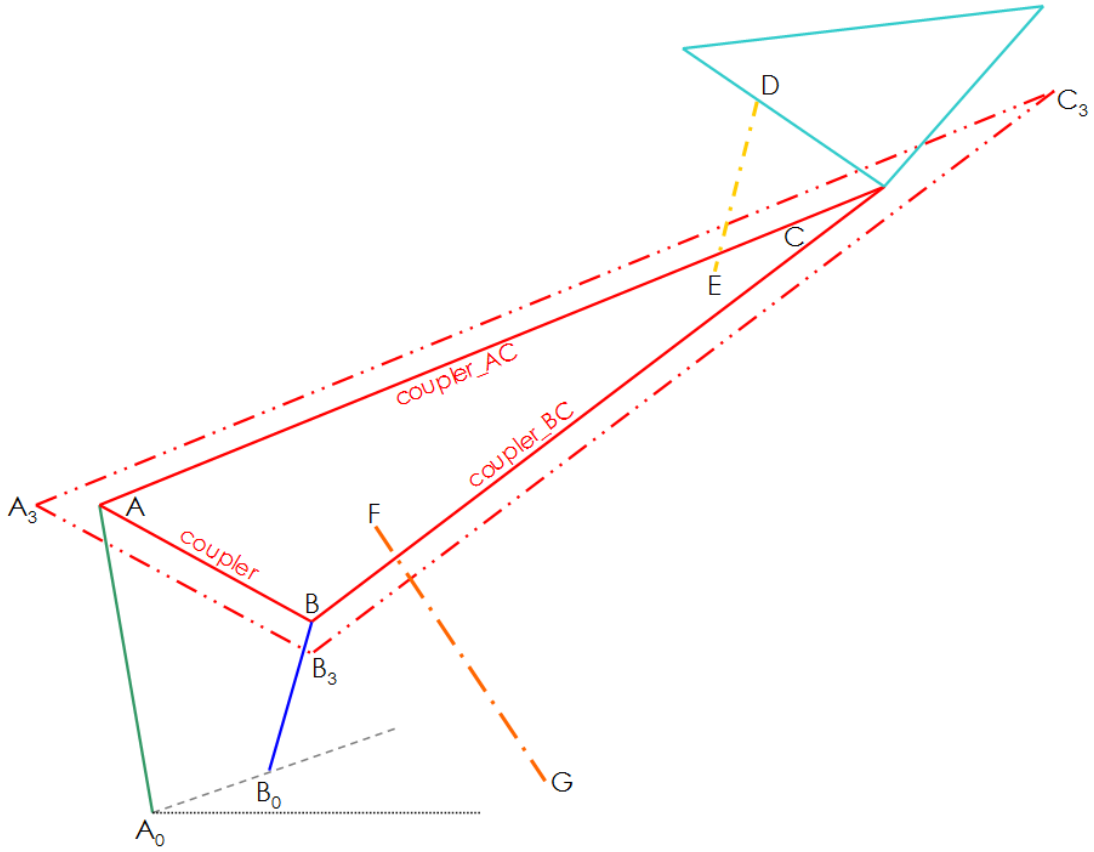

Figure 6-3 – The schematic view of a skid-steer loader lift arm mechanism

$$F_x = A_{3x} + cyl\_ran \cdot |A_3C_3| \cdot \cos(\beta_{coupler\_AC}) + cyl\_ran2 \cdot dist \cdot \cos(\beta_{coupler\_AC} + 3\pi/2) \tag{6.11}$$

$$F_y = A_{3y} + cyl\_ran \cdot |A_3C_3| \cdot \sin(\beta_{coupler\_AC}) + cyl\_ran2 \cdot dist \cdot \sin(\beta_{coupler\_AC} + 3\pi/2) \tag{6.12}$$

Two circles are drawn to determine the position of G in Figure 6-3. One circle having center at F and a radius of the closed length of the lift cylinders is drawn when the lift arm is at its lowest position. Plus, another circle having center at F and a radius of the full length of the lift cylinders is drawn when the lift arm is at its highest position.

The intersections of these two circles are possible positions for the fixed pivot of the lift cylinders. Both of the intersection points are checked whether it satisfies the continuity of the cylinder stroke criterion or not. After the fixed pivot of the lift cylinders are decided, the angle β_{s1} is defined as (6.13) to use in the force analysis.

$$\beta_{s1} = a\tan2((F_x - G_x);(F_y - G_y)) \tag{6.13}$$

To decide the position of D, a ratio cyl_ran3 is selected randomly. The definition cyl_ran3 is explained in (6.14) and the lengths defining this ratio can be seen in Figure 6-4.

$$cyl\_ran3 = \frac{|CD|}{|CC'|} \tag{6.14}$$

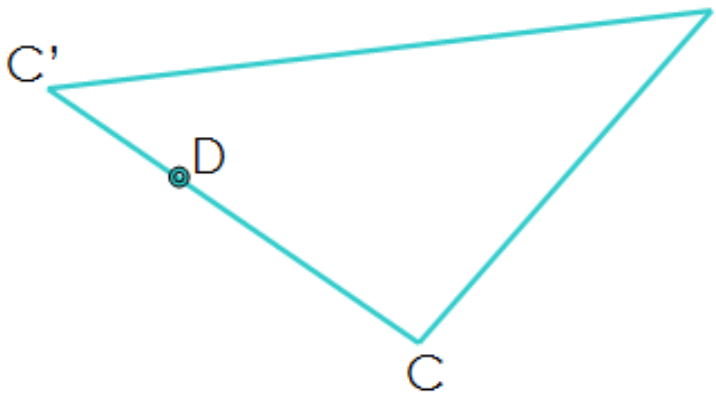

Figure 6-4 – The position of tilt cylinder pivot mounted on bucket

Like point G, two circles have to be drawn and their intersections should be found to locate the position of point E. The bucket is set to a position that satisfying the not spilling over any material to the top of the cabin criterion. A circle having center at D and a radius of the closed length of the tilt cylinders is drawn at that position. After that, the bucket is located at the dump angle position and another circle having center at D and a radius of the full length of the tilt cylinders is drawn. The intersections of these two circles are possible tilt cylinder coupler pivot locations. After selecting one of the intersection points, the coordinate of E is definite. The coordinate of D can be defined as (6.15) and (6.16) when (6.17) and (6.18) are substituted into (6.15) and (6.16).

$$D_x = C_x + cyl\_ran3 \cdot |CC'| \cdot \cos(-\pi - (\theta_{s_2} - \beta_{coupler\_EC})) \tag{6.15}$$

$$D_y = C_y + cyl\_ran3 \cdot |CC'| \cdot \sin(-\pi - (\theta_{s_2} - \beta_{coupler\_EC})) \tag{6.16}$$

where

$$\beta_{coupler\_EC} = a\tan2((C_x - E_x);(C_y - E_y)) \tag{6.17}$$

$$\theta_{s_2} = ang\cos(|EC|;|DC|;|s_2|) \tag{6.18}$$

where angcos gives the angle of the triangle having s_2 as opposite side and the $|DC|$ and $|EC|$ as other sides.

An illustration of the things explained above on a Microsoft Excel sheet can be seen in Figure 6-5.

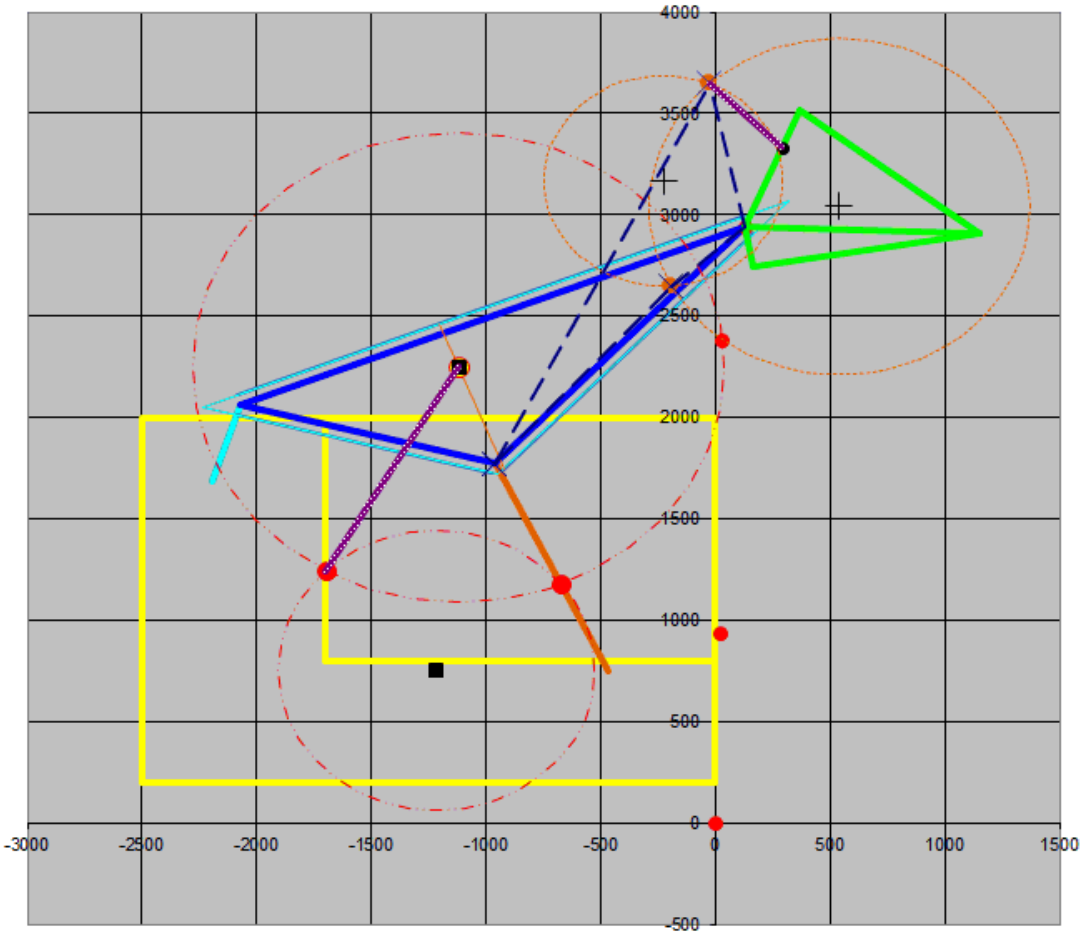

Figure 6-5 – A Microsoft Excel sheet explaining the synthesis of a Type II mechanism

6.2 TYPE I (INVERTED SLIDER) MECHANISM

A fixed pivot point for inverted-slider mechanism should be set. Target height is the most important factor while selecting the fixed pivot point. The vertical distance of the fixed pivot from the ground should be selected around half of the target height. If it is below half of the target height, at the highest position of the lift arm the hinge pin of the bucket will be far away from the truck that is to be loaded. If it is above that level, the length of the lift arm will be long. Therefore, the lift arm will be heavy

unnecessarily and the arc drawn by the hinge pin will be far away from the front of the cabin and a greater area will be needed for a loading cycle.

After the fixed pivot point A_0 is located, $arm1$ length, the length from the fixed pivot to the hinge pin, can be determined. At the lowest position of the hinge pin, the hinge pin is assumed to be at (0, Hmin). If the coordinates of A_0 is selected as (x_{A0}, y_{A0}) the length of $arm1$ can be calculated as (6.19).

$$arm1 = \sqrt{x_{A0}{}^2 + (y_{A0} - H_{\min})^2} \tag{6.19}$$

At the first stages of the design β_{arm1}, which can be seen in Figure 6-7, was the input of the mechanism. The coordinates of A_1 can be found when (6.22) is substituted in (6.20) and (6.21),

$$A_{1x} = A_{0x} + arm1 \cdot \cos(\beta_{arm1}) \tag{6.20}$$

$$A_{1y} = A_{0y} + arm1 \cdot \sin(\beta_{arm1}) \tag{6.21}$$

where

$$\beta_{arm1} = a\tan2((A_{1x} - A_{0x});(A_{1y} - A_{0y})) \tag{6.22}$$

The position of K on A_1A_1' is determined by a ratio cyl_ran3, which is selected randomly, and it can be defined as in (6.23).

$$cyl\_ran3 = \frac{|KA_1|}{|A_1A_1'|} \tag{6.23}$$

According to the not spilling over and dump angle criteria, the positions of K when the tilt cylinder is at its closed and fully opened conditions are set. Two circles have to be drawn to determine the position of the cylinder pivot mounted on the lift arm. One circle having center at K and a radius of the closed length of the tilt cylinders,

which satisfies the not spilling over to the top of the cab condition, is drawn. Plus, another circle having center at K and a radius of the full length of the tilt cylinders, which satisfies the dump angle criterion, is drawn. The circle having smaller radius can be seen in orange; the circle having larger radius can be seen in brown in Figure 6-6. The intersections, A_{21} and A_{22}, of these two circles are possible positions for the fixed pivot of the tilt cylinders. Both of the intersection points are checked whether they satisfy the continuity of the cylinder stroke criterion or not. After check, the pivot point is set as A_2, A_{21} in this case.

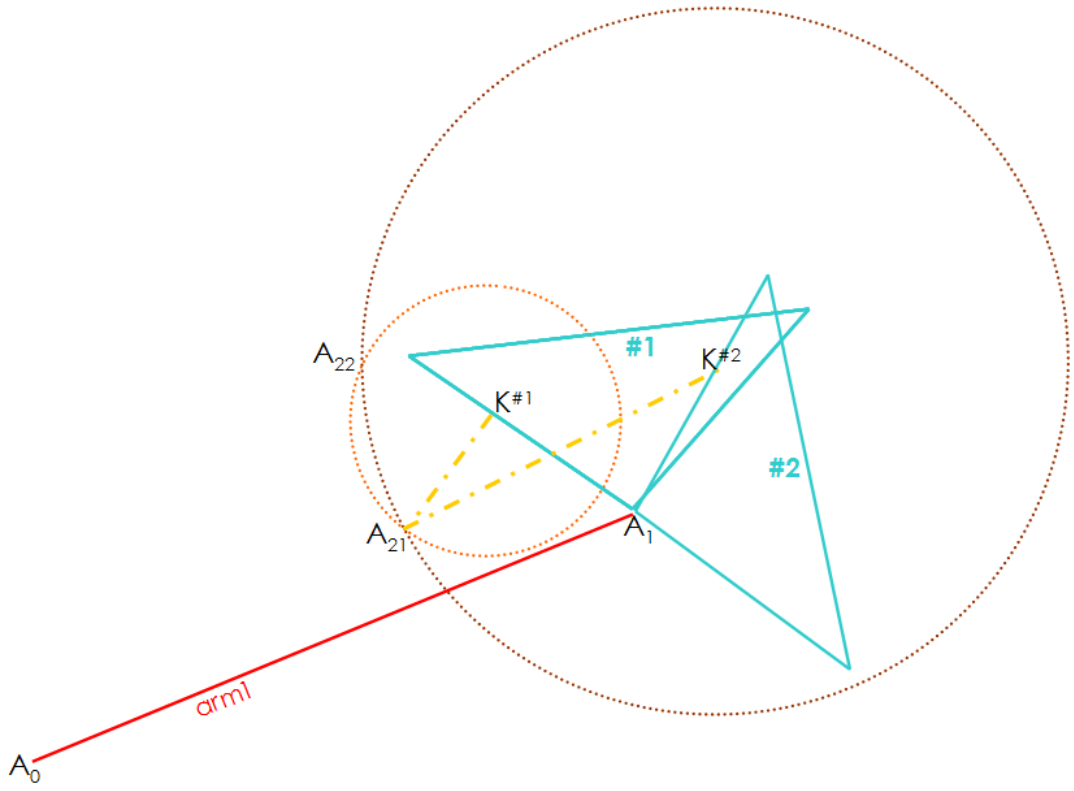

Figure 6-6 – The possible bucket cylinder pivot points

When A_2 is found, the pivot-to-pivot lengths of the lift arm, $arm2$ and $arm3$, can also be found. To determine the coordinates of A_2 at every position the equations (6.24) and (6.25) can be used if (6.26) is submitted to these equations.

$$A_{2x} = A_{0x} + arm2 \cdot \cos(\beta_{arm1} + \alpha_{arm3}) \tag{6.24}$$

$$A_{2y} = A_{0y} + arm2 \cdot \sin(\beta_{arm1} + \alpha_{arm3}) \tag{6.25}$$

where

$$\alpha_{arm3} = ang\cos(arm1; arm2; arm3) \tag{6.26}$$

The coordinates of K at every position can be calculated by using the equations (6.27) and (6.28) when (6.29) and (6.30) are submitted to these equations.

$$K_x = A_{1x} + cyl\_ran3 \cdot \left|A_1A_1'\right| \cdot \cos(-(\pi - \beta_{arm1} + \alpha_{arm2} + \theta_{s_2})) \tag{6.27}$$

$$K_y = A_{1y} + cyl\_ran3 \cdot \left|A_1A_1'\right| \cdot \sin(-(\pi - \beta_{arm1} + \alpha_{arm2} + \theta_{s_2})) \tag{6.28}$$

where

$$\alpha_{arm2} = ang\cos(arm1; arm3; arm2) \tag{6.29}$$

$$\theta_{s_2} = ang\cos(arm3; \left|A_1K\right|; s_2) \tag{6.30}$$

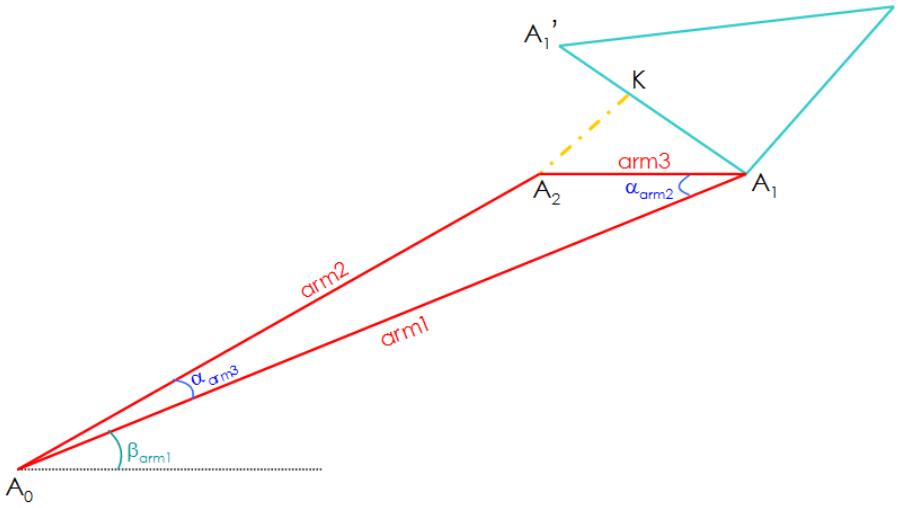

Figure 6-7 – The geometric properties of a lift arm having Type I mechanism for analysis

A greater triangular area is unnecessary for a Type I mechanism case. *arm*1 is a straight line that is drawn between A_0 and A_1. Actually, having a link like *arm*1 is impossible, because either skid-steer has tracks or crawler the link is not able to connect these two pivots directly, it should have a shape like shown with dots in Figure 6-8. Therefore it is not possible to mount a cylinder pivot below the line *arm*1.

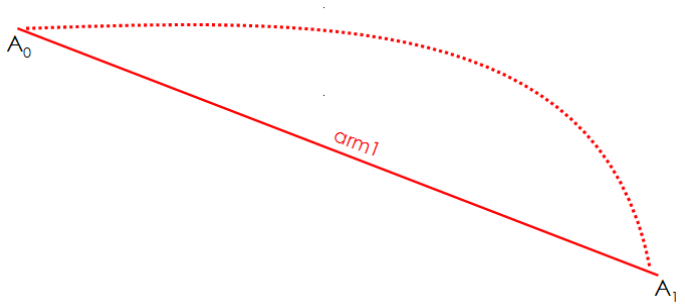

Figure 6-8 – The potential shape of the lift arm of a Type I mechanism

To decide the position of the lift cylinder pivot on lift arm two ratios cyl_ran and cyl_ran2 are selected randomly like in Type II case. The definition of cyl_ran2 is the same as the Type II case; cyl_ran is also very similar to the Type II mechanism and is defined in (6.31). Equations (6.32) and (6.33) show the x and y positions of point F.

$$cyl\_ran = \frac{|A_0F'|}{|A_0A_1|} \tag{6.31}$$

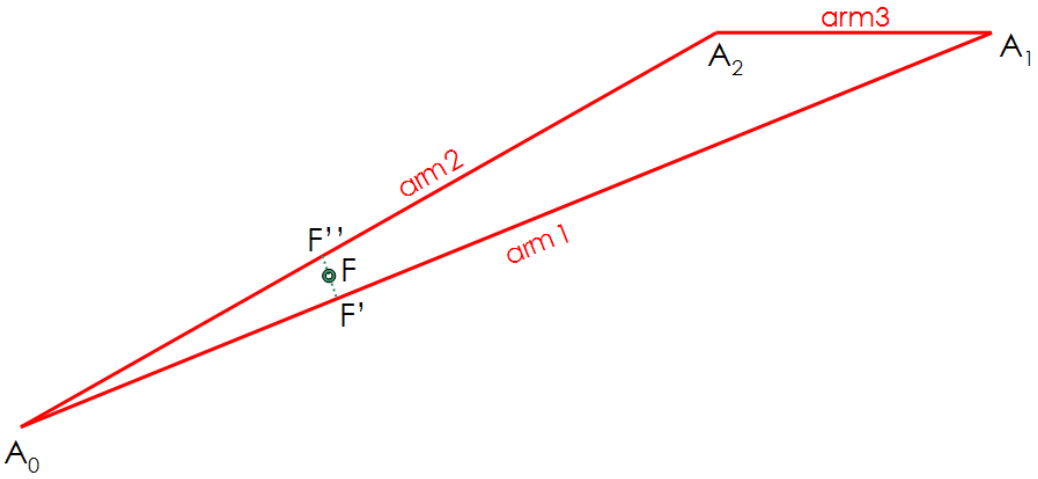

Figure 6-9 – The position of lift cylinder pivot mounted on coupler on a Type I mechanism

$$F_x = A_{0x} + cyl\_ran \cdot arm1 \cdot \cos(\beta_{arm1}) + cyl\_ran2 \cdot |F'F''| \cdot \cos(\beta_{arm1} + \pi/2) \tag{6.32}$$

$$F_y = A_{0y} + cyl\_ran \cdot arm1 \cdot \sin(\beta_{arm1}) + cyl\_ran2 \cdot |F'F''| \cdot \sin(\beta_{arm1} + \pi/2) \tag{6.33}$$

Same method explained in tilt cylinder case can also be applied here. To determine the fixed pivot of the lift cylinder, two circles having a center at F should be drawn. When the hinge pin is at (0, Hmin), the circle must have a radius equal to the closed length of the lift cylinder; when the hinge pin reaches the target height, the circle must have a radius equal to the fully opened length of the cylinder. The intersection points are possible fixed pivots and after check, one of them is selected to be the fixed pivot of the lift cylinder.

An illustration of the issues explained above on a Microsoft Excel sheet can be seen in Figure 6-10.

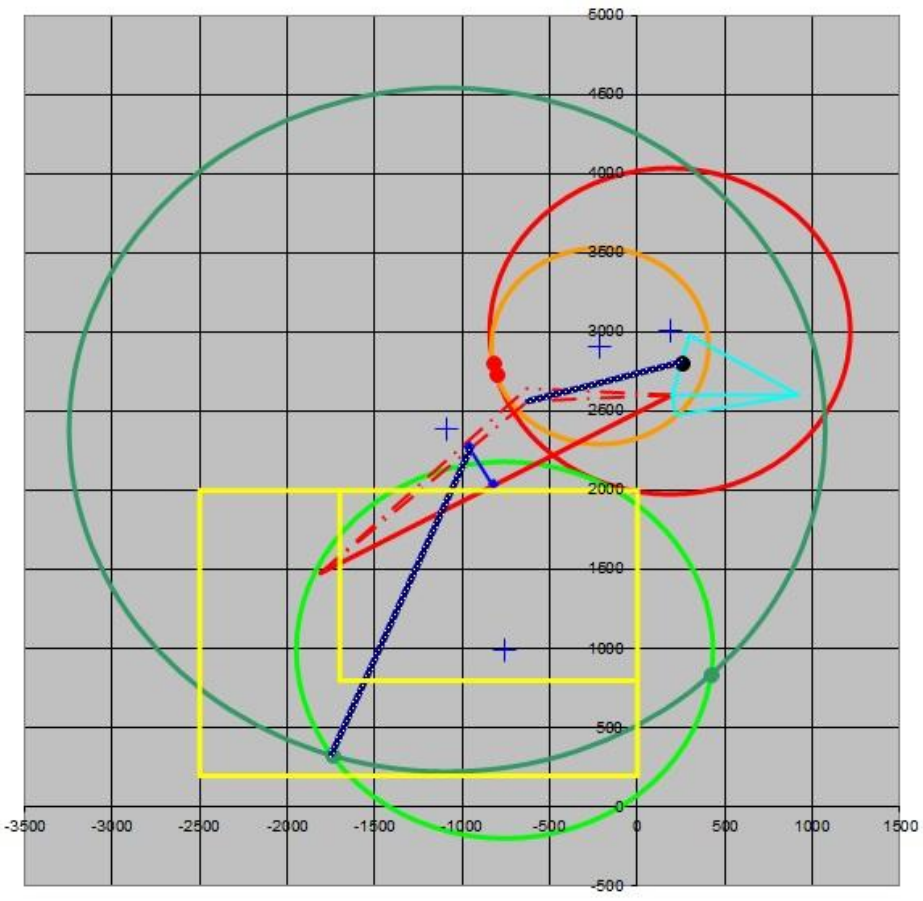

Figure 6-10 – A Microsoft Excel sheet explaining the synthesis of a Type I mechanism

CHAPTER 7

STATIC FORCE ANALYSIS

7.1 TYPE II (FOUR-BAR) MECHANISM

The free body diagram of a Type II mechanism can be seen in Figure 7-1. In horizontal and vertical direction total net force is zero and also moment about any point, B in this case, should be zero. The equations to calculate the unknown forces are (7.1), (7.2) and (7.3) when (7.4), (7.5) and (7.6) are submitted to these equations.

$$X \Rightarrow \left|\overrightarrow{F_{s1}}\right| \cdot \cos(\beta_{s_1} + \pi) + \left|\overrightarrow{F_A}\right| \cdot \cos(\pi + \theta_{12} + \alpha_{A0B0}) + \left|\overrightarrow{F_B}\right| \cdot \cos(\pi + \theta_{14} + \alpha_{A0B0}) = 0 \tag{7.1}$$

$$\begin{aligned} Y \Rightarrow & \left|\overrightarrow{F_{s1}}\right| \cdot \sin(\beta_{s_1} + \pi) + \left|\overrightarrow{F_A}\right| \cdot \sin(\pi + \theta_{12} + \alpha_{A0B0}) \\ & + \left|\overrightarrow{F_B}\right| \cdot \sin(\pi + \theta_{14} + \alpha_{A0B0}) - \left|\overrightarrow{F_{external}}\right| = 0 \end{aligned} \tag{7.2}$$

$$\begin{aligned} M(B) \Rightarrow & \left|\overrightarrow{F_{s1}}\right| \cdot |FB| \cdot \sin(\beta_{s_1} + \pi - \beta_{coupler\_BF}) \\ & \pm \left|\overrightarrow{F_A}\right| \cdot |AB| \cdot \sin(\pi + \theta_{12} + \alpha_{A0B0} - (\beta_{coupler\_BC} + \alpha_{AC})) \\ & + \left|\overrightarrow{F_{external}}\right| \cdot |BC| \cdot \sin(3\pi/2 - \beta_{coupler\_BC}) = 0 \end{aligned} \tag{7.3}$$

where

$$\beta_{coupler\_BC} = a\tan2((C_x - B_x);(C_y - B_y)) \tag{7.4}$$

$$\beta_{coupler\_BF} = a\tan2((F_x - B_x);(F_y - B_y)) \tag{7.5}$$

$$\alpha_{AC} = ang\cos(|AB|;|BC|;|AC|) \tag{7.6}$$

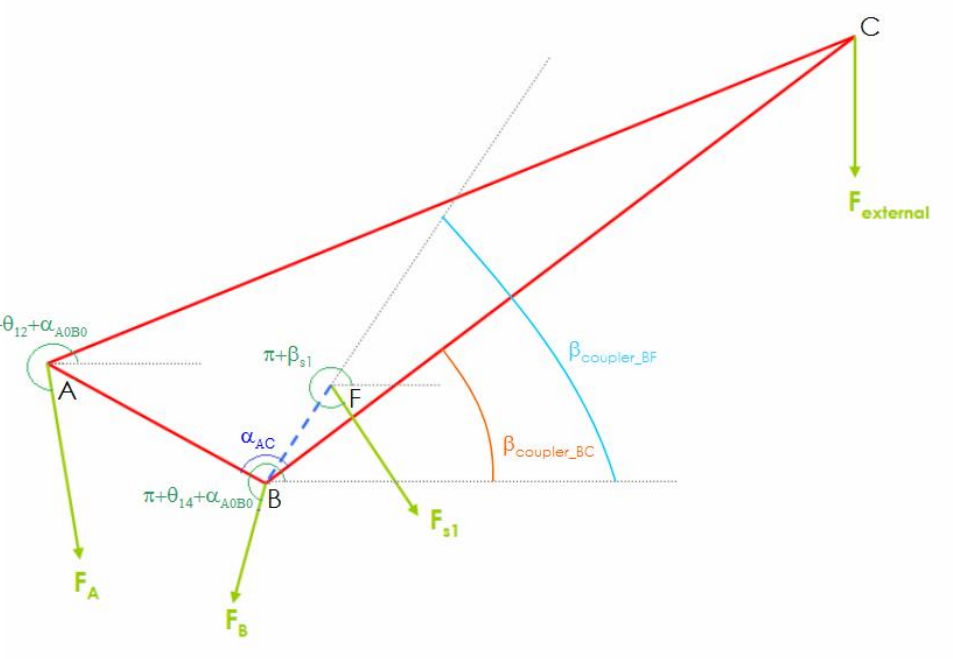

Figure 7-1 – The free body diagram of a Type II mechanism lift arm for static force analysis

The crank and rocker in the four-bar mechanism are binary links so they act as two force members. Besides, the lift cylinders can act as a two force member. Therefore the directions of $\overrightarrow{F_A}$, $\overrightarrow{F_B}$ and $\overrightarrow{F_{s_1}}$ are known. $\overrightarrow{F_{external}}$ is acted from the hinge pin to represent the weight of the diggings in bucket.

In this thesis, the properties of the tilt cylinders are used only for kinematics. To illustrate, the closed length and stroke of tilt cylinders are designed to satisfy the not spilling over and dump angle criteria. $\overrightarrow{F_{s_2}}$ is not included in this free body diagram because when $\overrightarrow{F_{external}}$ is applied from the hinge pin, the moment equation cannot be written for the bucket, in other words $\overrightarrow{F_{s_2}}$ is turn out to be zero.

The equations (7.1), (7.2) and (7.3) are used to calculate the unknowns, namely $\left|\overrightarrow{F_{Aox}}\right|$, $\left|\overrightarrow{F_{Aoy}}\right|$ and $\left|\overrightarrow{F_{s_1}}\right|$. There are 3 linear equations and 3 unknowns, so the system has a unique solution and can be solved by using linear algebra.

The structural shapes of the links are ambiguous. A finite element analysis is made after the selection of the best four-bar linkage, so the weights of the links are neglected in the static force analysis part.

Let A be the coefficient matrix, B be the vector of unknown forces and C be the forcing vector. The unknown forces, B, can be found by $B = A^{-1}C$. The matrix and vectors are defined in (7.7), (7.8) and (7.9).

$$A = \begin{vmatrix} \cos(\beta_{s_1} + \pi) & \cos(\pi + \theta_{12} + \alpha_{A0B0}) & \cos(\pi + \theta_{14} + \alpha_{A0B0}) \\ \sin(\beta_{s_1} + \pi) & \sin(\pi + \theta_{12} + \alpha_{A0B0}) & \sin(\pi + \theta_{14} + \alpha_{A0B0}) \\ \left|FB\right| \cdot \sin(\beta_{s_1} + \pi - \beta_{coupler\_BF}) & \left|AB\right| \cdot \sin(\pi + \theta_{12} + \alpha_{A0B0} - (\beta_{coupler\_BC} + \alpha_{AC})) & 0 \end{vmatrix} \tag{7.7}$$

$$B = \begin{vmatrix} \left|\overrightarrow{F_{s_1}}\right| \\ \left|\overrightarrow{F_A}\right| \\ \left|\overrightarrow{F_B}\right| \end{vmatrix} \tag{7.8}$$

$$C = \begin{vmatrix} 0 \\ F_{ext} \\ -F_{external} \cdot \left|BC\right| \cdot \sin(3\pi/2 - \beta_{coupler\_BC}) \end{vmatrix} \tag{7.9}$$

The kinematic analysis is performed by Microsoft Excel. When there are parametric equations and plenty of variables, Microsoft Excel is the most practical software. To illustrate, a parameter affecting most of the equations can be changed with just changing a cell or the effect of increasing or decreasing a parameter can easily be seen by a scroll bar.

7.2 TYPE I (INVERTED-SLIDER) MECHANISM

The free body diagram of the Type I (inverted-slider) mechanism can be seen in Figure 7-2. The total net force in horizontal and vertical directions and moment about any point should be zero. (7.10), (7.11) and (7.12) can be used to determine the unknowns if (7.13) are substituted into (7.12). β_{s1} is defined in (6.13) and β_{arm1} is defined in (6.22).

$$X \Rightarrow \left|\overrightarrow{F_{s_1}}\right| \cdot \cos(\beta_{s_1} + \pi) + \left|\overrightarrow{F_{A0x}}\right| = 0 \tag{7.10}$$

$$Y \Rightarrow \left|\overrightarrow{F_{s_1}}\right| \cdot \sin(\beta_{s_1} + \pi) + \left|\overrightarrow{F_{A0y}}\right| - \left|\overrightarrow{F_{external}}\right| = 0 \tag{7.11}$$

$$M(A_0) \Rightarrow \left|\overrightarrow{F_{s_1}}\right| \cdot \left|A_0F\right| \cdot \sin(\beta_{s_1} + \pi - (\beta_{arm1} + \alpha_{s_1}))$$
$$+ \left|\overrightarrow{F_{external}}\right| \cdot arm1 \cdot \sin(3\pi/2 - \beta_{arm1}) = 0 \tag{7.12}$$

where

$$\alpha_{s_1} = ang\cos(\left|A_0F'\right|; \left|A_0F\right|; \left|F'F\right|) \tag{7.13}$$

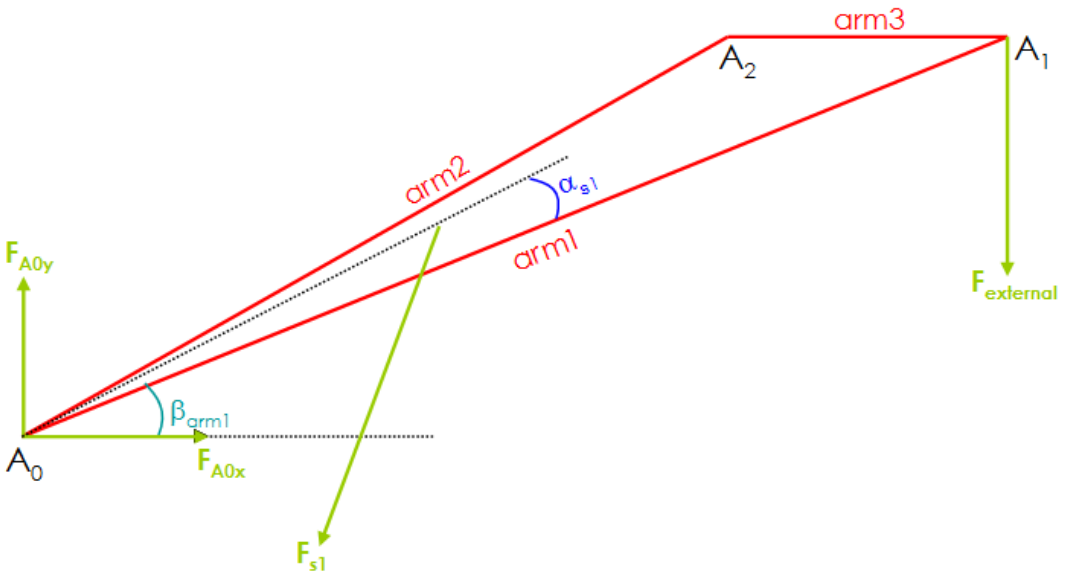

Figure 7-2 - The free body diagram of a Type I mechanism lift arm for static force analysis

Again, there are 3 linear equations and 3 unknowns, so the system has a unique solution and can be solved by using linear algebra. Solution explained in Type II case can also be used for inverted-slider (Type I) mechanism. The coefficient matrix A, the vector of unknown forces B and the forcing vector C can be seen in (7.14), (7.15) and (7.16).

$$A = \begin{vmatrix} \cos(\beta_{s_1} + \pi) & 1 & 0 \\ \sin(\beta_{s_1} + \pi) & 0 & 1 \\ |A_0F| \cdot \sin(\beta_{s_1} + \pi - (\beta_{arm1} + \alpha_{s_1})) & 0 & 0 \end{vmatrix} \tag{7.14}$$

$$B = \begin{vmatrix} \left|\overrightarrow{F_{s_1}}\right| \\ \left|\overrightarrow{F_{A0x}}\right| \\ \left|\overrightarrow{F_{A0y}}\right| \end{vmatrix} \tag{7.15}$$

$$C = \begin{vmatrix} 0 \\ F_{ext} \\ -F_{external} \cdot arm1 \cdot \sin(3\pi/2 - \beta_{arm1}) \end{vmatrix} \tag{7.16}$$

CHAPTER 8

APPLICATION OF GENETIC ALGORITHM

A general purpose genetic algorithm is used which is further altered to meet the needs of the mechanism synthesis problem. As a beginning, an initial population is created. Then, a fitness value is assigned to each individual by using an evaluation function. After the selection of the individuals, crossover and mutation are applied. The process of generating new populations continues up to achieve the termination condition.

8.1 PROBLEM DESCRIPTION

It is desired to increase the value of the objective function at every generation and select the best individual from the last generation. The objective function can be defined as in Equation (8.1).

$$f(x) = w_{min/max} \bullet D_{min/max}(x) + w_{max} \bullet D_{max}(x) + w_{tilt} \bullet D_{tilt}(x) + w_{rackback} \bullet D_{rackback}(x) \quad (8.1)$$

where $D_{min/max}(x)$, $D_{max}(x)$, $D_{tilt}(x)$ and $D_{rackback}(x)$ are the minimum force / maximum force on lift cylinders when a specific force is applied downwards from the hinge pin, the maximum force on lift cylinders when specific force is applied downwards from the hinge pin, the minimum transmission angle of the tilt cylinders and the rackback angle.

The ratio of the minimum force to maximum force is important for the stability of the force vs. cylinder stroke graph and the maximum force is important for the lift capacity to maximum height. The transmission angle of the tilt cylinders is important for the ability of the transmission of motion (and force) from the lift arm (input link) to

the bucket (output link). The bucket and the tilt cylinders are shown on figures just for kinematics. Therefore, a parameter that shows the capability of motion transfer should be in the objective function. The rackback angle should be in a range to achieve one of the design criteria: avoidance of spilling over any material at the highest position. Moreover, $w_{min/max}(x)$, $w_{max}(x)$, $w_{tilt}(x)$ and $w_{rackback}(x)$ are the weight factors for the variables of the objective function. At first, the values of the weight factors are started with an initial guess of importance of each input. Then, by increasing and decreasing the ratios, the tendency of the fitness value is observed and final weight factors are decided accordingly. The most important ones are the first two factors because the customer, the operator, is very connected with the lift capacity and the smoothness of the motion. This earth-moving machinery is for industry so the design should not be done just theoretically but should be done also practically. It is inevitable to close our ears to the desires of the buyers.

The general x variable depends on some other variables selected randomly by genetic algorithm. For a Type I mechanism, the variables are the x position of the lift arm joint mounted of the chassis, the target height, the positions of the joints of the lift and tilt cylinders, the dump angle, the closed lengths of the lift and tilt cylinders and the rollback angle on the ground. For a Type II mechanism, the variables are x and y positions of the hinge pin on the second, third and fourth prescribed positions, the change of angle of the lift arm on those prescribed positions, the angles defining the position of the fixed pivots on Burmester curves, the positions of the joints of the lift and tilt cylinders, the dump angle, the closed lengths of the lift and tilt cylinders, the dump angle, the rollback angle on the ground and the configuration of the Type II mechanism. On one hand, Figure 8-2 shows the variables used for Type I mechanism; on the other hand, Figure 8-3 shows the variables used for Type II mechanism.

8.2 FLOW CHART OF GENETIC ALGORITHM

The flow chart of genetic algorithm can be seen in Figure 8-1.

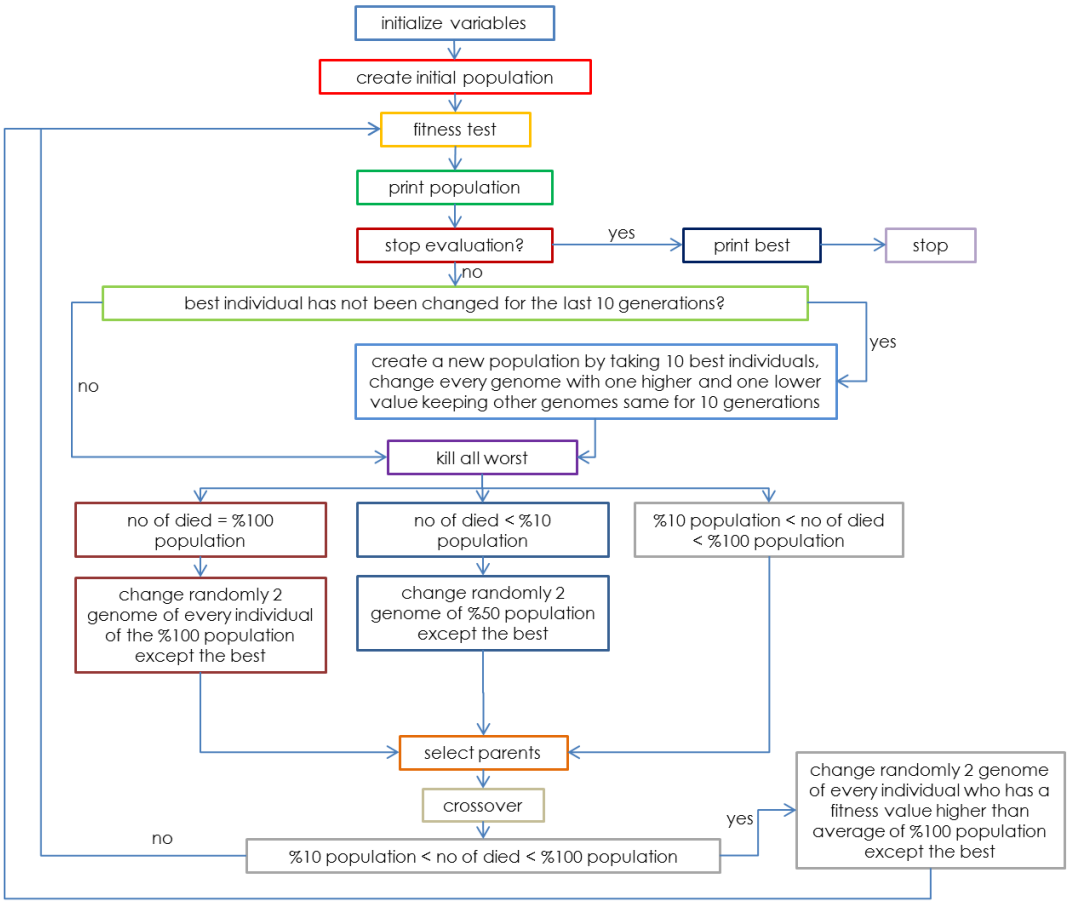

Figure 8-1 – Flow chart of genetic algorithm

There are some parameters that should be defined by the user before the initialization of the genetic algorithm. The parameters can be listed as maximum fitness to reach, population size, crossover probability, mutation probability, genome length and mutation genome number. Data structure of the program is made up of arrays. One of the arrays is the population array which holds all the information about the current generation. After crossover, new individuals are written over to selected parents. Data belonging to previous generations are erased as new generations are formed.

At the initialization stage of the algorithm initial parameter values (genomes) for the first generation are selected randomly between specified lower and higher limits. There are 9 genomes for each individual for Type I and 19 genomes for Type II mechanism. The lower and higher limits are determined according to the physical constraints on the mechanism size and constraints on the positions of the pivot points and these limits on the Microsoft Excel sheet can be seen in Figure 8-2 and Figure 8-3.

	min	max	
A0x	-2500	-1700	mm
target height	2900	3300	mm
cyl_lngth_1	0,01	1	ratio
cyl_lngth_3	0,01	1	ratio
cly_lngth_2	0,01	1	ratio
dump	45	50	degree
tilt retracted	500	800	mm
ground	25	35	degree
lift retracted	600	1200	mm

Figure 8-2 – The lower and upper limits of the parameters for Type I mechanism

	min	max	
del2-x	0	100	mm
del2-y	500	1000	mm
del3-x	0	200	mm
del3-y	1600	2400	mm
del4-x	0	300	mm
del4-y	2900	3300	mm
alfa-2	5	22	degree
alfa-3	17	55	degree
alfa-4	33	74	degree
beta-3	0	360	degree
beta-4	0	360	degree
cyl_ran2	0	1	ratio
cyl_ran	0	1	ratio
lift retracted	600	1600	mm
cyl_ran3	0	1	ratio
ground	25	35	degree
dump	45	50	degree
tilt retracted	500	800	mm
config1	-1	1	

Figure 8-3 – The lower and upper limits of the parameters for Type II mechanism

After the population is created, a fitness test is applied and a fitness value is assigned to each individual, which is calculated by the objective function described in problem description part. The Microsoft Excel sheets that show the fitness value of the individuals in the current generation can be seen in Figure 8-4 for Type I mechanism and Figure 8-5 for Type II mechanism. The condition that stops the evaluation is to have an individual having a fitness value equals to maximum fitness to reach.

CURRENT GENERATION								
1	**1**	**2**	**3**	**4**	**5**	**6**	**7**	**8**
A0x	-2010	-2170	-1800	-2170	-2000	-2130	-2170	-1900
target height	3120	2940	3210	3150	2910	2940	3220	3290
cyl_lngth_1	0,34	0,58	0,66	0,62	0,36	0,97	1	0,37
cyl_lngth_3	0,68	0,01	0,54	0,9	0,73	0,11	0,95	0,63
cly_lngth_2	0,49	0,26	0,9	0,32	0,62	0,69	0,65	0,39
dump	46,5	47,5	49,5	46,5	47	50	46,5	45,5
tilt retracted	670,00	550,00	580,00	710,00	560,00	530,00	660,00	750,00
ground	35,00	32,00	34,00	34,00	29,00	29,00	35,00	27,00
lift retracted	980,00	850,00	810,00	1080,00	830,00	890,00	880,00	740,00
fitness	**73,69**	**73,44**	**73,41**	**73,68**	**71,97**	**73,69**	**73,27**	**0,00**

Figure 8-4 – Fitness value of the individuals in the population for Type I mechanism

CURRENT GENERATION								
1	**1**	**2**	**3**	**4**	**5**	**6**	**7**	**8**
del2-x	60	60	60	60	60	60	60	60
del2-y	920	920	920	920	920	920	920	920
del3-x	30	30	30	30	30	30	30	30
del3-y	2380	2380	2380	2380	2380	2380	2380	2380
del4-x	110	110	110	110	110	110	110	110
del4-y	2940	2940	2940	2940	2940	2940	2940	2940
alfa-2	10,56	10,56	10,56	10,56	10,56	10,56	10,56	10,56
alfa-3	46,74	46,74	46,74	46,74	46,74	46,74	46,74	46,74
alfa-4	60,98	60,98	60,98	60,98	60,98	60,98	60,98	60,98
beta-3	55,7	55,7	55,7	55,7	55,7	55,7	55,7	55,7
beta-4	327,9	327,9	327,9	327,9	327,9	327,9	327,9	327,9
cyl_ran2	0,298	0,298	0,298	0,298	0,298	0,298	0,298	0,298
cyl_ran	0,402	0,402	0,402	0,402	0,402	0,402	0,402	0,402
lift retracted	1160	1160	1160	1160	1160	1160	1160	1160
cyl_ran3	0,286	0,294	0,291	0,29	0,285	0,287	0,281	0,283
ground	35	35	35	35	35	35	35	35
dump	46	46	46	46	46	46	46	46
tilt retracted	540	540	540	540	540	540	540	540
config1	-1	-1	-1	-1	-1	-1	-1	-1
fitness	**47,68**	**47,60**	**47,33**	**47,64**	**48,06**	**52,30**	**52,80**	**58,60**

Figure 8-5 – Fitness value of the individuals in the population for Type II mechanism

Before selecting the parents, another operation is run and the number of population that is going to be dead is calculated with kill all worst operator. It is the number of individuals having a fitness value lower than the average fitness value. A mutation process is applied according to the number of individuals that is going to be dead. If there is not any suitable individual in the population, selected number of genomes, 2 in this study, are mutated on each individual. Else if the number of individuals that is going to be dead is below 10% of the population, selected number of genomes, 2, of 50% numbers of individuals in the population is mutated. Moreover, the best individual is always kept without mutated.

In selecting operation 50% of the parents are selected randomly from the population, the other 50% parents are selected from the individuals who have a fitness value greater than the average. Selecting random parents keeps the variety of the population.

The genomes that change an output on the objective function are grouped together and 5 groups are created for Type I mechanism and 9 groups are created for Type II mechanism. A random number is selected. Crossover is achieved between parents on the genomes, which are the random number selected and the other numbers belonging that randomly selected number's group.

After that if the number of individuals that is going to be dead is below 100% and above 10% of the population, 2 randomly selected genomes are mutated on the individuals, who have a greater fitness value than the average fitness value.

After all these operations are completed, the new generation is evaluated again with fitness test and the operations continue up to the evaluation criterion is reached. The evaluation criterion is to reach the maximum fitness limit.

It is expected to have an individual having a fitness value greater than the previous generation's best individual's fitness value. If the best individual is not changed for 10 generations, the best 10 individual for Type I mechanism and 6 best individual for Type II mechanism are selected from the last generation. Their every single genome is increased and decreased by 1 while the other genomes are held constant to

reach the maxima. The maxima found can be local maxima, so a lot of trials have to be made to reach the global maxima.

The genetic algorithm is implemented on Microsoft Excel using built in Visual Basic for Applications editor (VBA). Figure 8-6 shows one of the sheets on Microsoft Excel for a Type I mechanism. The purple cells show the variables that are used to evaluate x on Equation (8.1) and selected randomly by genetic algorithm. The orange cells shows the physical limits of the machine and the pink cells are the parameters that are designated according to the physical constraints related with the mechanism.

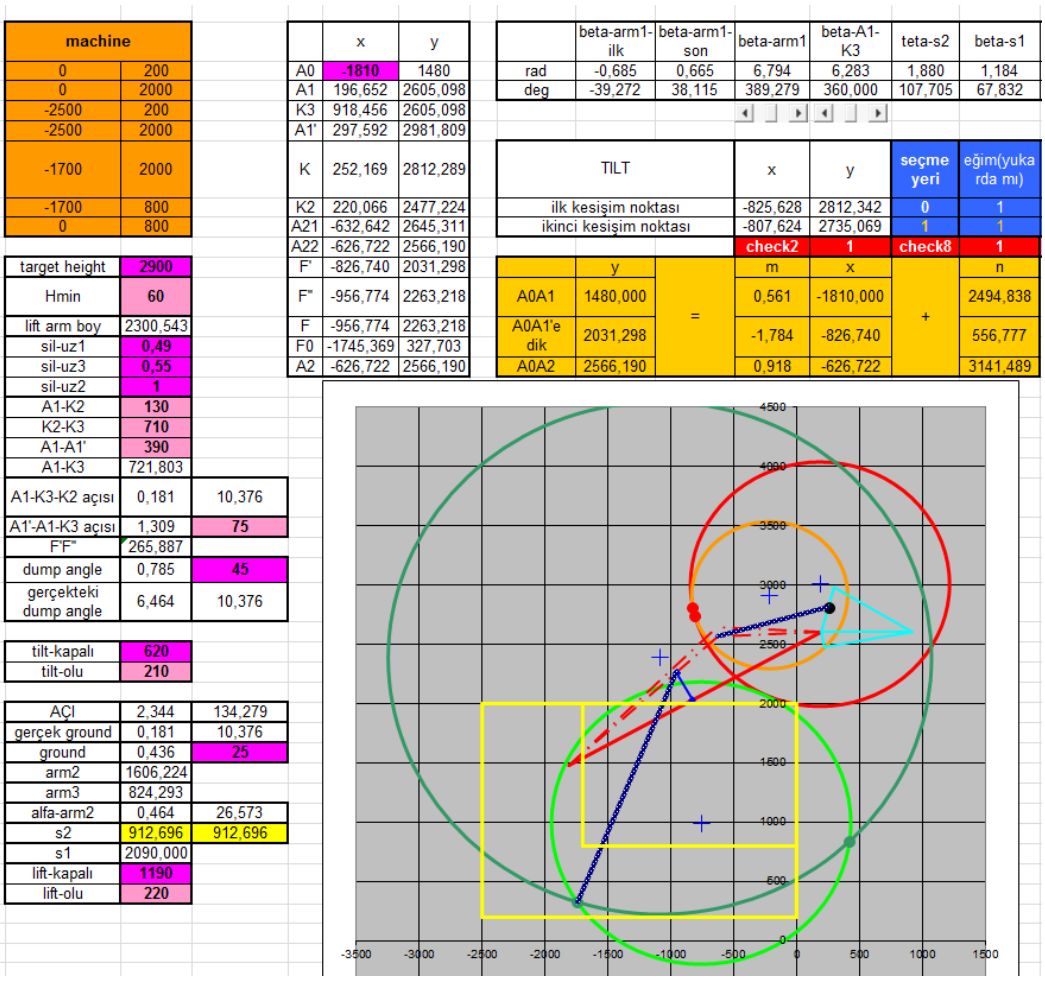

Figure 8-6 - The variables that genetic algorithm randomly select

8.3 RESULTS OF GENETIC ALGORITHM

8.3.1 TYPE I (INVERTED-SLIDER) MECHANISM

The genetic algorithm program in Microsoft Excel is built by using Visual Basic. An example of the development on individuals can be seen in Figure 8-7 for 50 and in Figure 8-8 for 150 generations. As explained above, one can see that the population could not find a better individual from 4th generation to 14th generation in Figure 8-7. Therefore, the increase and decrease for every genome by 1 unit is applied and one can easily see that the best individual in the generations from 15th to 25th has developed continuously.

After the values of the weight factors are finalized, the program is run approximately 400 times. In every run, the program is run for 255 generations. In every run, a local maximum is found. A few of them are formed same as the local maxima of another program. After many trials, the program is run with all local maxima's to find the global one, the best one, for both types of mechanisms.

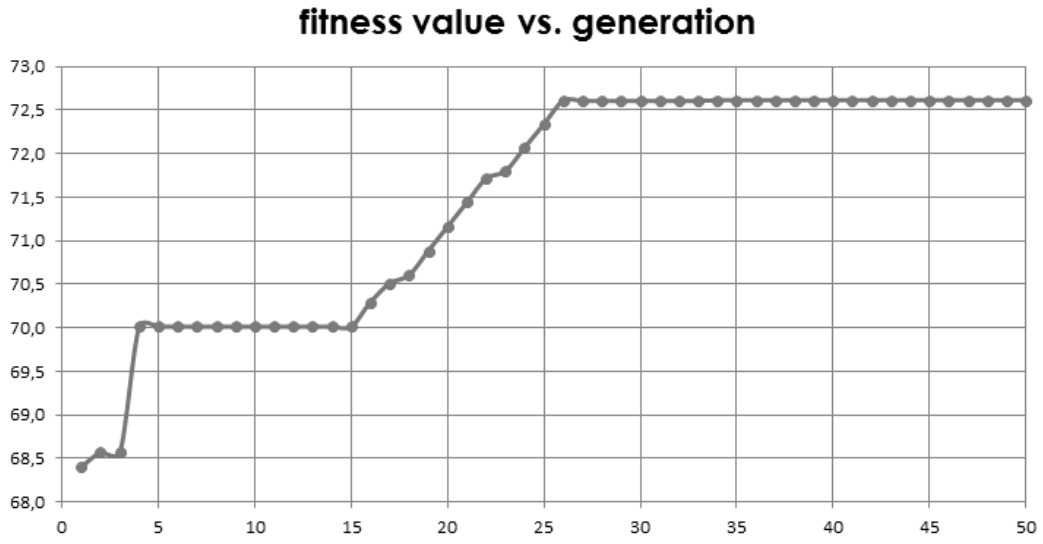

Figure 8-7 – The increase of the fitness value over 50 generations

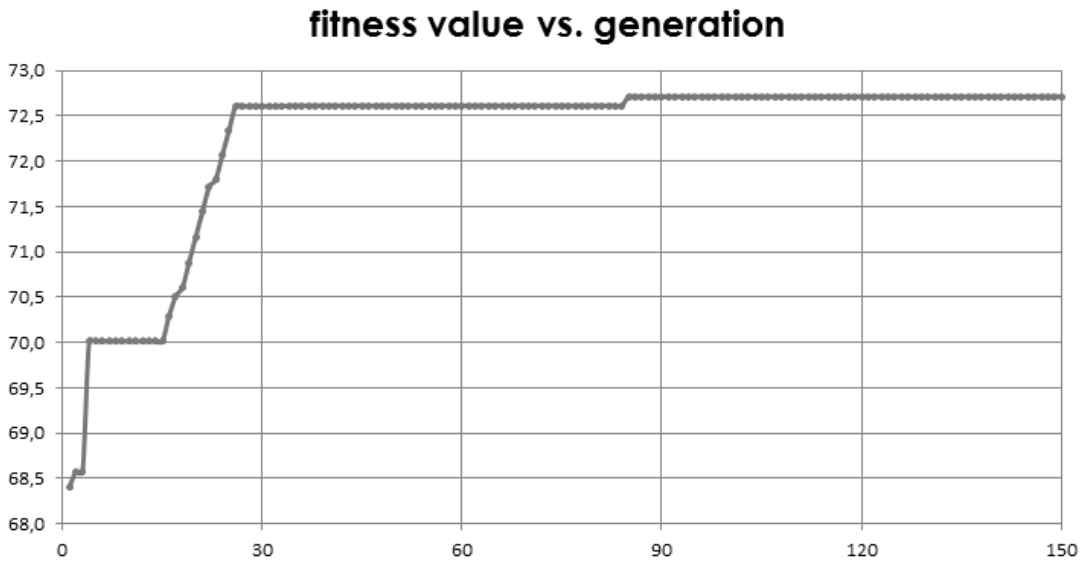

Figure 8-8 – The increase of the fitness value over 150 generations

The variables defining the best individual for Type I mechanism can be seen in Table 8-1 and the graph showing the joints and links can be seen in Figure 8-9. The red continuous straight line shows $|A_0A_1|$, the red dashed lines used to define the places of joints of lift and tilt cylinders on the lift arm. The lift and tilt cylinders are shown with dark blue lines with white dots on them. On one hand, the green dots at the intersection of dark and light green circles are possible joint places for lift cylinders on chassis; on the other hand, the red dots at the intersection of the orange and red circles are possible joint places for tilt cylinders on lift arm when the lift cylinders are at their maximum stroke. The blue plus signs show the center of the circles, meaning the beginning and the end of the cylinder strokes. The yellow continuous straight lines are used to define the machine. The right upper part of it is designed as window; the other part can be defined as chassis. The cyan lines show the bucket.

Table 8-1 – The variables for the best individual for Type I mechanism

A0x	-2020
target height	2900
cyl_lngth_1	0.48
cyl_lngth_3	0.45
cyl_lngth_2	0.92
dump	45
tilt retracted	540
ground	25
lift retracted	1200

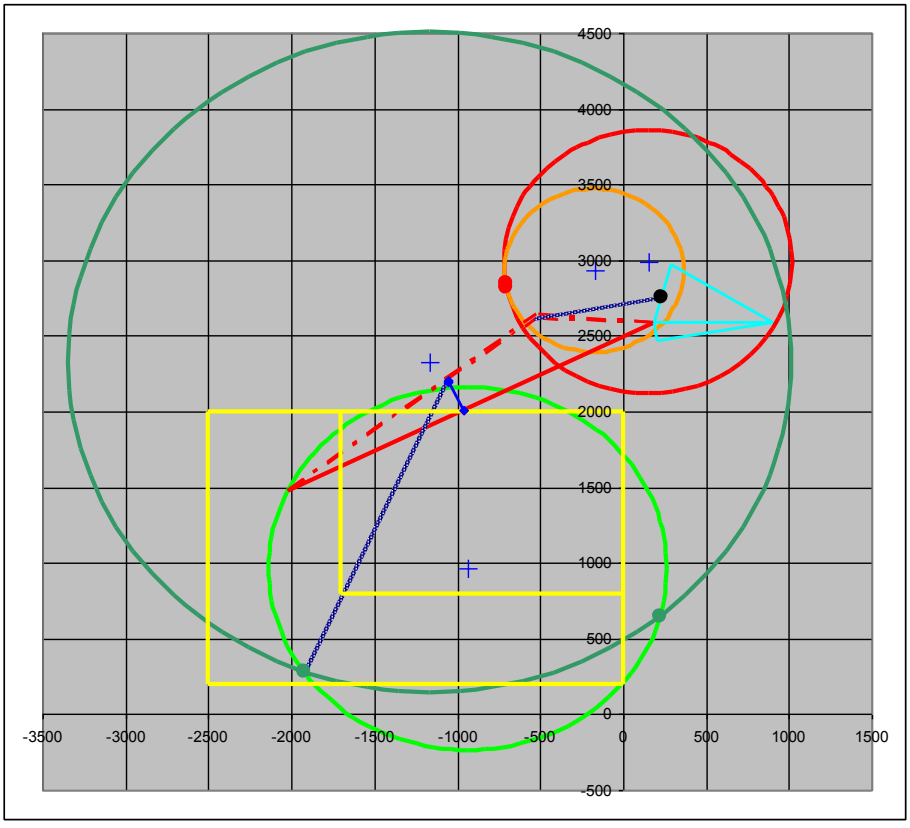

Figure 8-9 – The mechanism for the best individual for Type I mechanism

Breakout force is a vital parameter for earth-moving machinery. The breakout force is defined as maximum sustained upward vertical force, generated at a point 100 mm behind the leading edge of the bucket of a loader, or behind the foremost point of the cutting edge for a loader having a bucket with an irregular cutting-edge shape, by a lift or tilt cylinder, with the bottom of the bucket's cutting edge parallel to, and not more than 20 mm above, the ground reference plane [55]. The typical test arrangement of the breakout force for lift cylinders can be seen in Figure 8-10.

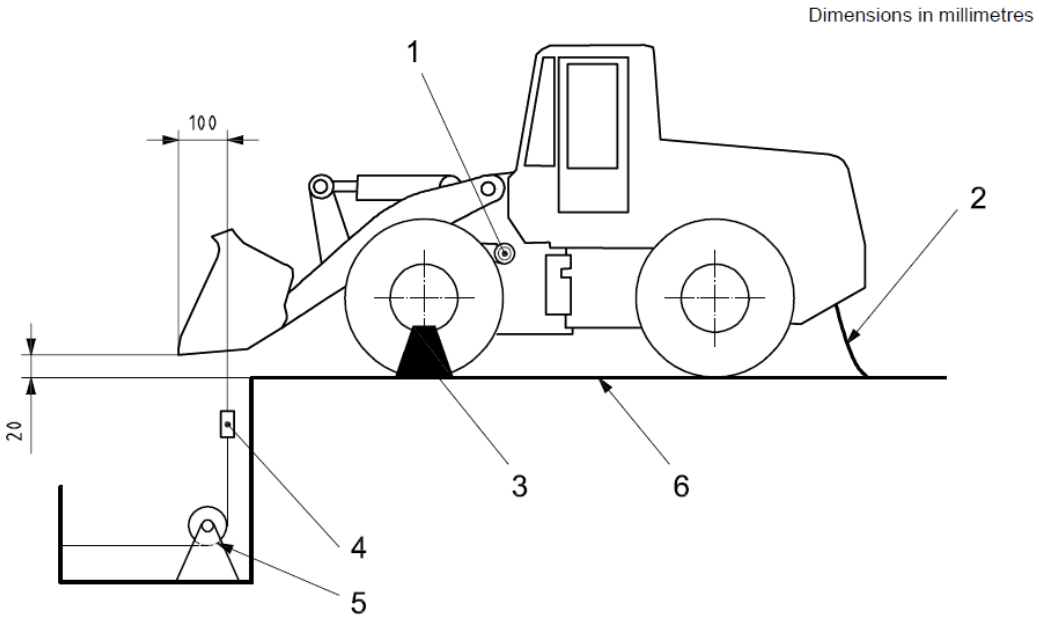

Key

1	lift cylinder	4	load cell
2	loose safety chain	5	pulley
3	support at axle centreline	6	GRP

Figure 8-10 – Typical test arrangement for breakout force on lift cylinders [55]

It is seen from benchmarking that the lift breakout forces changes from 1250 kg to 2250 kg when the machines having similar size of the machine in this thesis and

having Type I mechanism are compared. The target is to have the best mechanism, meaning that having the largest lift breakout force capacity. Therefore, having a lift breakout force higher than 2250 kg is the aim. When the bore diameter is selected as 60 mm and the working pressure is selected as 120 bars, the lift breakout force is 2645 kg. As a result, the goal is accomplished.

Apart from breakout force, the force that can be lifted from the hinge pin throughout the stroke can be seen in Figure 8-11. Moreover, the x component, y component and resultant forces occurred at A_0 joint can be seen in Figure 8-12.

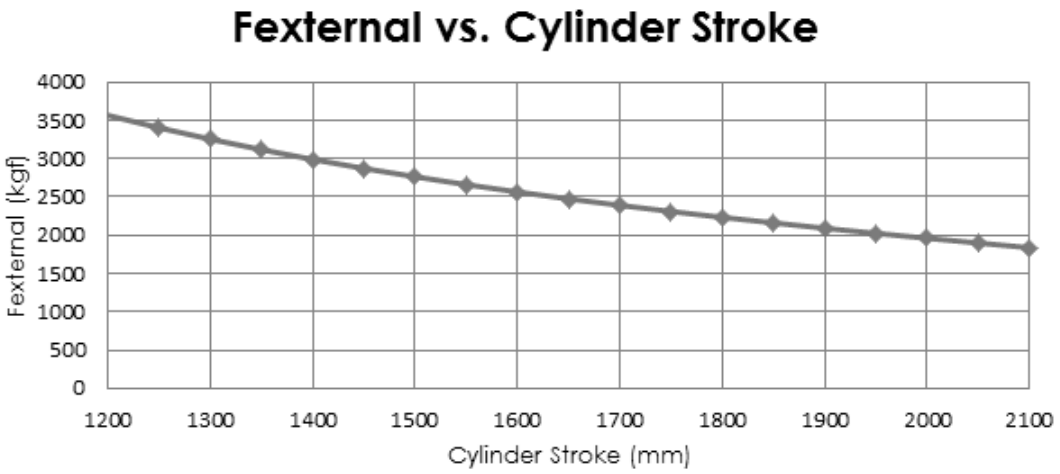

Figure 8-11 – Force that can be lifted from the hinge pin throughout the stroke

The forces supplied by the cylinders depend on 3 parameters; rod diameter, cylinder diameter and the pressure supplied for the motion of the cylinder. The cylinder diameter is greater than the rod diameter. The motion of the cylinders is supplied by hydraulic oil. If the hydraulic oil is transferred to cylinder section, the cylinder is extending under compressive load; on the contrary, if transferred to rod section, the cylinder is retracting under tension load.

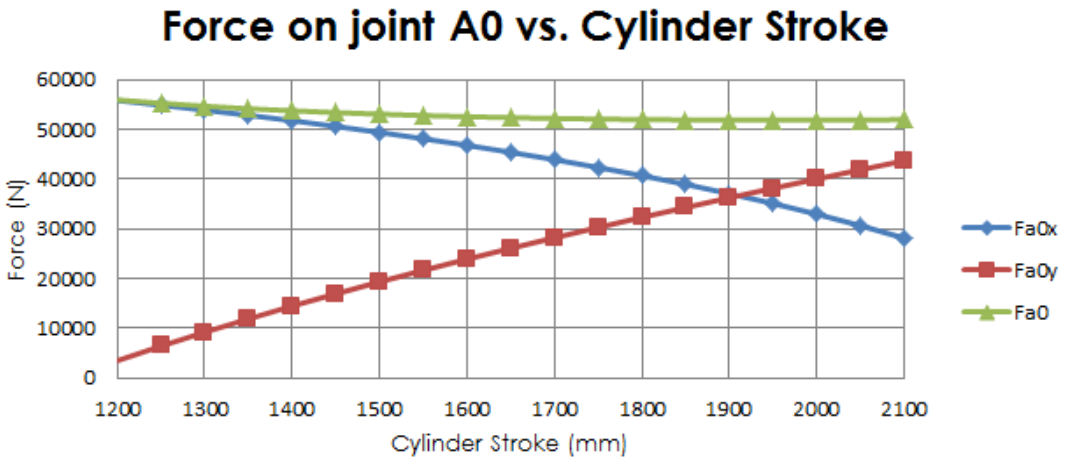

Figure 8-12 – Force on joint A_0 versus cylinder stroke graph

It should be checked whether the hydraulic cylinder is subjected to buckling or not. Therefore, a calculation should be carried out. Buckling can be calculated according to the following formula [56]:

Calculation according to Euler: $F = \frac{\pi^2 \cdot E \cdot I}{\nu \cdot L_K^{\,2}}$ if $\lambda > \lambda_g$ (8.2)

Calculation according to Tetmajer $F = \frac{\pi^2 \cdot E \cdot I}{4 \cdot \nu}$ if $\lambda \leq \lambda_g$ (8.3)

Where

E: modulus of elasticity in $\frac{N}{mm^2}$ = 210000 for steel (8.4)

d: piston rod diameter in mm = 40 (8.5)

I: moment of inertia in mm^4 = $\frac{d^4 \cdot \pi}{64}$ = $\frac{40^4 \cdot \pi}{64}$ = 125663.7 (8.6)

ν : safety factor = 1 (taken as 1 to calculate later) (8.7)

L_K : free buckling length in mm(can be seen from B in (8.13)) = L = 2180 (8.8)

λ : slenderness ratio = $\frac{4 \cdot L_K}{d}$ = $\frac{4 \cdot 2180}{40}$ = 218 (8.9)

R_e : yield strength of the piston rod material in $\frac{N}{mm^2}$ = 417 for AISI 4140 (8.10)

$$\lambda_g = \pi\sqrt{\frac{E}{0.8 \cdot R_e}} = \pi\sqrt{\frac{210000}{0.8 \cdot 417}} = 78.82 \quad (8.11)$$

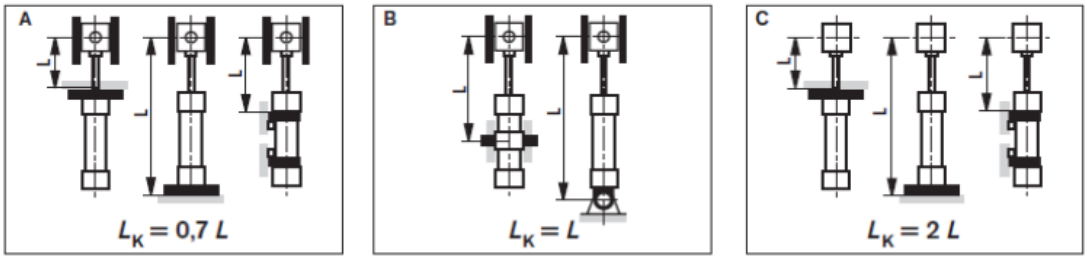

Figure 8-13 – The influence of the mounting style on the buckling length [56]

According to the comparison between slenderness ratios in Equations (8.9) and (8.11), calculation according to Euler, Equation (8.2), should be applied instead of Tetmajer, Equation (8.3). Equations (8.4), (8.5), (8.6), (8.7), (8.8), (8.10) are used to calculate the Equations (8.2) and (8.3).

According to Euler: $F = \frac{\pi^2 \cdot E \cdot I}{\nu \cdot L_K^{\,2}} = \frac{\pi^2 \cdot 210000 \cdot 125663.7}{1 \cdot 2180^2} = 54804\ \text{N}$ (8.12)

On the other hand, force in the cylinder can be calculated from Equation (8.13).

$$F(N) = \text{Pressure}(bar) \cdot Area(mm^2)/10 = \frac{120 \cdot \frac{\pi \cdot 60^2}{4}}{10} = 33929\ \text{N} \quad (8.13)$$

Therefore safety factor ν becomes 1.6 by dividing Equation (8.12) to (8.13).

8.3.2 TYPE II (FOUR-BAR) MECHANISM

A similar genetic algorithm program is also run many times for Type II mechanism. The best Type II mechanism is found after the program is run with all local maxima's. The variables defining the best individual for Type II mechanism can be seen in Table 8-2 and the graph showing the joints and links can be seen in Figure 8-14.

The yellow continuous straight lines are used to define the machine. The right upper part of it is designed as window; the other part can be defined as chassis. The dark blue continuous straight lines are used to define the lift arm, and the triangle formed by light blue lines outside the dark blue triangle parallel to dark blue lines are used to define the possible joint area for lift cylinders on lift arm. The orange and blue lines connecting the chassis and the lift arm are rocker and crank of four-bar. The lift and tilt cylinders are shown with purple lines with white dots on them. On one hand, the red dots at the intersection of red dashed circles are possible joint places for lift cylinders on chassis; on the other hand, the orange dots at the intersection of the orange dashed circles are possible joint places for tilt cylinders on lift arm when the lift cylinders are at their maximum stroke. The blue plus signs show the center of the orange circles, meaning the beginning and the end of the tilt cylinder strokes, and the black square signs show the center of the red circles, meaning the beginning and the end of the lift cylinder strokes. The green lines show the bucket.

Table 8-2 – The variables for the best individual for Type II mechanism

del2-x	50
del2-y	920
del3-x	70
del3-y	2380
del4-x	0
del4-y	2910
alfa-2	10.55
alfa-3	46.04
alfa-4	61.01
beta-3	53.9
beta-4	327.5
cyl_ran2	0.025
cyl_ran	0.402
lift retracted	1180
cyl_ran3	0.323
ground	34
dump	45.5
tilt retracted	590
config1	-1

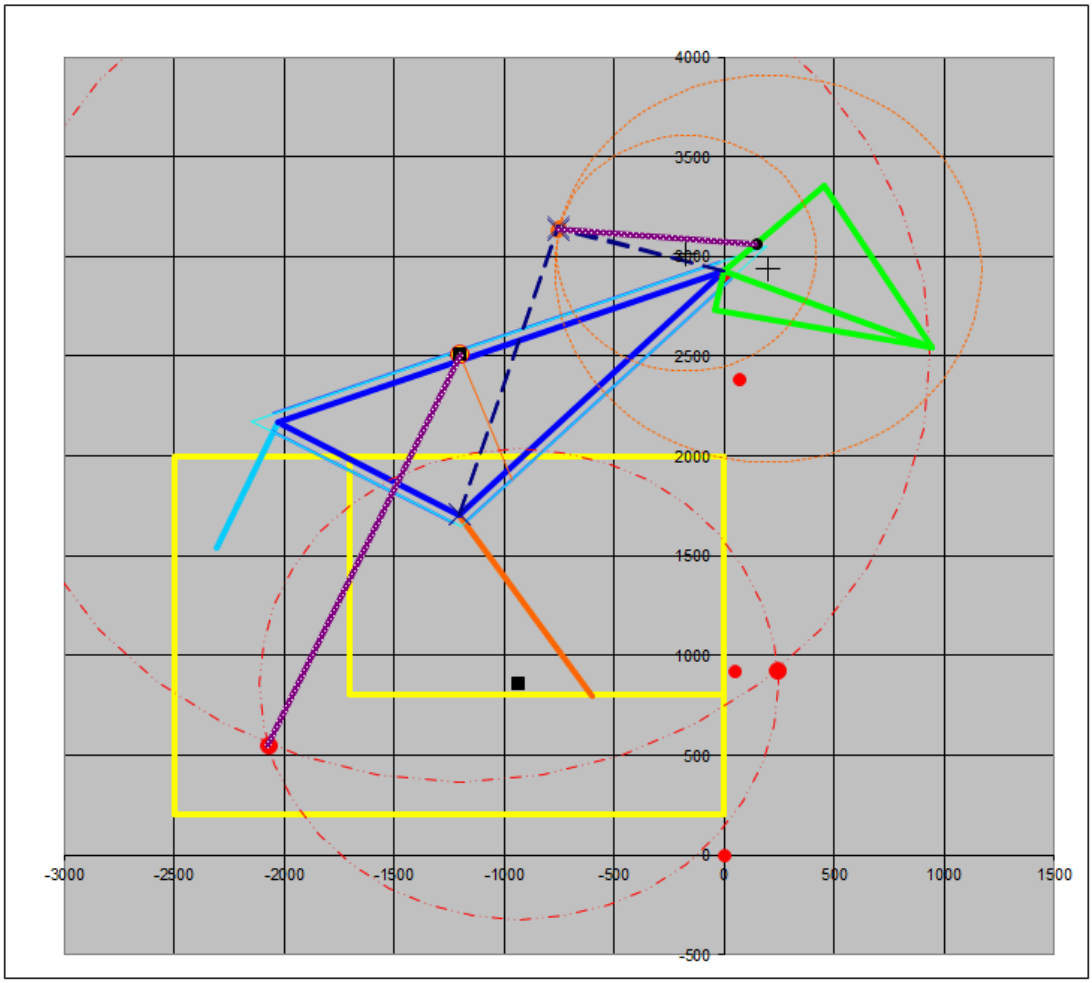

Figure 8-14 – The mechanism for the best individual for Type II mechanism

It is seen from benchmarking that the breakout forces changes from 1250 kg to 1500 kg when the machines having similar size of the machine in this thesis and having Type II mechanism are compared. Like the previous one, having a lift breakout force higher than the largest one, 1500 kg, is the aim. Having a lift breakout force higher than 1500 kg is achieved also with Type II mechanism by selecting 60 mm as bore diameter and 120 bars as working pressure. With this selection, the lift breakout force is 1825 kg.

Moreover, the force that can be lifted from the hinge pin throughout the stroke can be seen in Figure 8-15. Furthermore, forces on rocker and crank links can be seen in Figure 8-16.

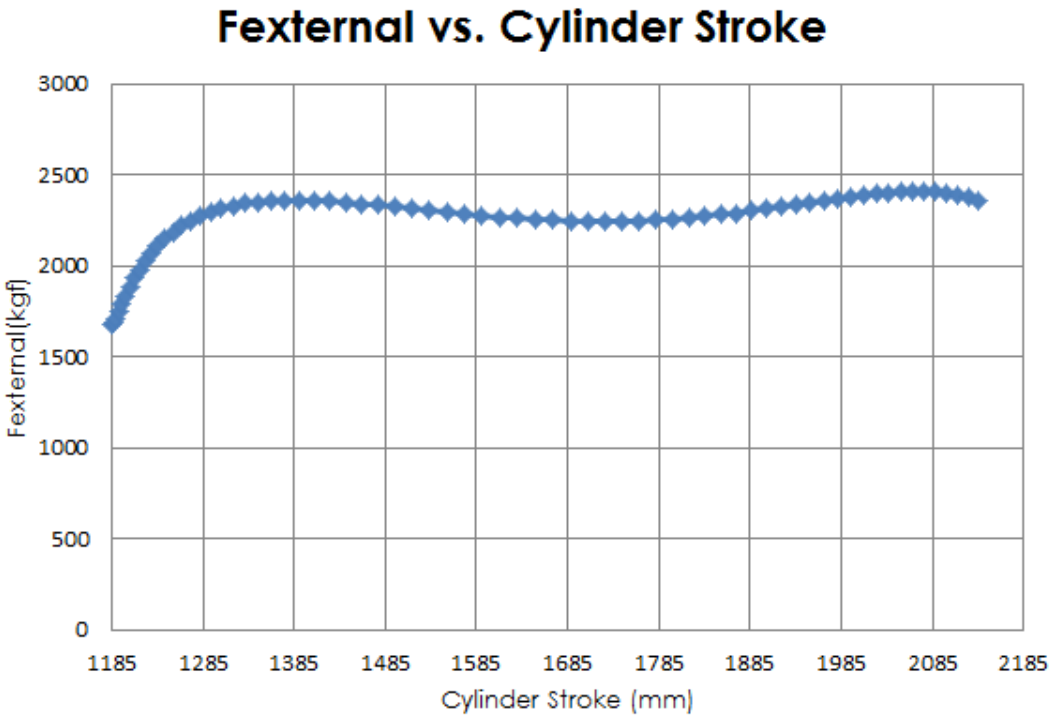

Figure 8-15 – Force that can be lifted from the hinge pin throughout the stroke

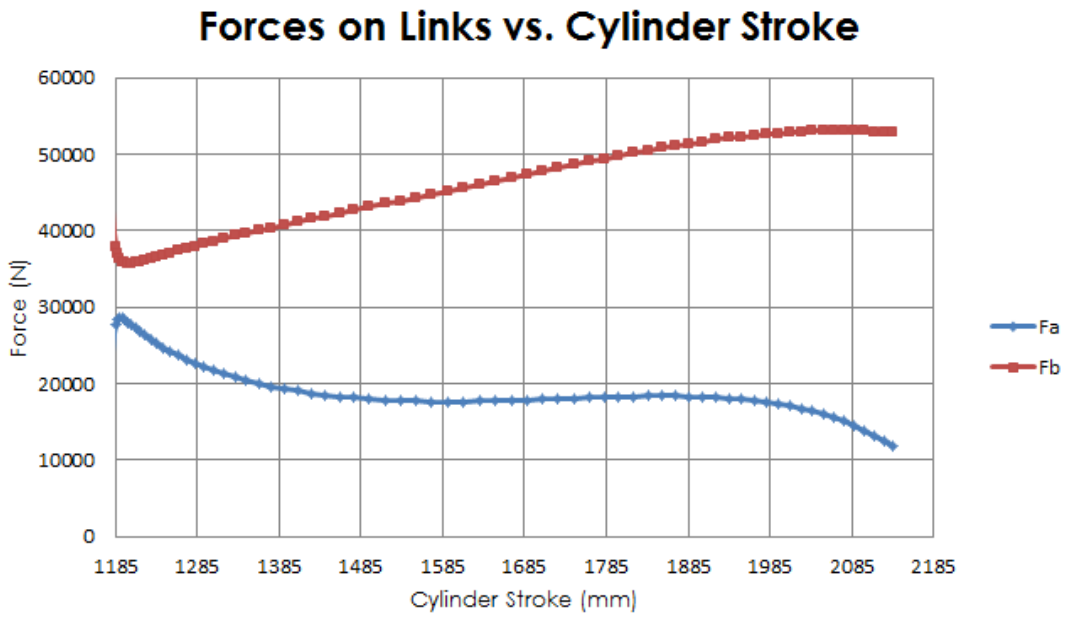

Figure 8-16 – Forces on rocker and crank links versus cylinder stroke graph

When equations (8.9) and (8.11) compared for free buckling length of 2140 mm, safety factor of 1, yield strength of piston rod material of 417 MPa for AISI 4140, piston rod diameter of 40 mm, moment of inertia of 125663.7 mm^4 and modulus of elasticity of 210 GPa for steel, it is seen that λ=214 $> \lambda_g$=63.13. Therefore, calculation according to Euler, equation (8.2), should be used. On one hand, from Euler equation the force which causes buckling is calculated as 56872 N, on the other hand the force in the cylinder is calculated from equation (8.13) as 33929 N for a bore diameter of 60 mm and working pressure of 120 bars. Therefore, safety factor ν becomes 1.7 by dividing Equation (8.12) to (8.13).

CHAPTER 9

FINITE ELEMENT ANALYSIS

9.1 FOR TYPE I (INVERTED-SLIDER) MECHANISM

The structural shape of lift arm for Type I mechanism, whose joints are designed according to the results of genetic algorithm, is created and can be seen in Figure 9-1. A new coordinate system is defined as x axis is in $|A_0A_1|$ direction and y axis is perpendicular to $|A_0A_1|$ direction. The new coordinate system and side view of the lift arm can be seen in Figure 9-2. A force versus lift cylinder stroke table is formed, which can be seen in Table 9-1, and given to MSC. Marc-Mentat.

Table 9-1 – Force applied from the hinge pin versus lift cylinder stroke

lift cylinder stroke (mm)	y-component (N)	x-component (N)
1200	-28632	20127
1250	-28225	17868
1300	-27795	15743
1350	-27341	13734
1400	-26862	11829
1450	-26357	10016
1500	-25823	8286
1550	-25259	6630
1600	-24664	5042
1650	-24034	3515
1700	-23366	2044
1750	-22659	624
1800	-21907	-748
1850	-21106	-2075
1900	-20250	-3361
1950	-19331	-4606
2000	-18341	-5811
2050	-17268	-6977
2100	-16093	-8101

Figure 9-1 – The structural shape of lift arm for Type I mechanism

Figure 9-2 – The side view of the lift arm for Type I mechanism

The side plates and intermediate plates between two side plates are meshed with shell meshes. These plates are thin enough to use shell meshes. Surfaces of the shell meshes are created at the middle of the plates. On the other hand, the cylinder between left and right arms and the cylinders between two side plates at the hinge pin and at the joint where chassis and lift arm combined are meshed with solid meshes.

In finite element analysis, the joint that is at the intersection of chassis and lift arm, the joint that is at the intersection of lift cylinder and lift arm are fixed in x, y, z directions and x, y rotations. The view representing the reaction forces formed at these joints can be seen in Figure 9-2.

The results at every step of the Table 9-1 are very similar to each other, so 3 of them, namely 1st, 10th, 19th are shown in Figure 9-3, Figure 9-4 and Figure 9-5 respectively. Furthermore, detailed views of stress concentrated areas are shown in Figure 9-6, Figure 9-7 and Figure 9-8.

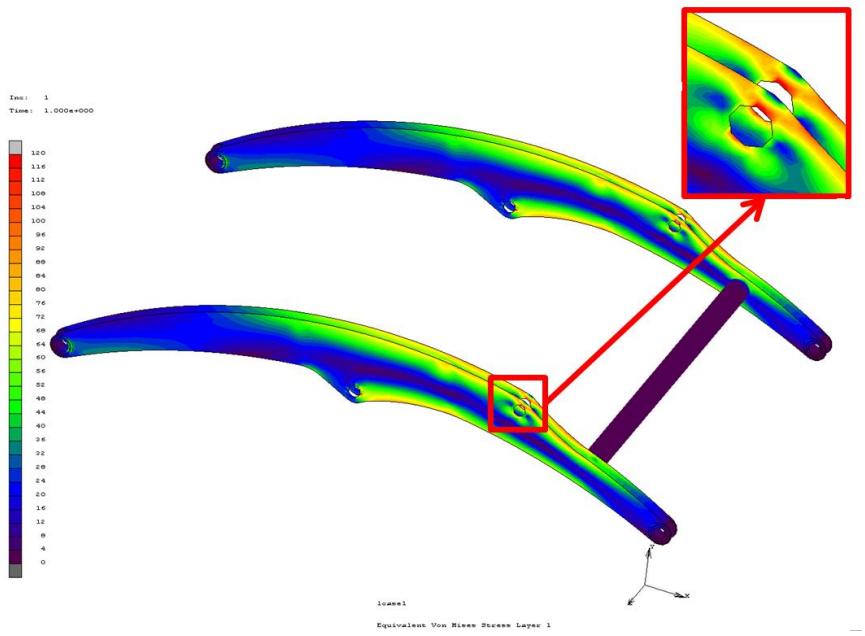

Figure 9-3 – The equivalent Von Mises stress distribution when lift cylinder is 1200 mm

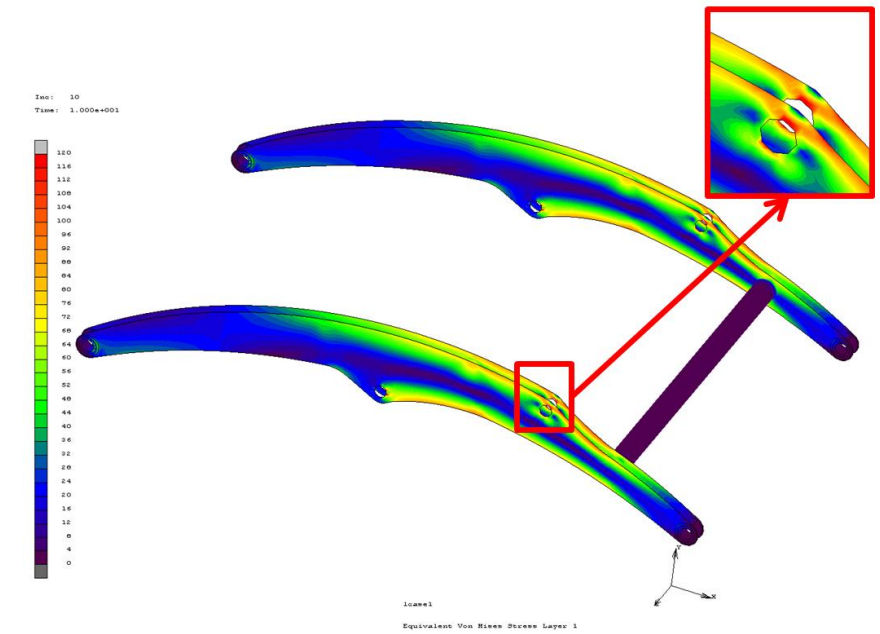

Figure 9-4 – The equivalent Von Mises stress distribution when lift cylinder is 1650 mm

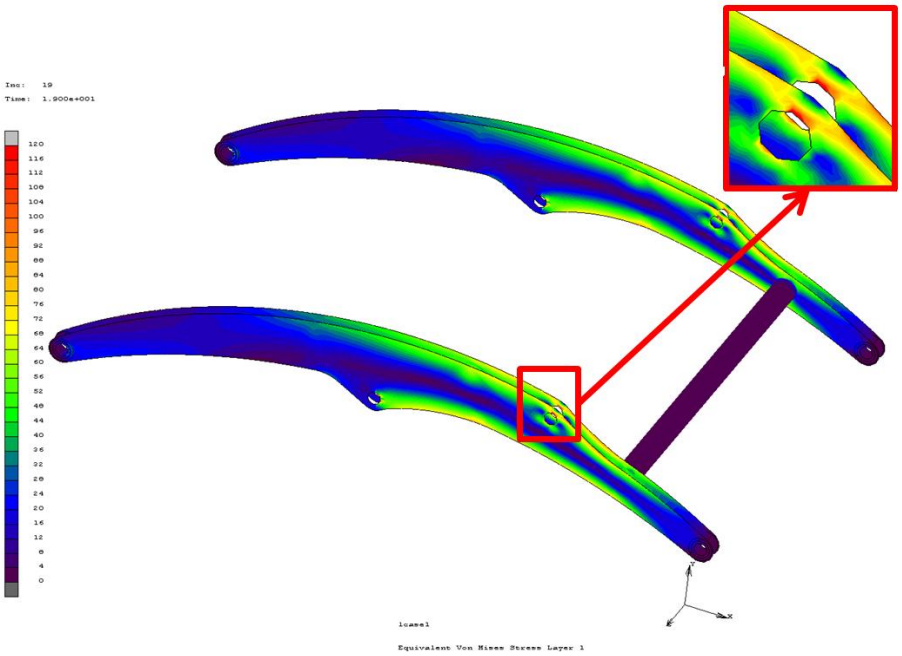

Figure 9-5 – The equivalent Von Mises stress distribution when lift cylinder is 2100 mm

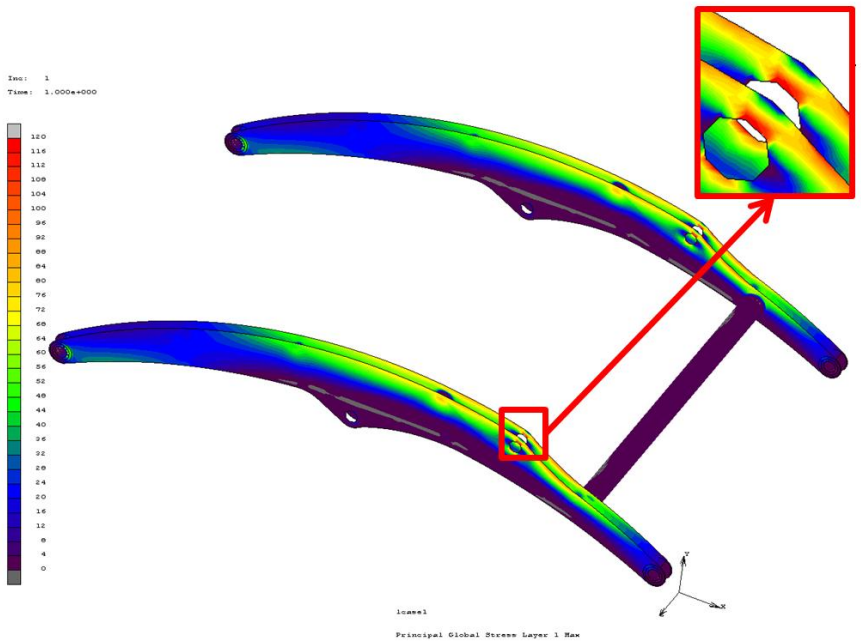

Figure 9-6 – The detailed view of stress distribution when lift cylinder is 1200 mm

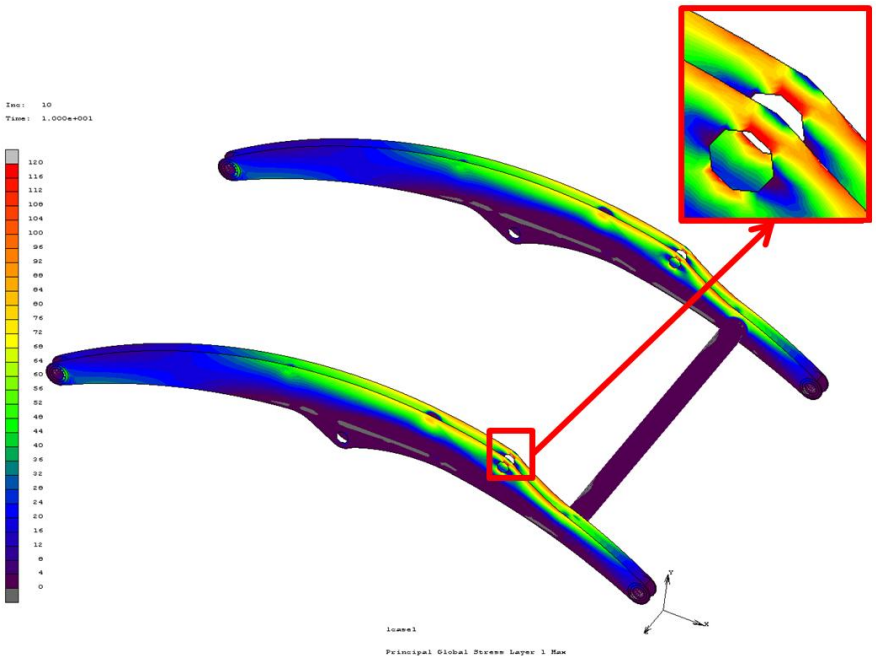

Figure 9-7 – The detailed view of stress distribution when lift cylinder is 1650 mm

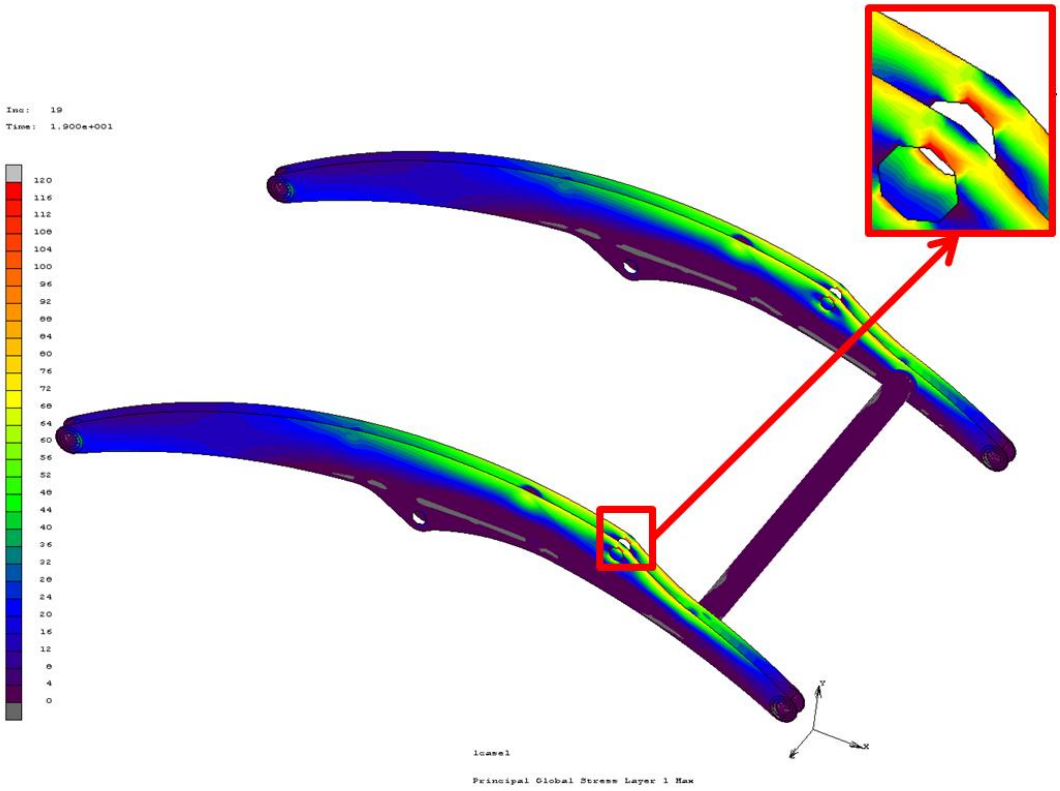

Figure 9-8 – The detailed view of stress distribution when lift cylinder is 2100 mm

Maximum Von Mises stress seen in the lift arm for Type I mechanism is 120 MPa. Therefore, the safety factor is 3.

Another structural shape is created according to the designated joints and this disjunctive structural shape can be seen in Figure 9-9. Furthermore, the side view of the disjunctive lift arm can be seen in Figure 9-10.

In this disjunctive lift arm, the structural shape is created by bending sheet metal. The bended sheet metals for one side of the lift arm are formed from 2 pieces and welded together. The meshing concept and the boundary conditions are same as described in structural shape of lift arm for Type I alternative 1 mechanism.

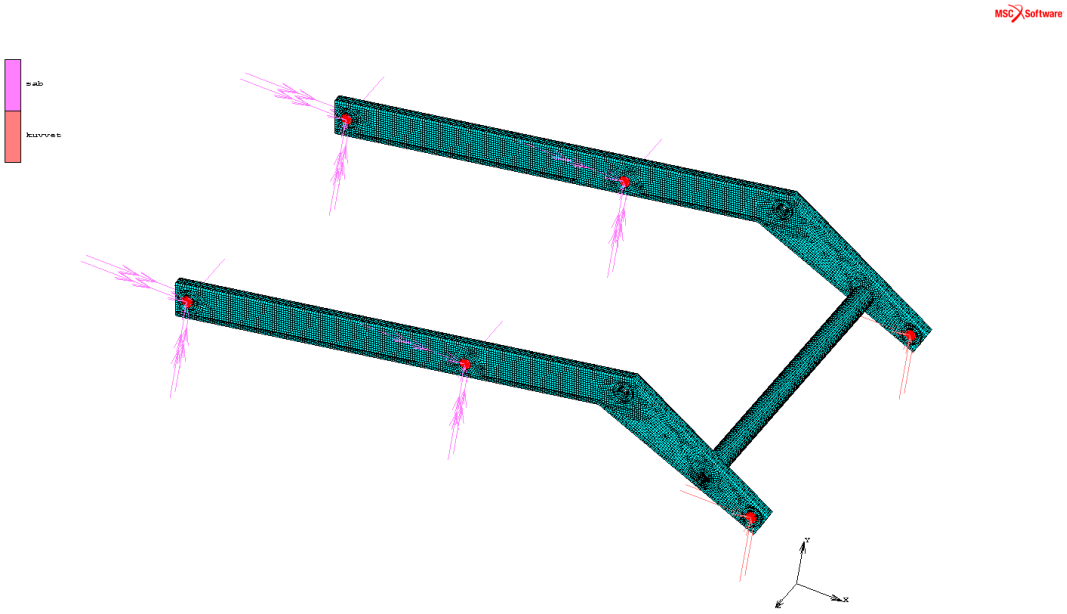

Figure 9-9 – The structural shape of alternative 2 lift arm for Type I mechanism

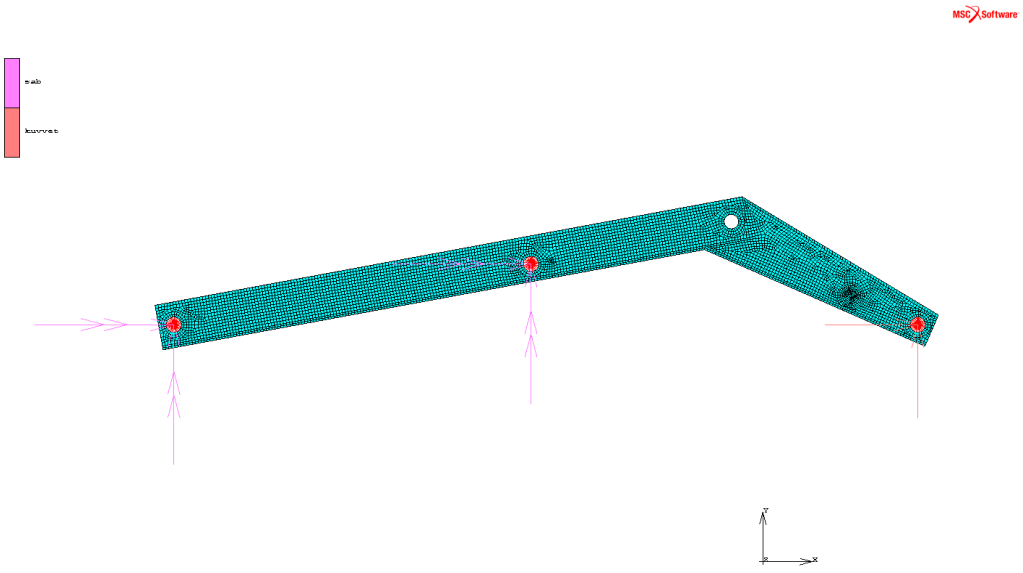

Figure 9-10 – The side view of the alternative 2 lift arm for Type I mechanism

The results at every step of the table, which can be seen in Table 9-1 are very similar to each other, so 3 of the Von Mises stress distribution, namely 1st, 10th, 19th are shown in Figure 9-11, Figure 9-12 and Figure 9-13. Moreover, detailed views of stress concentrated areas of the alternative 2 lift arm can be seen in Figure 9-14, Figure 9-15 and Figure 9-16.

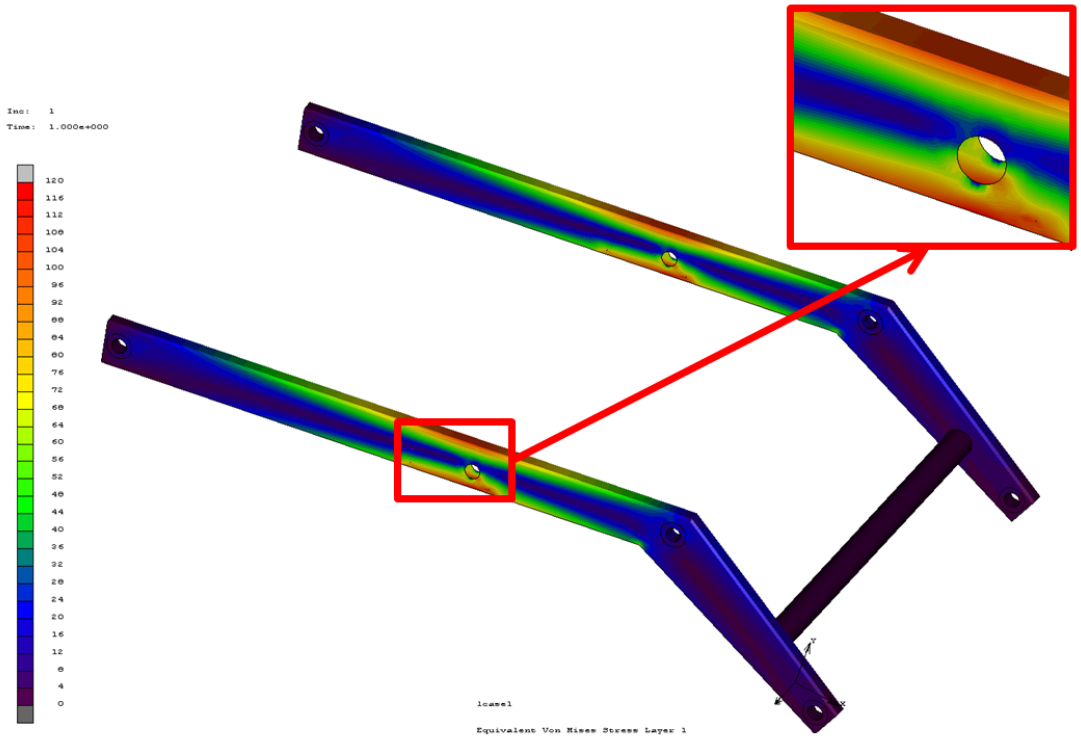

Figure 9-11 – The equivalent Von Mises stress distribution of alternative 2 lift arm when lift cylinder is 1200 mm

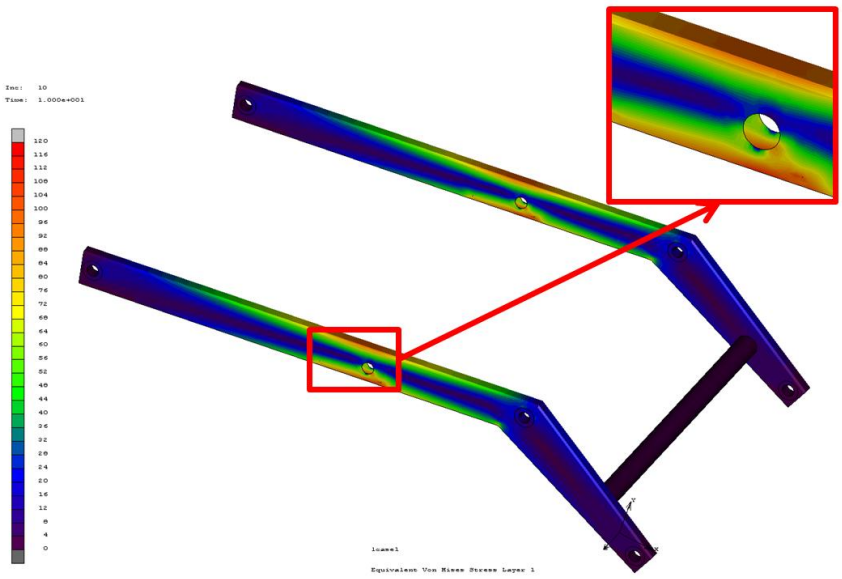

Figure 9-12 – The equivalent Von Mises stress distribution of alternative 2 lift arm when lift cylinder is 1650 mm

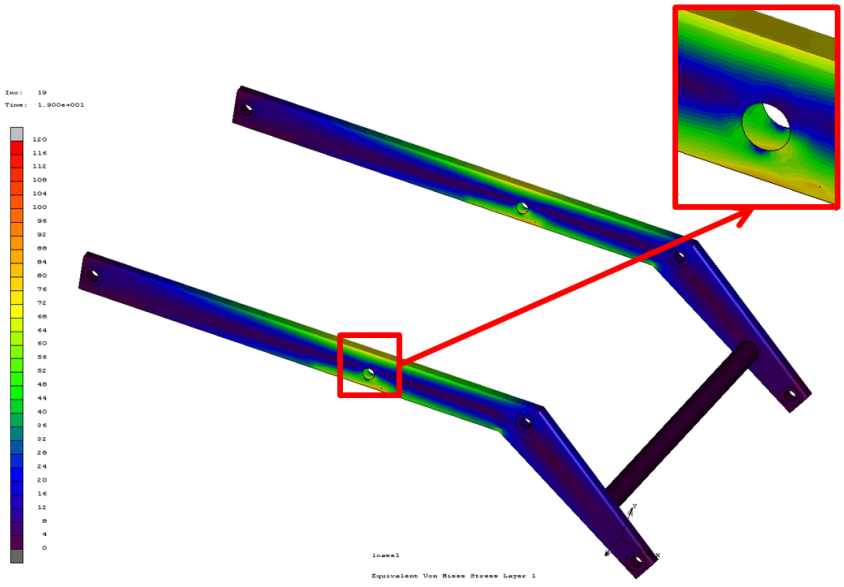

Figure 9-13 – The equivalent Von Mises stress distribution of alternative 2 lift arm when lift cylinder is 2100 mm

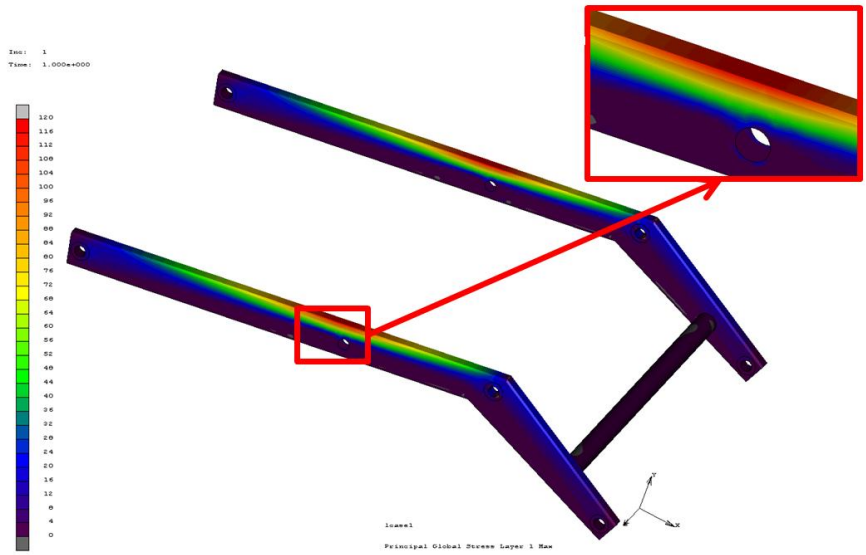

Figure 9-14 – The detailed view of stress distribution of alternative 2 lift arm when lift cylinder is 1200 mm

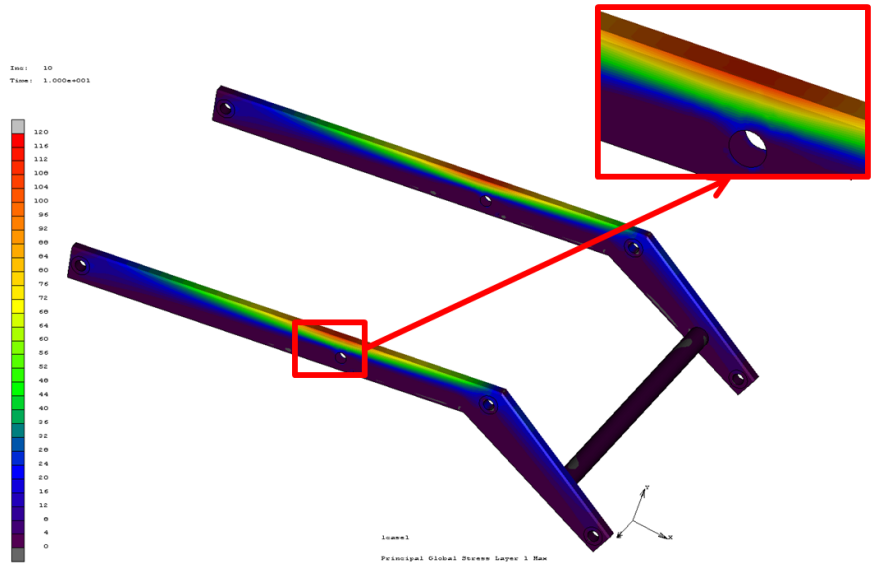

Figure 9-15 – The detailed view of stress distribution of alternative 2 lift arm when lift cylinder is 1650 mm

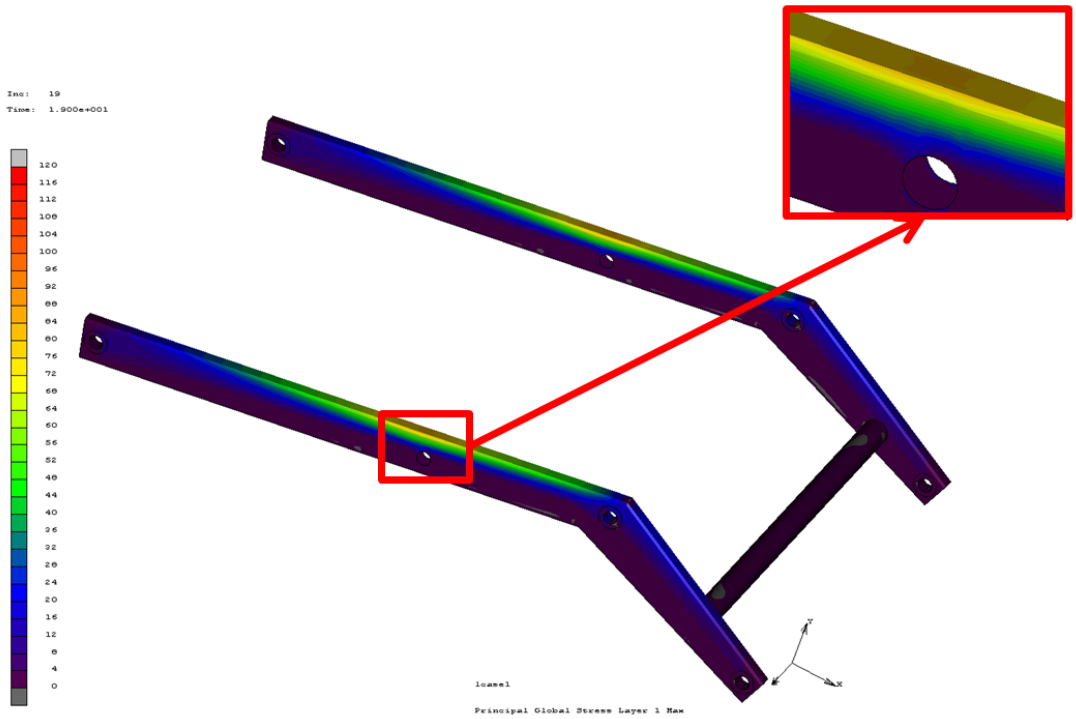

Figure 9-16 – The detailed view of stress distribution of alternative 2 lift arm when lift cylinder is 2100 mm

Maximum Von Mises stress seen in alternative 2 lift arm for Type I mechanism is also 120 MPa. Therefore, the safety factor is again 3.

However, on one hand the thickness of the sheet metals on the side of the alternative 1 lift arm is 6 mm and the intermediate plates thickness are 10 mm; on the other hand the thickness of sheet metals used in alternative 2 lift arm is 10 mm. The masses of constructions are 152 kg for alternative 1 lift arm and 203 kg for alternative 2 lift arm.

9.2 FOR TYPE II (FOUR-BAR) MECHANISM

The structural shape of lift arm of Type II mechanism, whose joints are optimized by using genetic algorithm, can be seen in Figure 9-17. A new coordinate system is defined as x axis is in $|A_0A_1|$ direction and y axis is perpendicular to $|A_0A_1|$ direction, like Type I mechanism. The new coordinate system and side view of the lift arm can be seen in Figure 9-18. A force versus lift cylinder stroke table is formed, which can be seen in Table 9-2, and given to program.

Table 9-2 – Force applied from the hinge pin versus lift cylinder stroke

lift cylinder stroke (mm)	y-component (N)	x-component (N)	lift cylinder stroke (mm)	y-component (N)	x-component (N)	lift cylinder stroke (mm)	y-component (N)	x-component (N)
1181	-19174	5662	1360	-22561	5115	1818	-20979	-7302
1182	-16849	5129	1375	-22665	4773	1836	-20874	-7819
1183	-15948	4987	1391	-22743	4403	1853	-20769	-8332
1185	-15667	5014	1407	-22796	4006	1870	-20663	-8841
1187	-15702	5127	1424	-22826	3585	1887	-20554	-9345
1190	-15915	5284	1441	-22834	3142	1903	-20441	-9843
1193	-16234	5464	1459	-22822	2680	1919	-20323	-10335
1196	-16615	5652	1477	-22791	2200	1935	-20198	-10819
1200	-17034	5839	1495	-22743	1706	1950	-20065	-11296
1205	-17472	6018	1514	-22680	1200	1966	-19923	-11763
1210	-17918	6182	1533	-22604	684	1981	-19770	-12219
1215	-18364	6328	1552	-22517	159	1995	-19604	-12663
1221	-18802	6451	1572	-22421	-371	2009	-19425	-13094
1228	-19228	6549	1591	-22318	-905	2023	-19230	-13509
1235	-19638	6618	1611	-22209	-1443	2037	-19018	-13907
1243	-20030	6656	1630	-22097	-1981	2051	-18787	-14286
1252	-20400	6661	1650	-21982	-2521	2064	-18537	-14643
1261	-20746	6632	1669	-21865	-3060	2076	-18266	-14977
1271	-21068	6567	1688	-21749	-3598	2089	-17972	-15285
1282	-21364	6467	1707	-21634	-4135	2101	-17655	-15565
1293	-21633	6330	1726	-21520	-4669	2113	-17311	-15812
1305	-21874	6157	1745	-21408	-5201	2124	-16941	-16025
1318	-22087	5947	1764	-21298	-5731	2135	-16543	-16200
1331	-22273	5703	1782	-21190	-6258			
1345	-22431	5425	1800	-21084	-6781			

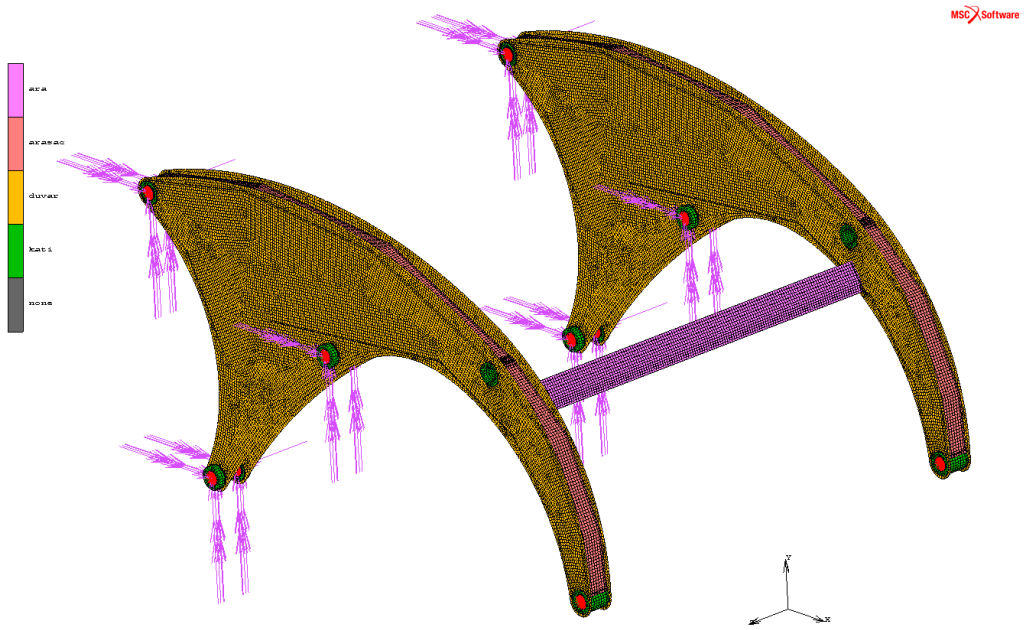

Figure 9-17 – The structural shape of lift arm for Type II mechanism

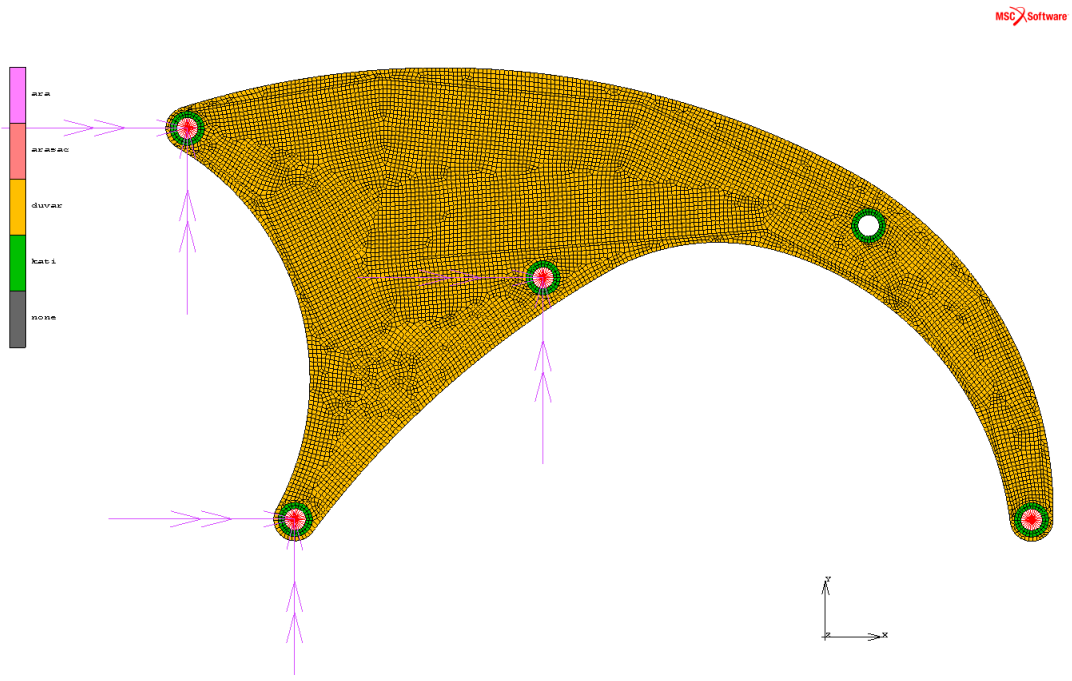

Figure 9-18 – The side view of the lift arm for Type I mechanism

The concept of using shell and solid meshes are same with Type I mechanism.

The joint which is at the intersection of rocker and lift arm, the joint which is at the intersection of crank and lift arm and the joint which is at the intersection of lift cylinder and lift arm are fixed in x, y, z directions and x, y rotations. The view representing the reaction forces formed at these joints can be seen in Figure 9-18.

The results at every step of Table 9-2 are very similar to each other, so 4 of them, namely 1st, 25th, 50th, 71th are shown in Figure 9-19, Figure 9-20, Figure 9-21 and Figure 9-22 respectively. Moreover, detailed views of stress concentrated areas are shown in Figure 9-23, Figure 9-24, Figure 9-25 and Figure 9-26.

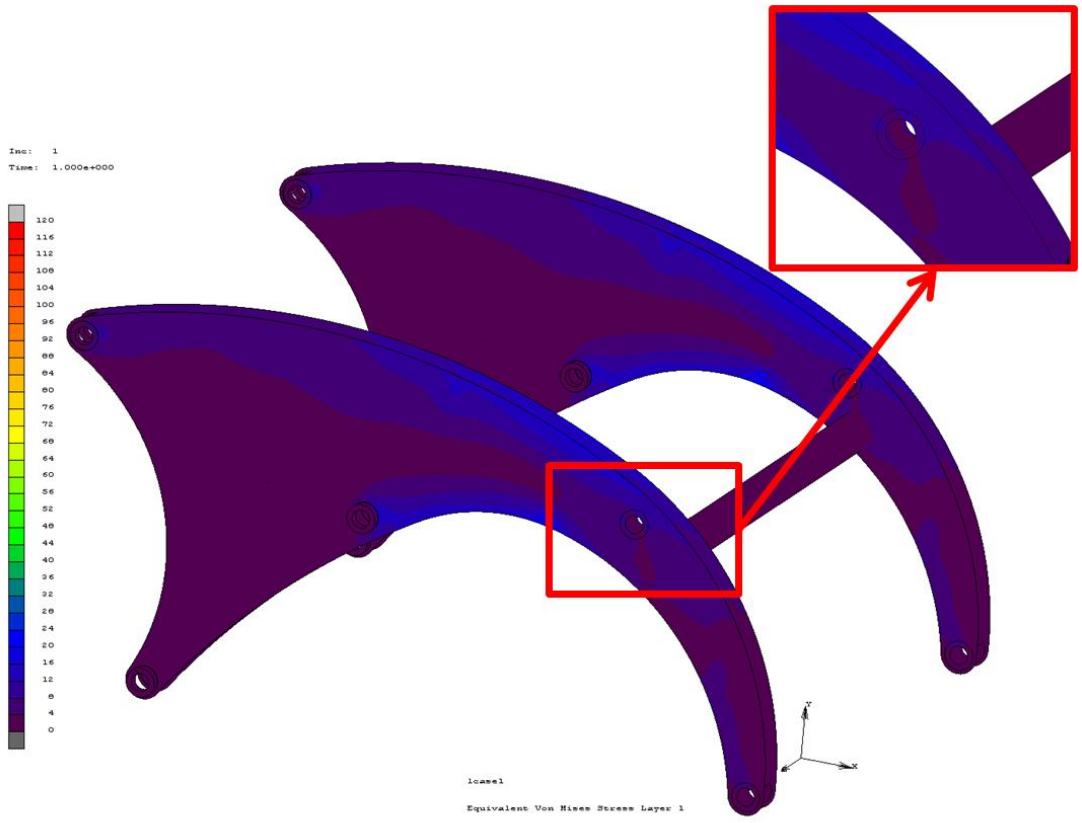

Figure 9-19 – The equivalent Von Mises stress distribution when lift cylinder is 1180 mm

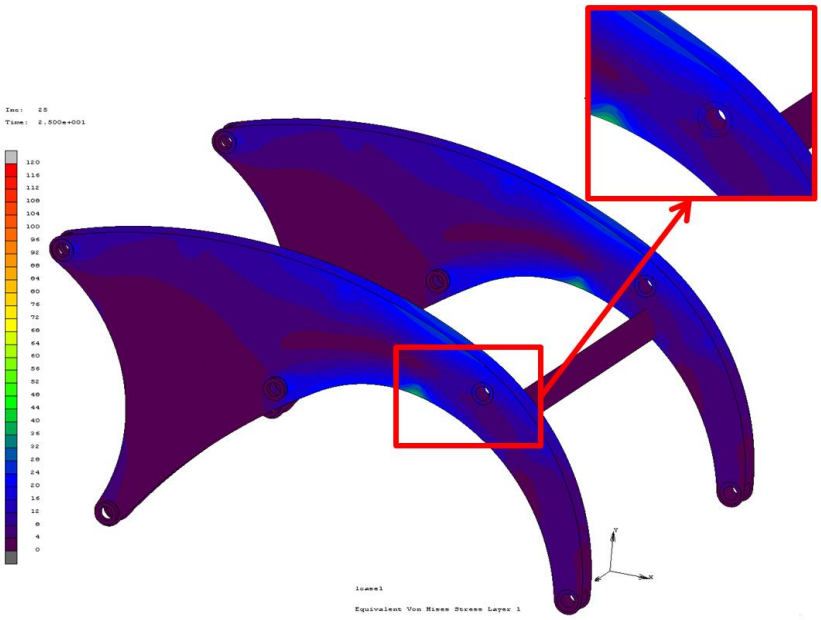

Figure 9-20 – The equivalent Von Mises stress distribution when lift cylinder is 1345 mm

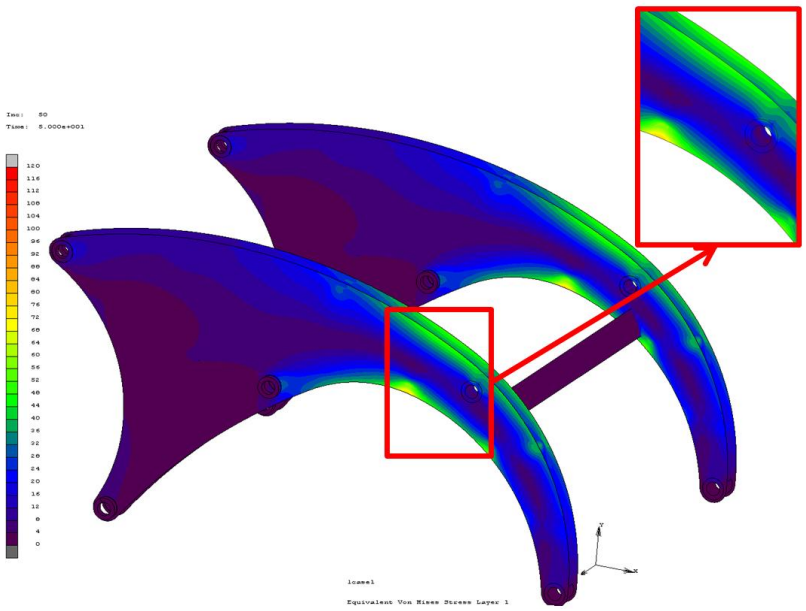

Figure 9-21 – The equivalent Von Mises stress distribution when lift cylinder is 1800 mm

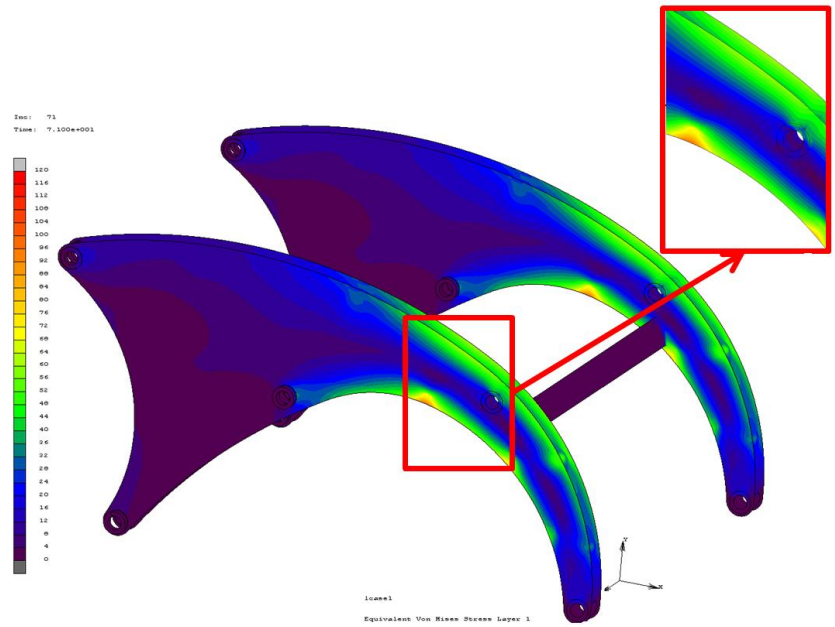

Figure 9-22 – The equivalent Von Mises stress distribution when lift cylinder is 2135 mm

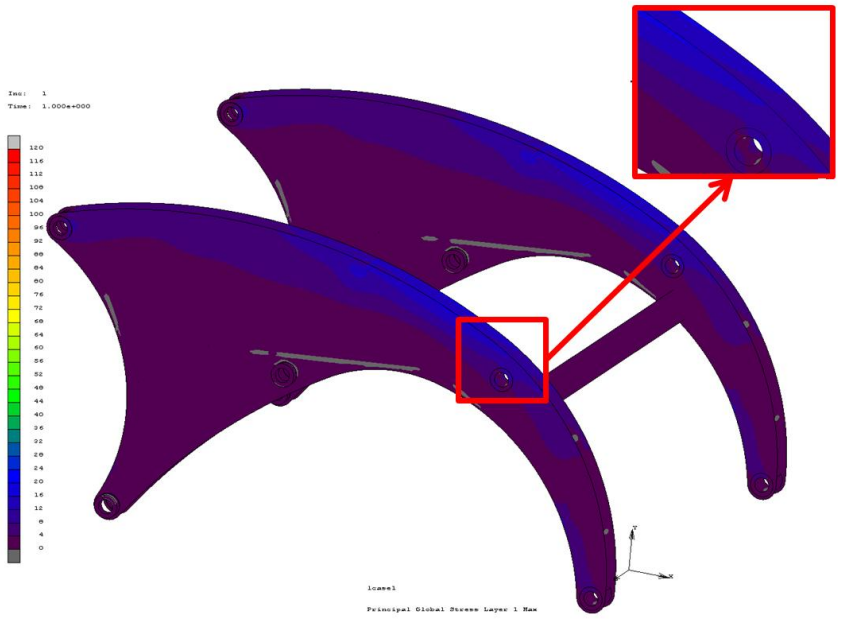

Figure 9-23 – The detailed view of stress distribution when lift cylinder is 1180 mm

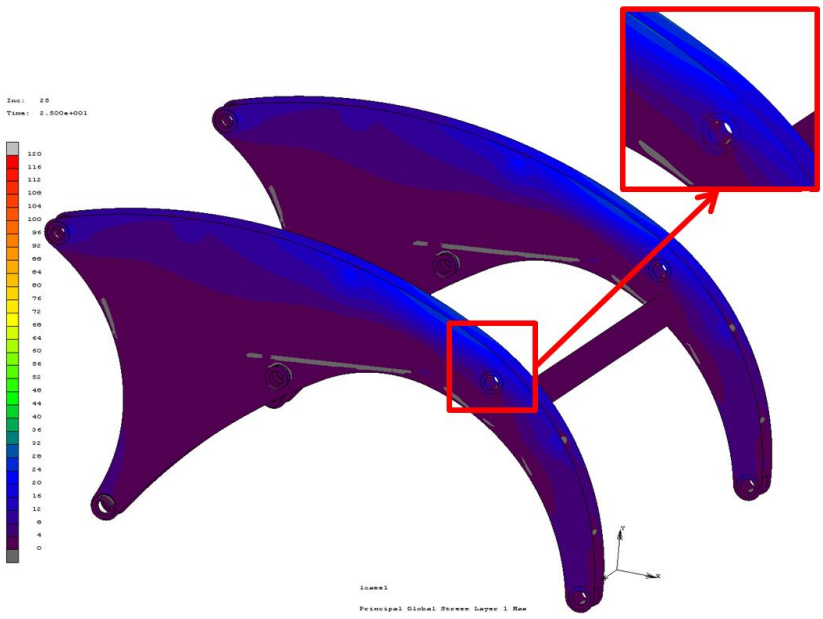

Figure 9-24 – The detailed view of stress distribution when lift cylinder is 1345 mm

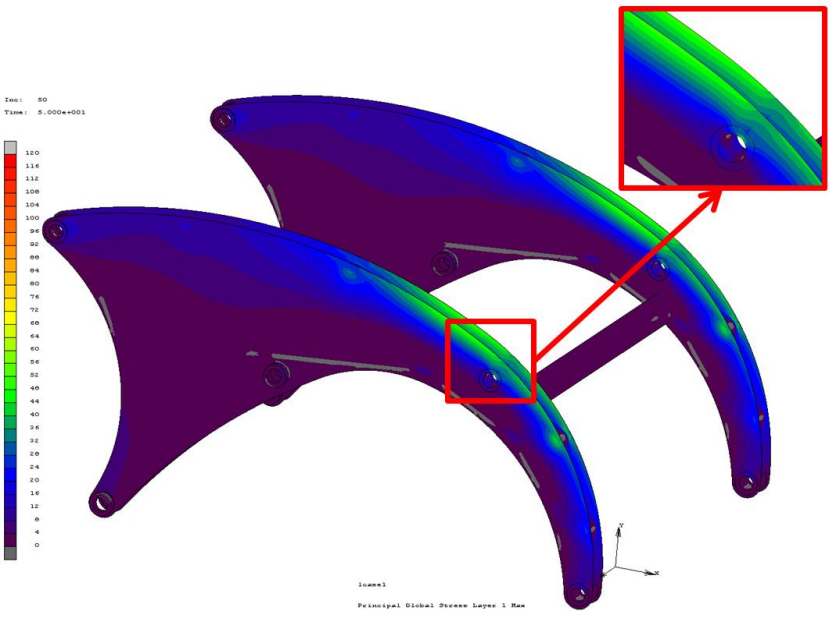

Figure 9-25 – The detailed view of stress distribution when lift cylinder is 1800 mm

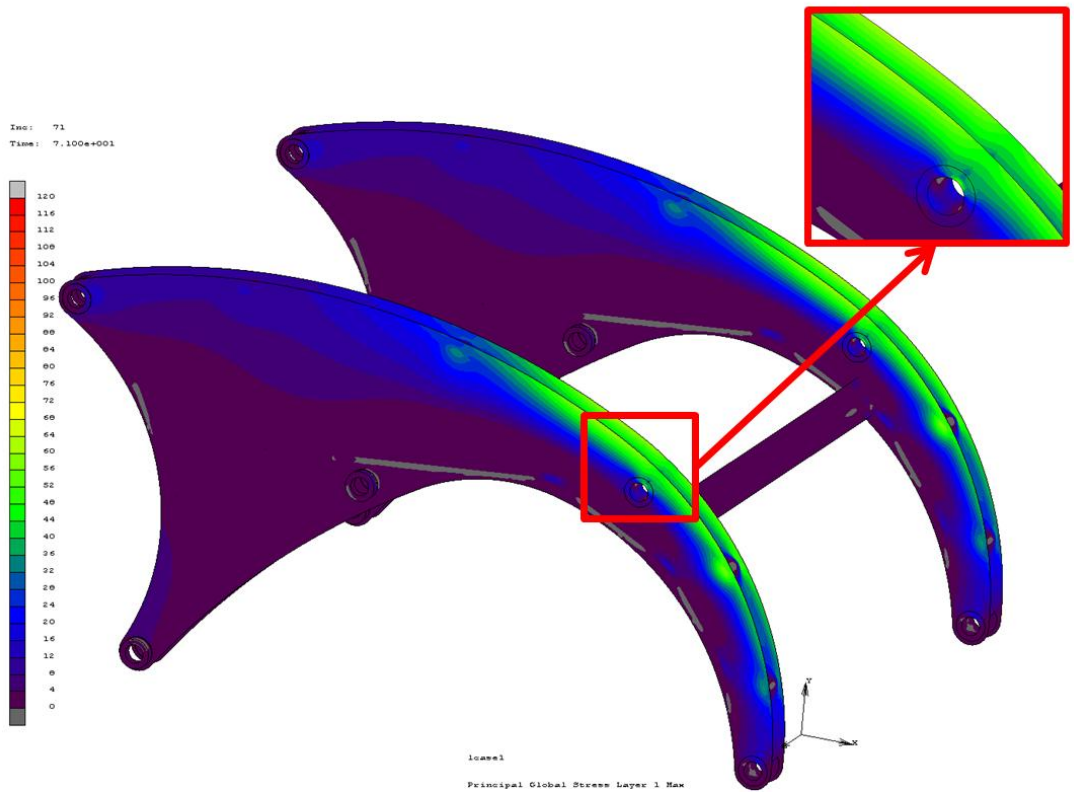

Figure 9-26 – The detailed view of stress distribution when lift cylinder is 2135 mm

Maximum Von Mises stress seen in the lift arm for Type II mechanism is 120 MPa. Therefore, the safety factor is 3.

The mechanism consisting of rocker, crank and lift arm can be seen in Figure 9-27.

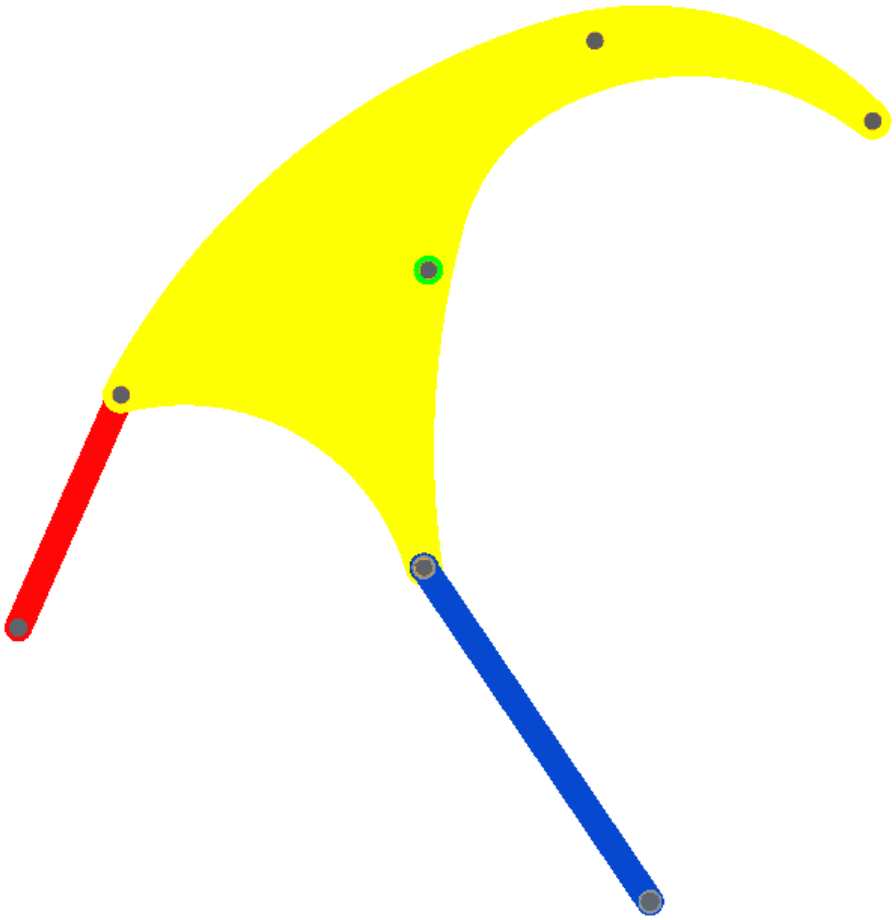

Figure 9-27 – The schematic view of alternative I lift arm for Type II mechanism

From Figure 8-16, it can be seen that the maximum force on crank is 28572 N. A finite element analysis is performed at the most critical time, namely when maximum force occurs. The crank is a two-force member, so the force is applied accordingly. The results can be seen in Figure 9-28. The maximum stress occurred in crank is 28 MPa.

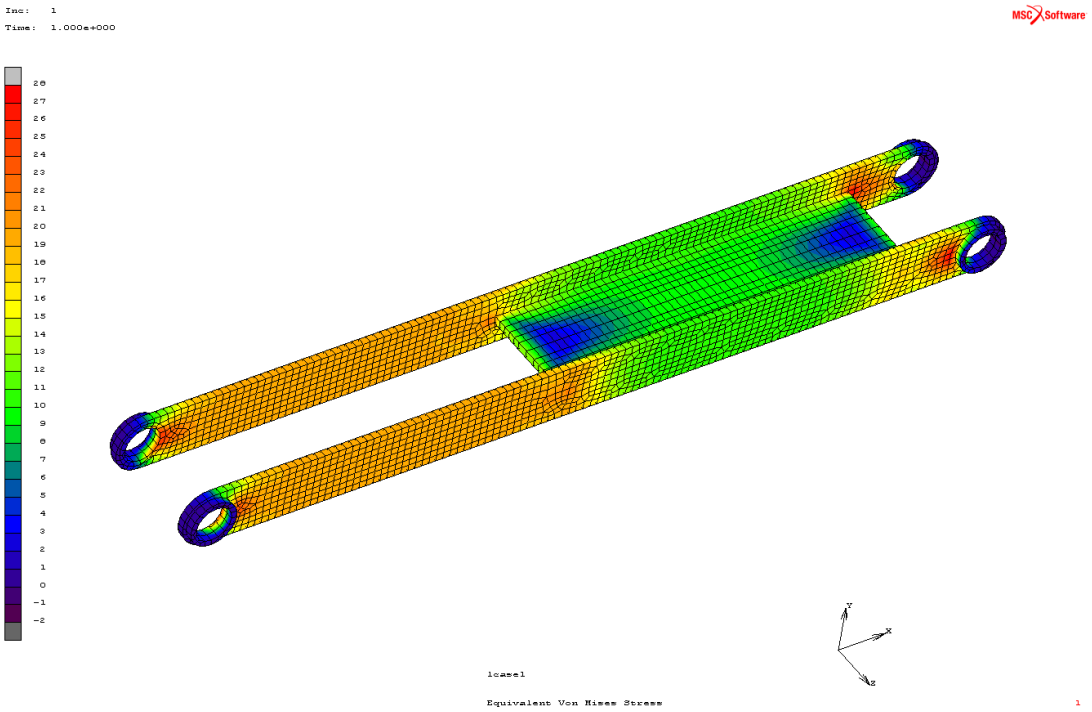

Figure 9-28 – The detailed view of stress distribution when lift cylinder is 2135 mm

From Figure 8-16, it can be seen that the maximum force on two rockers are 53068 N. The thickness of the rocker plate is 20 mm and the width is 75 mm. Therefore nominal stress can be calculated from Equation (9.1). K_t, which is shown in Equation (9.2), should be taken as 2.2 [57], so maximum stress becomes 116.75 MPa. The safety factor is calculated as 3 with these calculations.

$$\sigma_0 = \frac{F}{A_0} = \frac{F}{(\omega - d)\cdot t} = \frac{53068}{(75-50)\cdot 20\cdot 2} = 53.07 \ \text{MPa} \tag{9.1}$$

stress concentration factor: $K_t = \frac{\sigma_{max}}{\sigma_0}$ (9.2)

According to the finite element results which can be seen in Figure 9-19, Figure 9-20, Figure 9-21 and Figure 9-22 the triangular shape on the left of the lift arm is unnecessary for strength of the structure. That part is a pointless mass and the triangular shape is changed by subtracting the inner part of it. The new structural shape of lift arm can be seen in Figure 9-29. Moreover, the side view of the new structural shape can be seen in Figure 9-30.

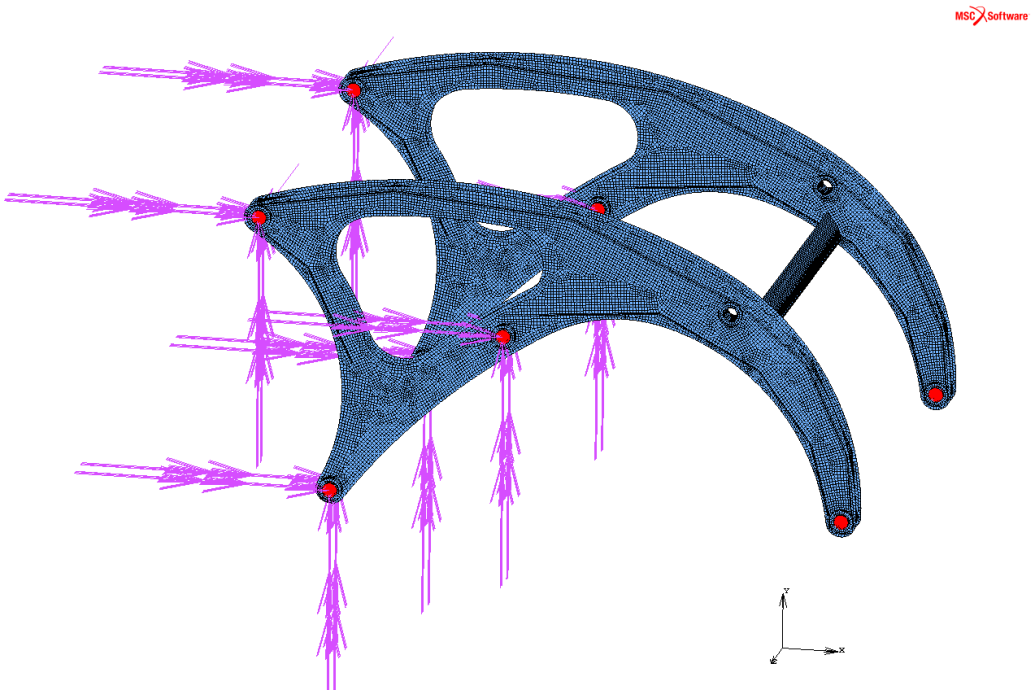

Figure 9-29 – The structural shape of alternative 2 lift arm for Type II mechanism

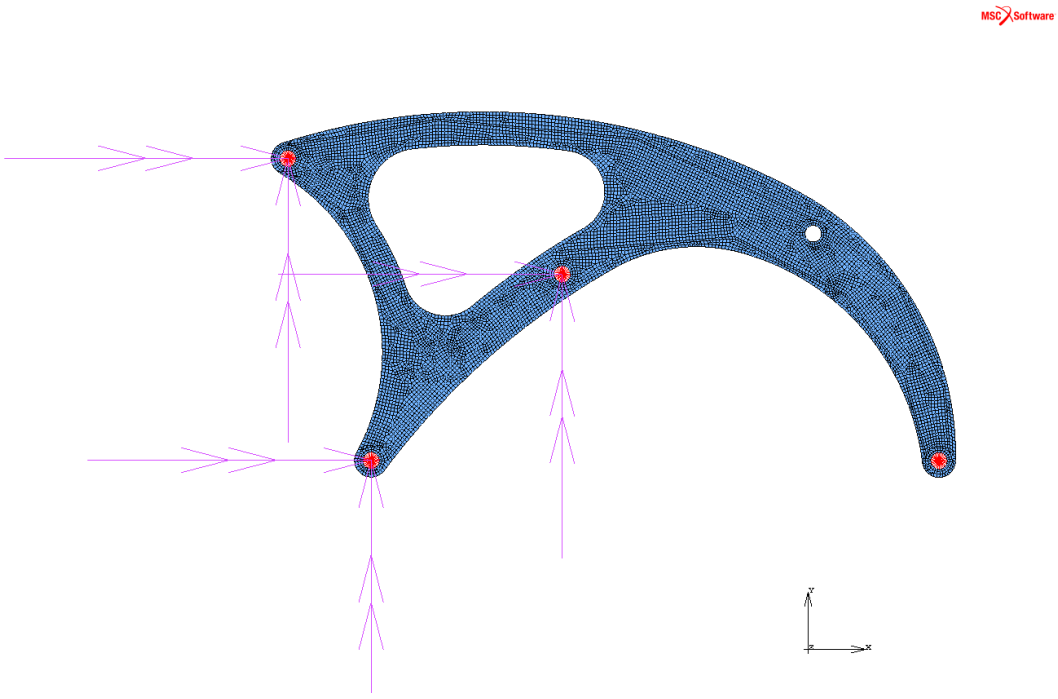

Figure 9-30 – The side view of the alternative 2 lift arm for Type I mechanism

As in the first alternative in Type II mechanism, the results at every step of the table, which can be seen in Table 9-2 are similar. Therefore, 4 of the Von Mises stress distribution, namely 1st, 25th, 50th, 71th are shown in Figure 9-31, Figure 9-32, Figure 9-33 and Figure 9-34. Moreover, detailed views of stress concentrated areas of the alternative 2 lift arm can be seen in Figure 9-35, Figure 9-36, Figure 9-37 and Figure 9-38 respectively.

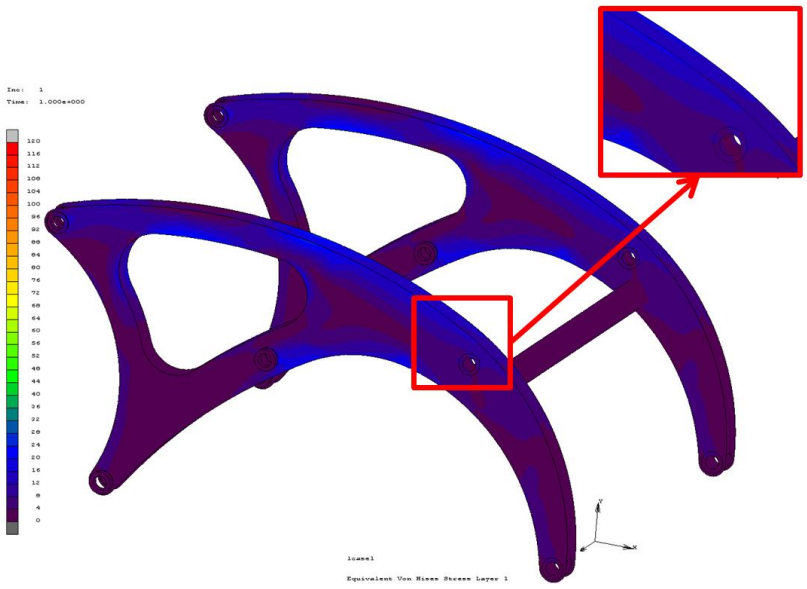

Figure 9-31 – The equivalent Von Mises stress distribution of alternative 2 lift arm when lift cylinder is 1180 mm

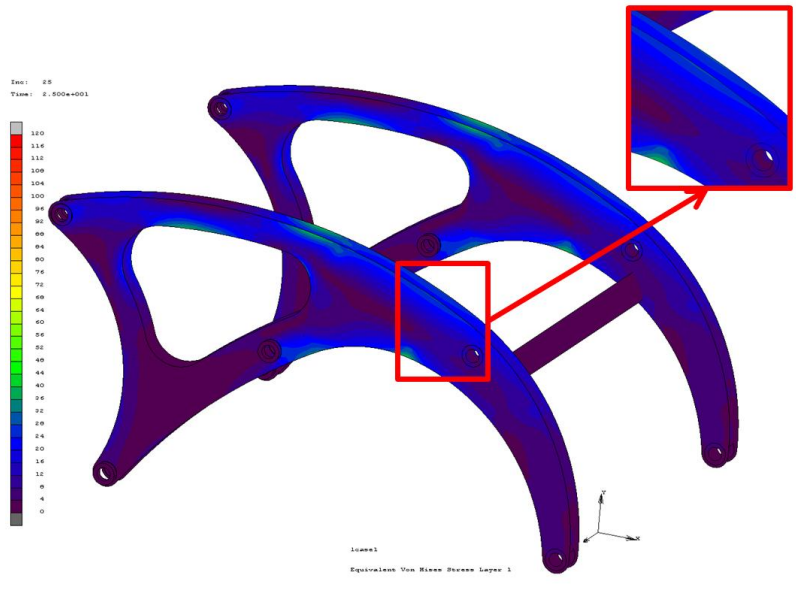

Figure 9-32 – The equivalent Von Mises stress distribution of alternative 2 lift arm when lift cylinder is 1345 mm

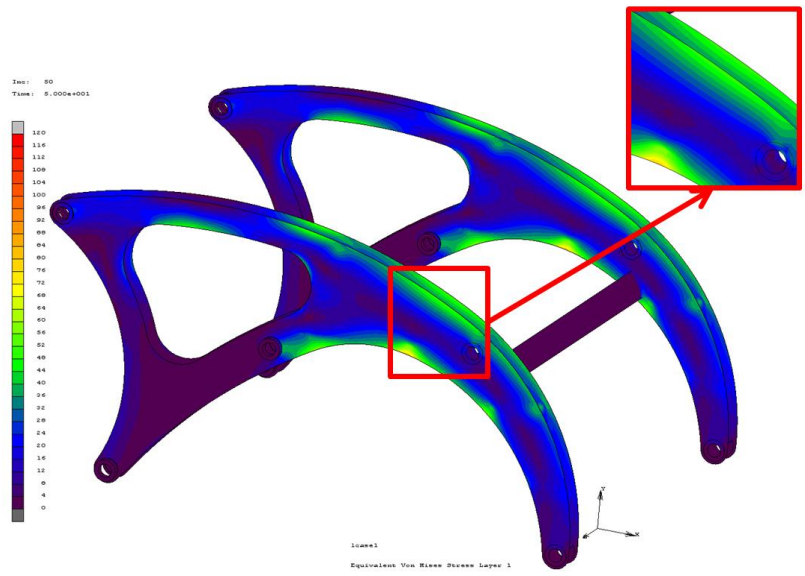

Figure 9-33 – The equivalent Von Mises stress distribution of alternative 2 lift arm when lift cylinder is 1800 mm

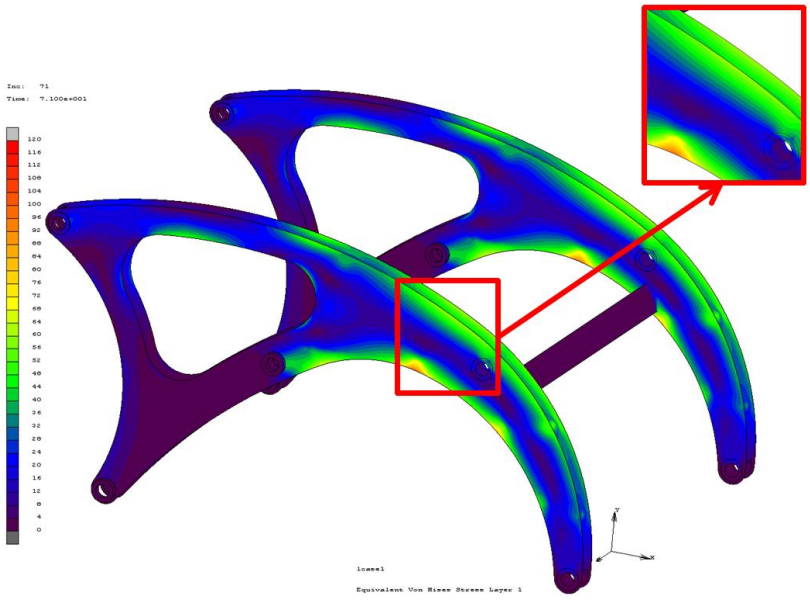

Figure 9-34 – The equivalent Von Mises stress distribution of alternative 2 lift arm when lift cylinder is 2135 mm

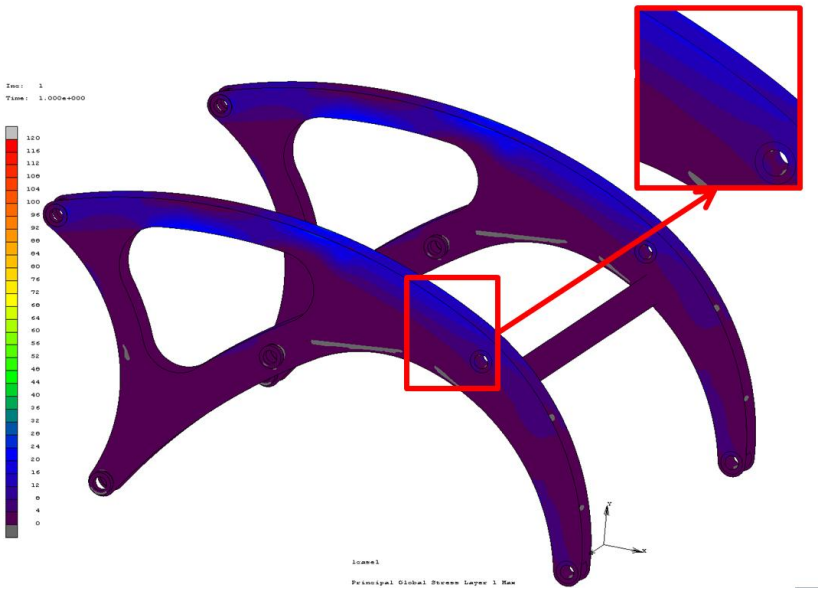

Figure 9-35 – The detailed view of stress distribution of alternative 2 lift arm when lift cylinder is 1180 mm

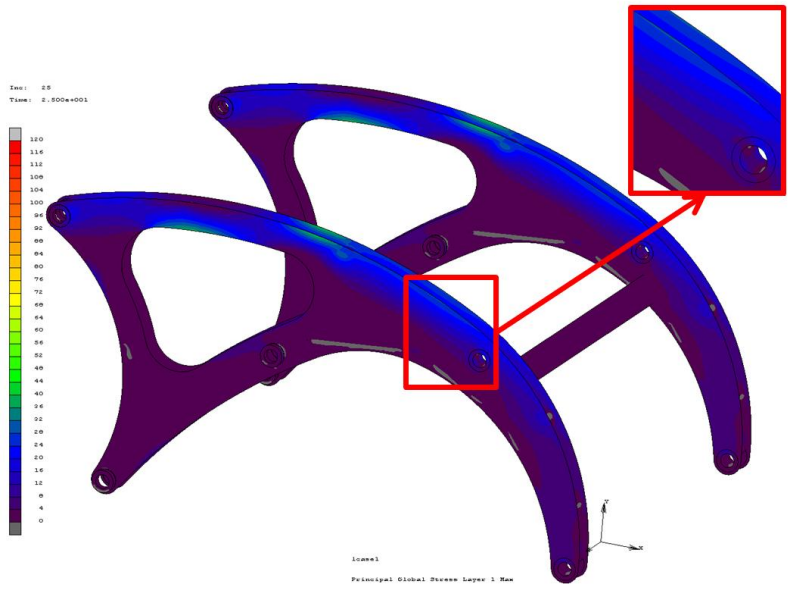

Figure 9-36 – The detailed view of stress distribution of alternative 2 lift arm when lift cylinder is 1345 mm

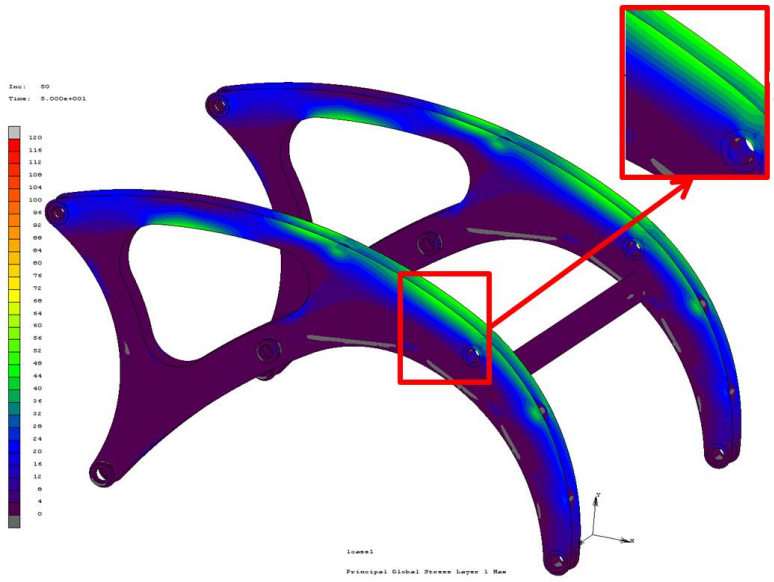

Figure 9-37 – The detailed view of stress distribution of alternative 2 lift arm when lift cylinder is 1800 mm

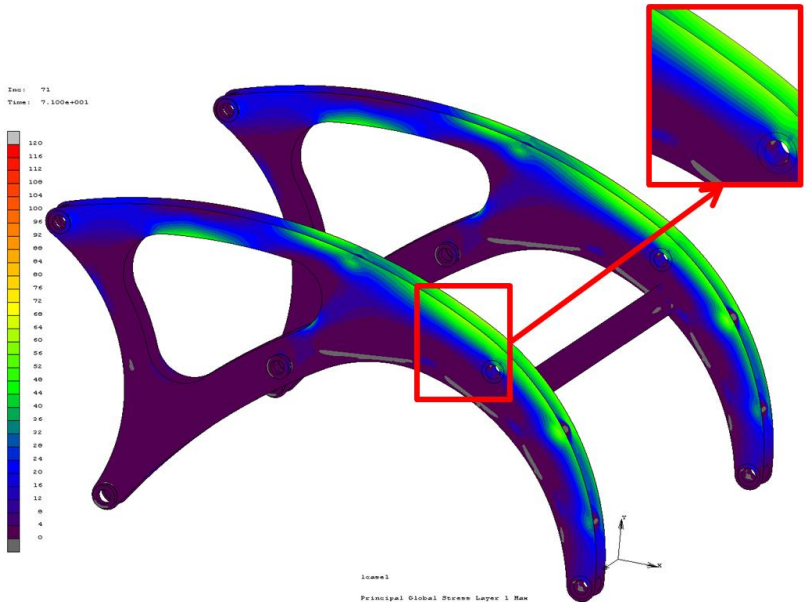

Figure 9-38 – The detailed view of stress distribution of alternative 2 lift arm when lift cylinder is 2135 mm

Maximum Von Mises stress seen in alternative 2 lift arm for Type II mechanism is also 120 MPa. Therefore, the safety factor is again 3.

In the first alternative the mass of the lift arm is 231 kg and in the second alternative the mass of the lift arm is 180 kg. Besides, the second alternative is still far away from safety factor of 3. Therefore, a new analysis is made by changing the thickness of the sheet metals from 6 mm to 4 mm. The most critical step is 71th so it is enough to look over that step only. Maximum Von Mises stress and detailed global stress of the 71th step can be seen in Figure 9-39 and Figure 9-40 respectively.

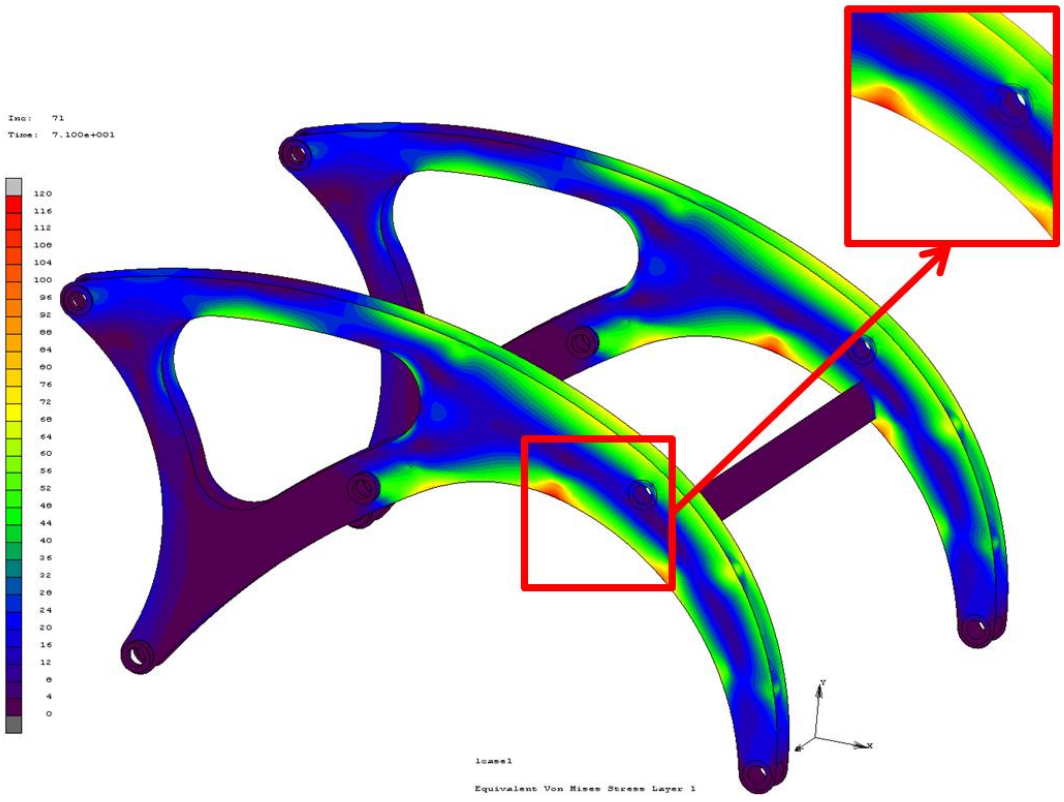

Figure 9-39 – The equivalent Von Mises stress distribution of alternative 3 lift arm when lift cylinder is 2135 mm

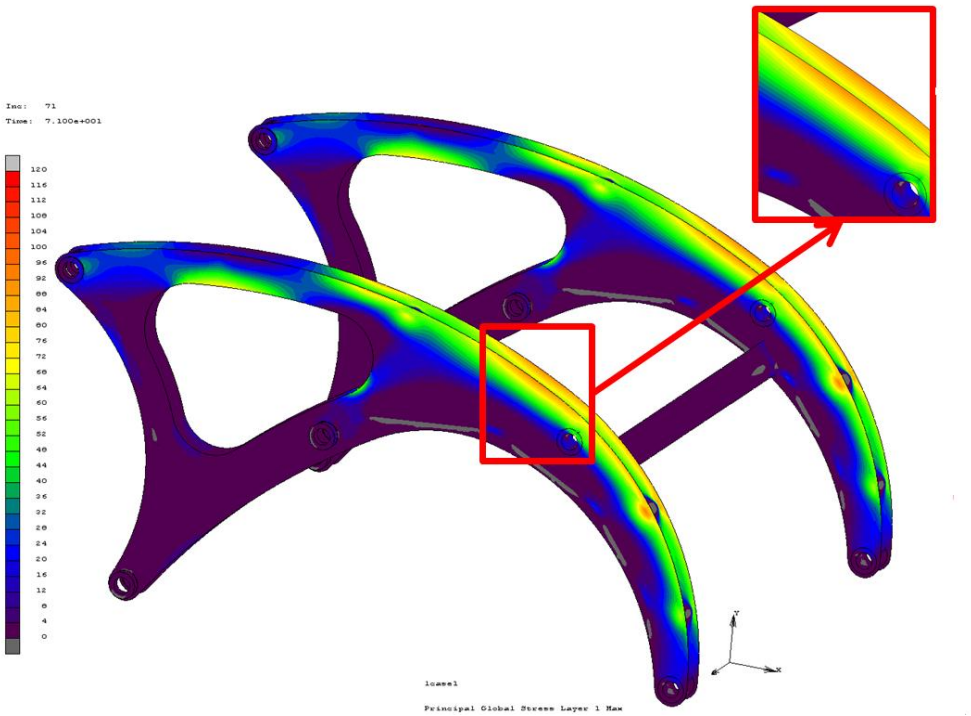

Figure 9-40 – The detailed view of stress distribution of alternative 3 lift arm when lift cylinder is 2135 mm

Finally, maximum Von Mises stress seen in alternative 3 lift arm for Type II mechanism becomes 120 MPa and the safety factor becomes 3. The mass of this alternative is 125 kg.

Another structural shape is created according to the designated joints and this disjunctive structural shape and its side view can be seen in Figure 9-41 and Figure 9-42 respectively.

The meshing concept and the boundary conditions are same as described in structural shape of lift arm for Type II alternative 1, 2, 3 mechanisms. The Von Mises stress distribution, namely 1st, 25th, 50th and 71th are shown in Figure 9-43, Figure 9-44, Figure 9-45, Figure 9-46 and detailed stress distributions on stress concentrated areas can be seen in Figure 9-47, Figure 9-48, Figure 9-49, Figure 9-50. The alternative 4 lift arm is composed of 6 mm sheet metals and has a mass of 147 kg.

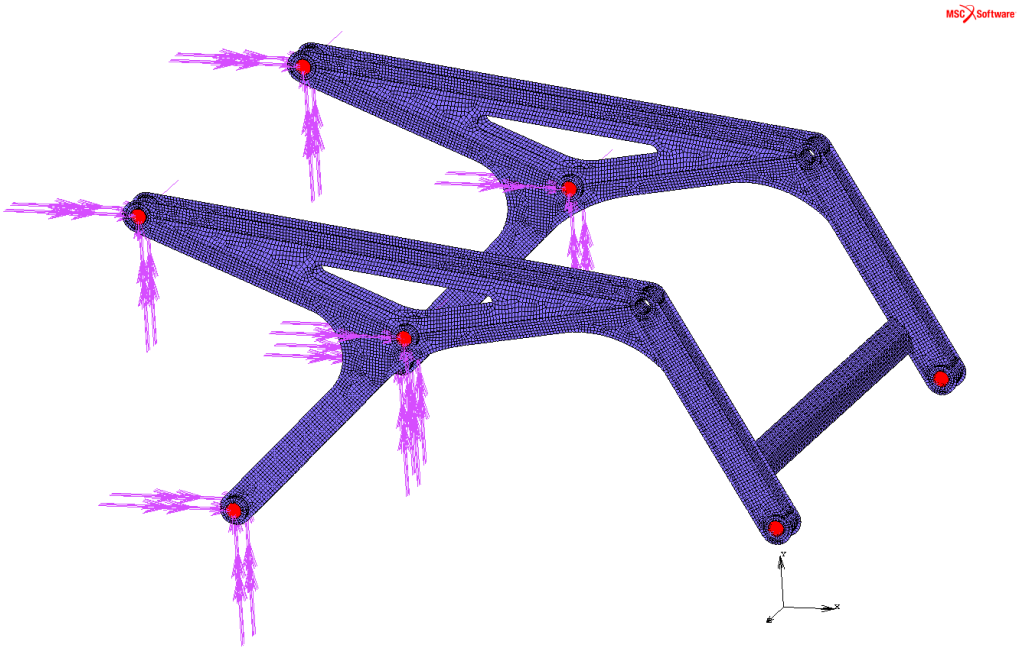

Figure 9-41 – The structural shape of alternative 4 lift arm for Type II mechanism

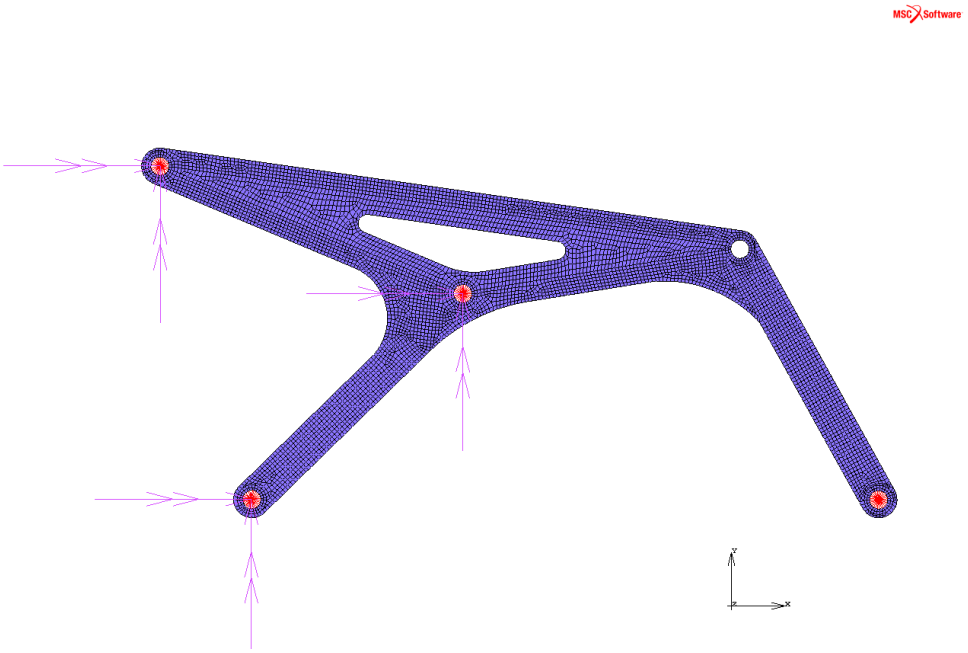

Figure 9-42 – The side view of the alternative 4 lift arm for Type II mechanism

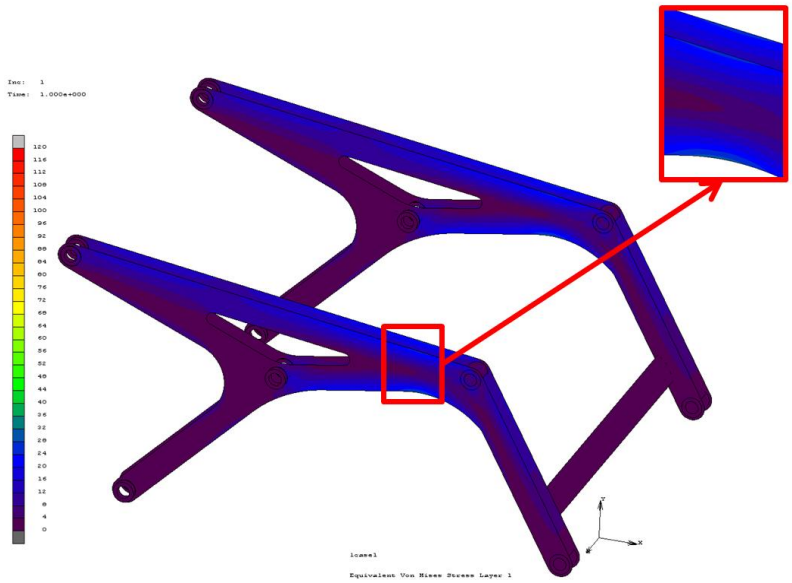

Figure 9-43 – The equivalent Von Mises stress distribution of alternative 4 lift arm when lift cylinder is 1180 mm

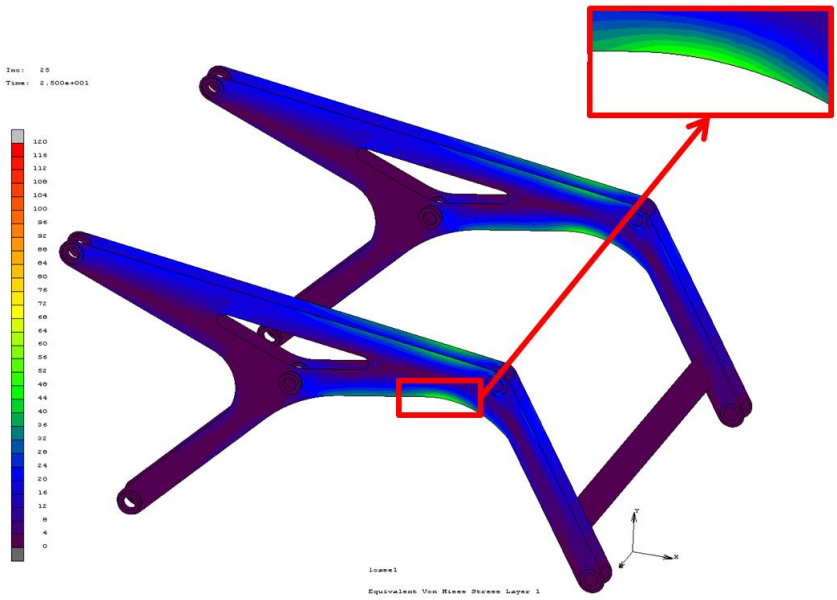

Figure 9-44 – The equivalent Von Mises stress distribution of alternative 4 lift arm when lift cylinder is 1345 mm

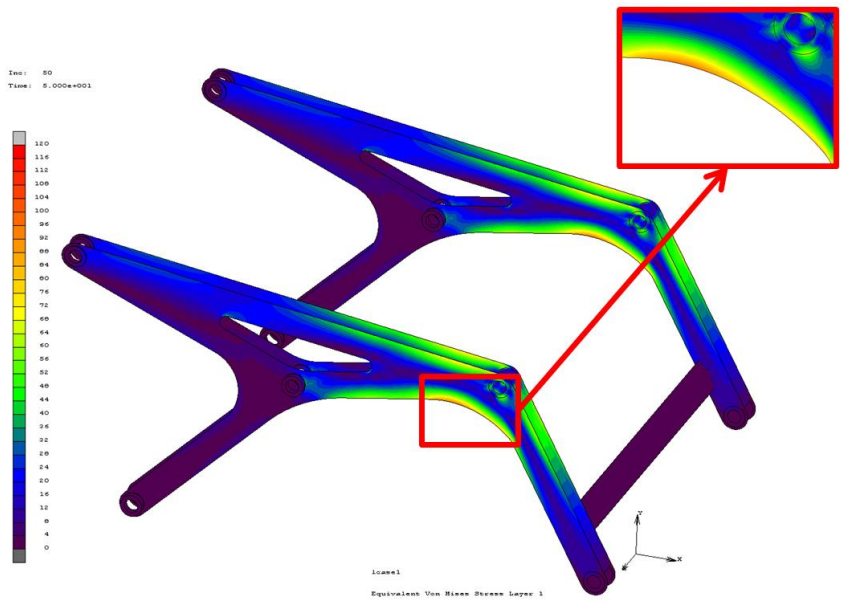

Figure 9-45 – The equivalent Von Mises stress distribution of alternative 4 lift arm when lift cylinder is 1800 mm

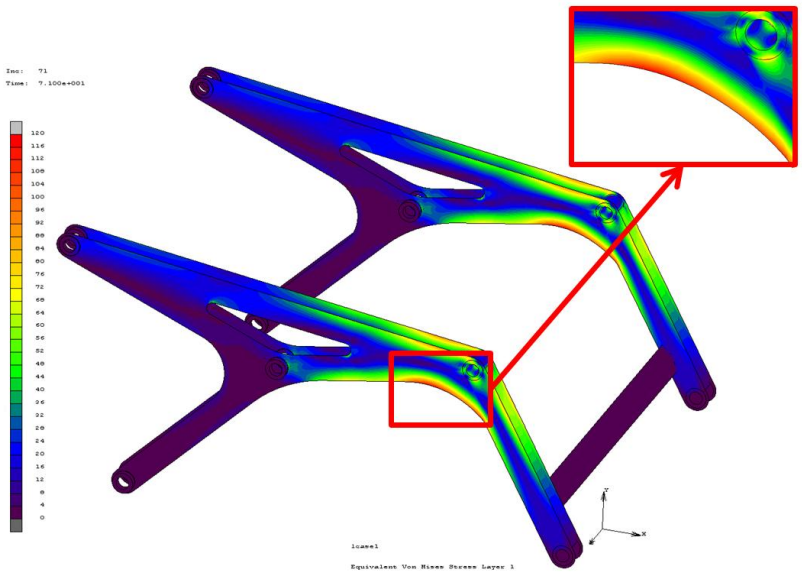

Figure 9-46 – The equivalent Von Mises stress distribution of alternative 4 lift arm when lift cylinder is 2135 mm

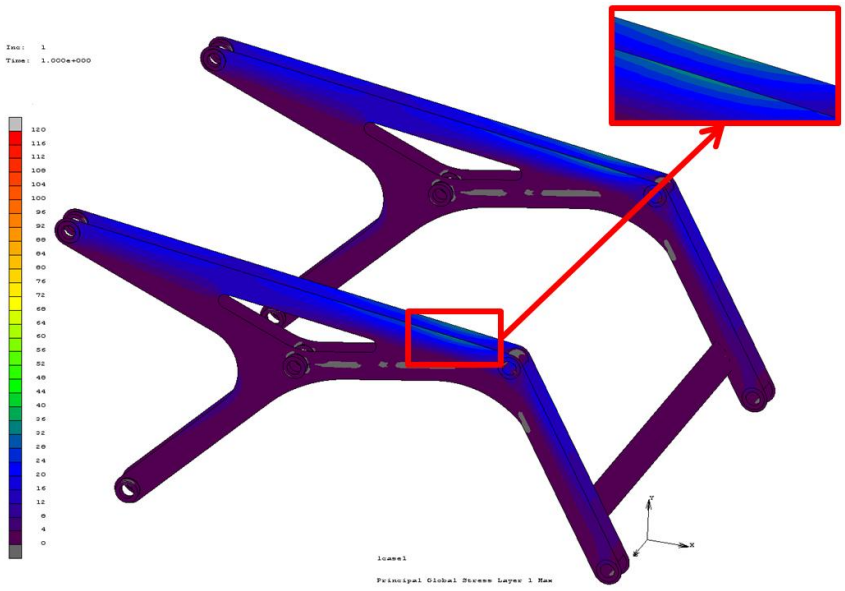

Figure 9-47 – The detailed view of stress distribution of alternative 4 lift arm when lift cylinder is 1180 mm

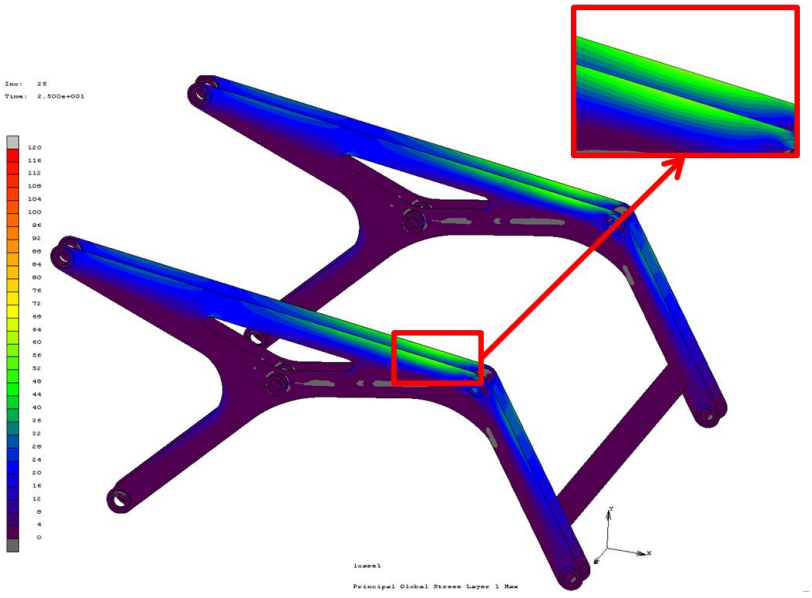

Figure 9-48 – The detailed view of stress distribution of alternative 4 lift arm when lift cylinder is 1345 mm

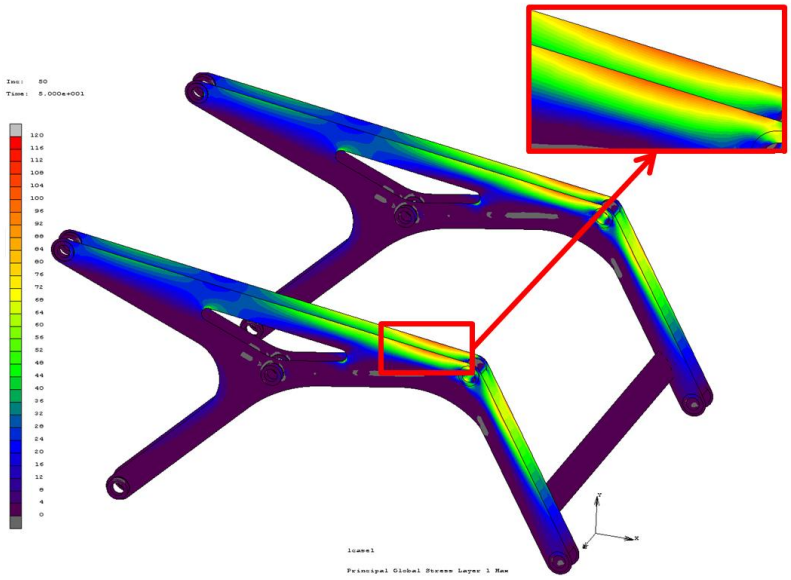

Figure 9-49 – The detailed view of stress distribution of alternative 4 lift arm when lift cylinder is 1800 mm

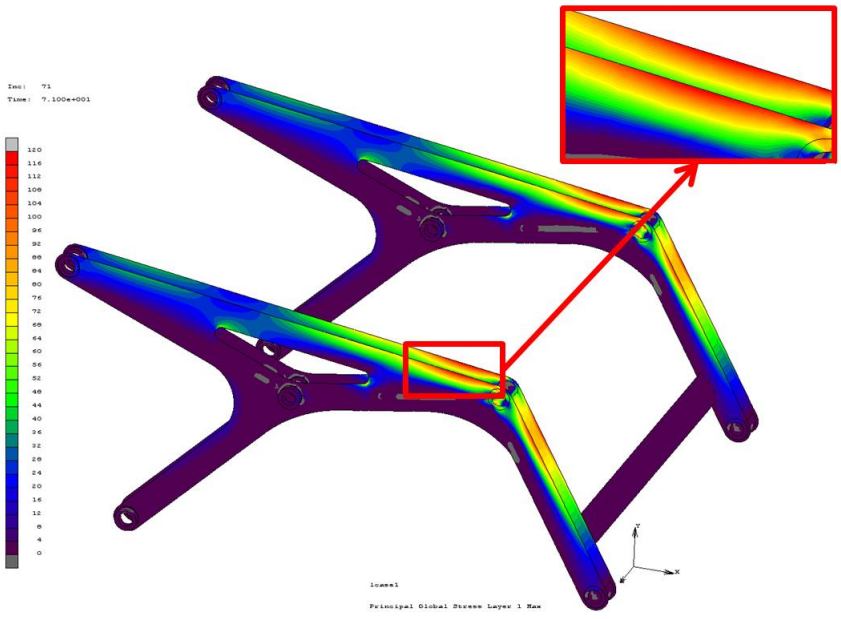

Figure 9-50 – The detailed view of stress distribution of alternative 4 lift arm when lift cylinder is 2135 mm

CHAPTER 10

RESULTS, DISCUSSION AND CONCLUSION, FUTURE WORK

The two types of skid-steer loaders according to their lift arm is either 9 links or 11 links complex mechanism. Besides, it is desired to improve several outputs while satisfying the design criteria. Therefore, classical methods of synthesis cannot be applied and genetic algorithm is selected for its multi-criteria optimization ability with constraints. In this study, a genetic algorithm program is implemented to Microsoft Excel to design a skid-steer loader mechanism.

In this thesis, genetic algorithm is used as an intermediate step for decision making. With the genetic algorithm program, the mechanism synthesis is performed to determine the basic link dimensions for the mechanism of the loader. The best individual is improved from first generation to last generation, and when the fitness value of the individual cannot grow anymore, the optimization is stopped. A final optimization is made between all best individuals from all trials and the ultimate best individual is selected for both types of mechanism. The path of the hinge pin of Type II mechanism can be seen in red in Figure 10-1. Besides, the path of the hinge pin of Type I mechanism can be seen in orange in Figure 10-2.

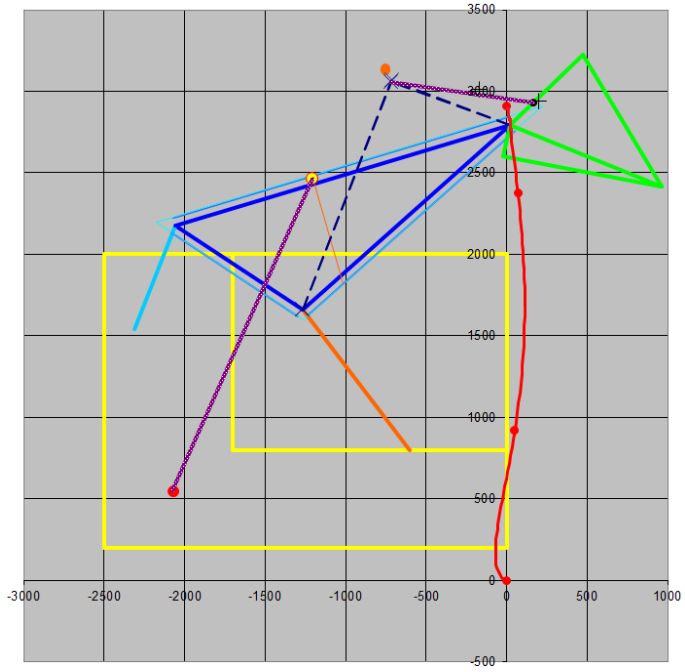

Figure 10-1 – The path of the hinge pin of the best Type II mechanism

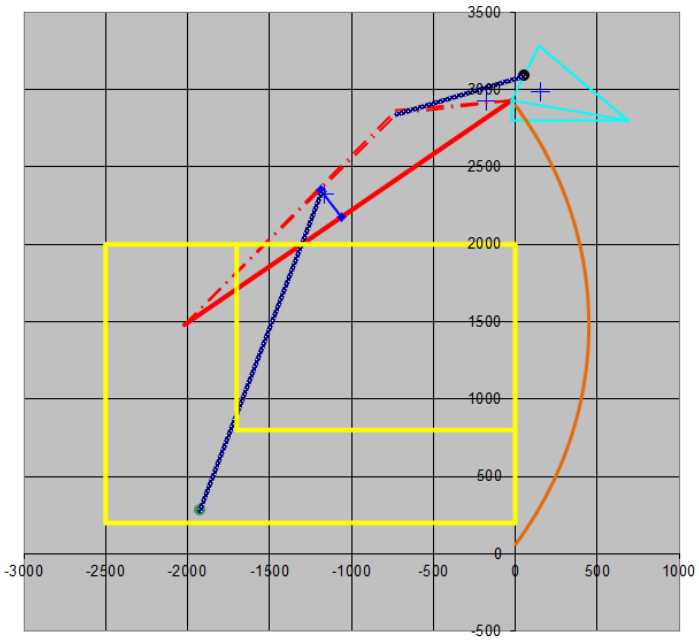

Figure 10-2 – The path of the hinge pin of the best Type II mechanism

It should not be forgotten that with different weight factors the mechanism that is going to be found will be different, most probably, from the ones found in this thesis. Besides, with different fitness function parameters the mechanism again will be different from these ones. Moreover, with different initial populations the best mechanism again will be different, but this disadvantage of diversity on the results can be eliminated by running the program many times. The crucial thing is not to find a solution after many runs of the program but to develop a method for the solution of the problem. The parameters and weight factors of the fitness function can change abundantly for other problems but if the method can be understood it is possible to adapt this method to any problem.

After synthesis, the hydraulic cylinders dimensions and working pressure of the loader mechanism is selected according to static force analysis results. 3D modeling of the loader mechanism is made and it is improved according to the results of finite element analysis. The vital thing that should not be forgotten is that the aim of the thesis is not shape optimization. Shape optimization is beyond the topic of this thesis. The shape of the skid-steer loader mechanisms is constructed from the experience of Hidromek Inc. and from the inspection of the other companies' skid-steer loader models. For Type I mechanism, the structural shape of alternative 1 is better than alternative 2 because it has similar maximum Von Mises stress while alternative 1 is 152 kg and alternative 2 is 203 kg. For Type II mechanism, the structural shape of alternative 3 is the best one because it has the least mass, 125kg, among others.

Each alternative satisfy all design criteria. Moreover, they are capable of lifting more mass through the cylinder stroke and they have higher breakout forces than the other machines having same size. From the benchmark study, it is seen that there are exiguous properties, listed on the brochures, to compare. The most important property from the exiguous properties is the breakout force. The tables that show the comparison of the breakout forces for both mechanisms can be seen in Table 10-1 and in Table 10-2. The breakout force for the best mechanism found in this thesis is 2645 kg for Type I mechanism and 1825 kg for Type II mechanism.

Table 10-1 – The comparison of average breakout forces of competitors for Type I mechanism

Competitor Number	Average Breakout Forces of a Company (kg)
Competitor 1	1260
Competitor 2	1435
Competitor 3	1870
Competitor 4	2200
Competitor 5	2250

Table 10-2 – The comparison of average breakout forces of competitors for Type II mechanism

Competitor Number	Average Breakout Forces of a Company (kg)
Competitor 1	1240
Competitor 2	1500
Competitor 3	1360
Competitor 4	1410

The genetic algorithm program can be applied to any skid-steer loader mechanism whose criteria are specified.

As mentioned in the Introduction Chapter, the designer has to use his/her intuition and experience while selecting the most suitable mechanism dimensions out of the possible combinations, that is why the designer plays a major role in design. It should not be forgotten that the design is something subjective. According to the specifications of the designer, many different solutions can be found for same problem. The important thing is to specify the parameters and their weight factors that should be maximized.

The synthesis can be improved either by decreasing the increment of parameters of by enlarging the lower and upper limits of parameters. Besides, changing the possible pivot positions, the sizes of both the machine and the cab, can be another improvement method.

The alternatives in this thesis are just examples for structural shape of the lift arm. They can be improved various ways. In this thesis, genetic algorithm is used to optimize the mechanism not the structural shape. A genetic algorithm program can be written optimizing the structural shape of this optimized mechanism.

REFERENCES

[1] ISO 6165, Earth-moving Machinery - Basic Types - Identifications and Terms and Definitions, 2006.

[2] ISO 7131, Earth-moving Machinery - Loaders - Terminology and Commercial Specifications, 2009.

[3] Bobcat, http://www.bobcat.com/loaders/skidsteer/ , 15 June 2011.

[4] JCB, http://www.jcb.com/products/MachineOverview.aspx?RID=12 , 15 June 2011.

[5] Çakır, M. K., *Structural Optimization of a Trainer Aircraft Wing by Using Genetic Algorithm*, Department of Mechanical Engineering, Middle East Technical University, September 2008.

[6] New Holland, http://europe.construction.newholland.com/family.php , 15 June 2011.

[7] Hartenberg, S. R., Denavit, J., *Kinematic Synthesis of Linkages*, McGraw-Hill Book Company, USA, 1964.

[8] Chase, T. R., Erdman, A. G., Riley, D. R., *Improved Center-Point Curve Generation Techniques for Four-Precision Position Synthesis Using the Complex Number Approach*, Transactions of ASME, Vol. 107, September, 1985.

[9] Harrisberger, L., *Mechanization of Motion*, John Wiley & Sons Inc., New York, 1961.

[10] Erdman, A. G., Sandor, G. N., *Mechanism Design Analysis and Synthesis Volume I*, 2nd edition, Prentice Hall, New Jersey, 1991.

[11] Sandor, G. N., *A General Complex Number Method for Plane Kinematic Synthesis with Applications*, Ph. D. Dissertation, Department of Mechanical Engineering, Columbia University, 1959.

[12] Freudenstein, F., Sandor, G. N., *Synthesis of Path-Generating Mechanisms by Means of a Programmed Digital Computer*, ASME Journal of Engineering for Industry, Vol. 81B, No. 2, pp. 159-168, 1959.

[13] Burmester, L., *Lehrbuch der Kinematik*, A. Felix Verlag, Germany, 1888.

[14] Erdman, A. G., Sandor, G. N., *Kinematic Synthesis of a Geared Five-Bar Function Generator*, Journal of Engineering for Industry, Vol. 93B, No. 1, pp. 157-164, 1971.

[15] Erdman, A. G., Sandor, G. N., *Advanced Mechanism Design: Analysis and Synthesis Volume II*, Prentice Hall, USA, 1984.

[16] McCarthy, J. M., *The Opposite Pole Quadrilateral as a Compatibility Linkage for Parameterizing the Center-point Curve*, Journal of Mechanical Design, Vol. 115, No. 2, pp. 332-336, 1993.

[17] Murray, A., McCarthy, J. M., *Center-point Curves Through Six Arbitrary Points*, Journal of Mechanical Design, Vol. 119, No. 1, pp. 33-39, 1997.

[18] Myszka, D. H., Murray, A. P., *Identifying Sets of Four and Five Positions that Generate Distinctive Center-Point Curves*, Proceedings of the ASME 2009 International Design Engineering Technical Conferences & Computers and Information in Engineering Conference, IDETC/CIE 2009, San Diego, California, USA, September, 2009.

[19] Loerch, R. J., Erdman, A. G., Sandor, G. N., *On the Existence of Circle-Point and Center-Point Circles for Three-Precision Point Dyad Synthesis*, Journal of Mechanical Design, pp. 554-562, 1979.

[20] Rigelman, G. A., Kramer, S. N., *A Computer-Aided Design Technique for the Synthesis of Planar Four-Bar Mechanisms Satisfying Specified Kinematic and Dynamic Conditions*, Journal of Mechanisms, Transmissions and Automation in Design, Vol. 110, No. 263, September 1988.

[21] Filemon, E., *Useful Ranges of Center-Point Curves for Design of Crank and Rocker Linkages*, Mechanisms and Machine Theory, Vol. 7, pp. 47-53, 1972.

[22] Chen, Y., Fu, J., *A Computational Approach for Determining Location of Burmester Solutions with Fully Rotatable Cranks*, Mechanism and Machine Theory, Vol. 34, Issue 4, pp. 549-558, 1999.

[23] Lee, M. Y., Erdman, A. G., Faik, S., *A Generalized Performance Sensitivity Methodology for Four-Bar Mechanisms*, Mechanism and Machine Theory, Vol. 34, pp. 1127-1139, 1999.

[24] Erdman, A. G., *Computer Aided Mechanism: Now and the Future*, Special 50th Anniversary Design Issue, Vol. 117, No. 93, June 1995.

[25] Rubel, A. J., Kaufman, R. E., *KINSYN 3: A New Human-Engineering System for Interactive Computer Aided Design of Planar Linkages*, ASME Journal of Engineering for Industry, Vol. 99, No. 2, 1988.

[26] Erdman, A. G., Gustafson, J., *LINCAGES: Linkage INteractive Computer Analysis and Graphically Enhanced Synthesis Packages*, Technical Report 77-DET-5, American Society of Mechanical Engineers, 1977.

[27] Erdman, A. G., *LINCAGES: Linkage INteractive Computer Assisted Geometrically Enhanced Synthesis – A Powerful Mechanism Design Software*, Online, Available: http://www.me.umn.edu/labs/lincages/ , January 2011.

[28] Alankuş, O. B., *Computer Aided Design of Mechanisms*, Ms. Thesis, Department of Mechanical Engineering, Middle East Technical University, March 1979.

[29] Polat, M., *Computer Aided Synthesis of Planar Mechanisms*, Ms. Thesis, Department of Mechanical Engineering, Middle East Technical University, March 1985.

[30] Sezen, A. S., *Development of an Interactive Visual Planar Mechanism Synthesis and Analysis Program by Using Delphi Object Oriented Programming Environment*, Ms. Thesis, Department of Mechanical Engineering, Middle East Technical University, June 2001.

[31] Demir, E., *Kinematic Design of Mechanisms in a Computer Aided Design Environment*, Ms. Thesis, Department of Mechanical Engineering, Middle East Technical University, May 2005.

[32] Holte, J. E., *Two Precision Position Synthesis of Planar Mechanisms with Approximate Position and Velocity Constraints*, Ph. D. Dissertation, University of Minnesota, December 1996.

[33] Mlinar, J. R., *An Examination of the Features of the Burmester Field and the Linear Solution Geometry of Dyads and Triads*, Ph. D. Dissertation, University of Minnesota, August 1997.

[34] Duran, Y., *Design of a Mechanism for Opening Hatchback Car Baggage Door*, Ms. Thesis, Department of Mechanical Engineering, Middle East Technical University, September 2009.

[35] Holland, J. H., *Adaptation in Natural and Artificial Systems*, The MIT Press, 1975.

[36] Goldberg, D. E., *Genetic Algorithms in Search and Machine Learning*, Addison-Wesley Longman Publishing Co. Inc., Boston, USA, 1989.

[37] Suganthan, P. N., *Structural Pattern Recognition Using Genetic Algorithms*, Pattern Recognition, Vol. 35, Issue 9, pp. 1883-1893, September 2002.

[38] Jakiela, M. J., Chapman, C., Duda, J., Adewuya, A. and Saitou, K., *Continuum Structural Topology Design with Genetic Algorithms*, Computer Methods in Applied Mechanics and Engineering, Vol. 186, Issues 2-4, pp. 339-356, June 2000.

[39] Hasançebi, O., Erbatur, F., *Evaluation of Crossover Techniques in Genetic Algorithm Based Optimum Structural Design*, Computers and Structures, Vol. 78, Issues 1-3, pp. 435-448, November 2000.

[40] Nanakorn, P., Meesomklin, K., *An Adaptive Penalty Function in Genetic Algorithms for Structural Design Optimization*, Computers and Structures, Vol. 79, Issues 29-30, pp. 2527-2539, November 2001.

[41] İpek, L., *Optimization of Backhoe-Loader Mechanisms,* Ms. Thesis, Department of Mechanical Engineering, Middle East Technical University, August 2006.

[42] Uzer, C. C., *Shape Optimization of an Excavator Boom by Using Genetic Algorithm*, Ms. Thesis, Department of Mechanical Engineering, Middle East Technical University, June 2008.

[43] Özbayramoğlu, E., *Shape Optimization of Wheeled Excavator Lower Chassis*, Ms. Thesis, Department of Mechanical Engineering, Middle East Technical University, August 2008.

[44] Chen, W. H., *A Genetic Algorithm for 2D Shape Optimizatio*n, Ms. Thesis, Department of Mechanical Engineering, Middle East Technical University, August 2008.

[45] Lawrance, M. H., *Material Handling Apparatus – Front Lift Type,* United States Patent Office 3215292, November 1965.

[46] Ashcroft, D. A., Todd, R. R., *Method of Lifting a Skid-steer Loader Bucket*, United States Patent 5542814, August 1996.

[47] Roan, T. J., Albright, L. E., *Folding Lift Arm Assembly for Skid-Steer Loader*, World Intellectual Property Organization WO 2004/104304 A2, December 2004.

[48] Wykhuis, L. A., O'Neill, M. J., *Lift Arm and Control Linkage Structure for Loader Buckets*, Canadian Patent 1166198, April 1982.

[49] Cormidi, http://www.cormidi.it/site_eng.html , 16 June 2011.

[50] Gehl, http://www.gehl.com/const/prodpg_eseries.html , 16 June 2011.

[51] Volvo Construction Equipment, http://www.volvoce.com/constructionequipment/na/en-us/products/skidsteerloaders/pages/introduction.aspx , 17 June 2012.

[52] Caterpillar, http://www.uk.cat.com/equipment/skid-steer-loaders , 15 June 2012.

[53] Hyundai Heavy Industries Europe, http://www.hyundai.eu/products/skid-steer-loaders/ , 18 June 2012.

[54] Renner, G., Ekárt, A., *Genetic algorithms in computer aided design*, Computer-Aided Design 35 pp. 709–726, 2003.

[55] ISO 14397-2, Earth-moving Machinery – Loaders and Backhoe Loaders – Part 2: Test Method for Measuring Breakout Forces and Lift Capacity to Maximum Lift Height, 2007.

[56] Rexroth Bosch Group, *Hydraulic Cylinders Tie Rod Design*, pp. 30, 2004.

[57] Shingley, J. E., Mischke, C. R., Budynas, R. G., *Mechanical Engineering Design*, Seventh Edition, pp. 147 and pp. 985, 2003.

[58] Linkage function genetator, http://en.wikipedia.org/wiki/File:Linkage_function_generator.png , 25 June 2012.

[59] Kinzel, E. C., Schmiedeler, J.P., Pennock, G.R., *Kinematic Synthesis for Finitely Separated Positions Using Geometric Constraint Programming*, Journal of Mechanical Design, Vol. 128, No. 1079, September 2006.

APPENDIX A

HISTORY OF KINEMATICS AND TYPES OF SYNTHESIS

Ampere defined kinematics as "the study of the motion of mechanisms and methods of creating them." [15]. The first part of the definition deals with the kinematic analysis; on the other hand the second part deals with the kinematic synthesis. The very first step in a machine design process is the kinematic synthesis of the mechanism because when starting to design a machine, the motion of the mechanism to be created is known. Therefore, the mechanism satisfying the desired motion should be developed. In other words, kinematic synthesis deals with the systematic design of mechanisms for a given performance.

The areas of synthesis can be grouped in two categories, namely type synthesis and dimensional synthesis. Type synthesis gives answers to questions like which type of mechanism is suitable for a given motion requirement, how many degrees of freedom is required, how many links should be needed and in which configuration, etc. Besides, dimensional synthesis seeks answers for determining the dimensions and the starting position of the mechanism of preconceived type for a specified task and prescribed performance. Optimization synthesis and prescribed position synthesis are two approaches that are generally used for dimensional synthesis. In optimization synthesis, the error between the desired output and the output generated by the mechanism is tried to be minimized. However, in prescribed position synthesis, a mechanism satisfying the desired output at some prescribed finite number of positions is searched.

According to the desired tasks, prescribed position synthesis can be categorized into three groups; namely function generation, path generation and motion generation. In function generation, the input and the output motions are correlated. In other words, if an output of $y = f(x)$ is desired with an input of x, than function generation

is the solution for the problem. A schematic view of a function generator can be seen in Figure A-1.

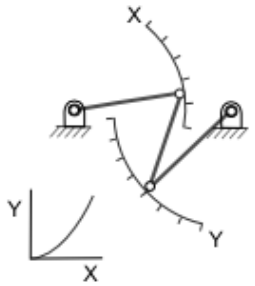

Figure A-1 – Function Generator [58]

In path generation, the motion of a single point is controlled without considering the angular rotations of the moving plane. This time, input link motion is correlated with the position change of a point on a floating link. If the path points are to be correlated with time, the task is called path generation with prescribed timing. A schematic view of a path generator can be seen in Figure A-2.

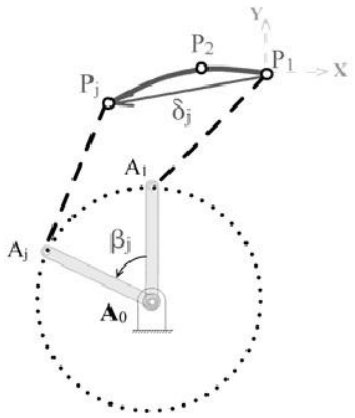

Figure A-2 – Path Generator [31]

Motion generation can be defined as the controlled translation and rotation of a moving reference frame relative to a fixed reference frame [59]. The difference of motion generation from the other two generations is that the input link motion is not prescribed. In this study, synthesis with four prescribed positions will be taken into consideration when a four-bar mechanism is designed. α_2, $\overrightarrow{\delta_2}$, α_3, $\overrightarrow{\delta_3}$, α_4 and $\overrightarrow{\delta_4}$ are the parameters for four multiply separated positions. A schematic view of a path generator can be seen in Figure A-3.

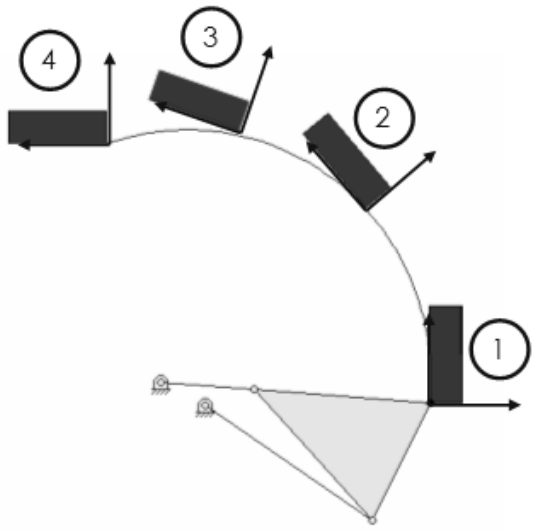

Figure A-3 – 4 prescribed positions for a typical motion generator

A circle-point curve is the locus of feasible moving pivot locations for a planar four-bar mechanism that will lead the coupler through the prescribed positions. Moreover, a center-point curve is the corresponding center of every circle-point. The objective of prescribed position synthesis is to find the circle-point and its corresponding center-point that satisfies the known prescribed positions. Theoretically, there are ∞^2 solutions for three multiply separated, ∞ solutions for four multiply separated and at most 6 solutions for five multiply separated positions.